

CHAPTER 1

Charge Transport in DNA

1.1 INTRODUCTION

The discovery of the double helical structure of DNA in 1953 defines a new era for molecular biology and biochemistry. It not only reveals the pivotal role of DNA as the carrier of genetic information in cells, but also implicates that DNA may have some unique physical properties and other biological functions.¹ The inner core of DNA double helix is composed of a stacked array of heterocyclic aromatic base pairs, wrapped within a negatively charged sugar phosphate backbone (Figure 1.1). As such, the DNA double helix represents a well-defined molecular π -stack which resembles a one-dimensional aromatic crystal. Numerous solid state π -stacked arrays have been identified, and these materials tend to exhibit semiconductor or conductor behavior, especially in the presence of dopants.²⁻⁴ Shortly after the elucidation of the double helical structure of DNA, by analogy, it was suggested that DNA might have special electronic properties and function as a charge mediator.^{1, 5} Indeed, whether double helical DNA, owing to its π -stacked structure, might be an effective conduit for charge transport (CT) has intrigued physicists, chemists, and biologists for more than 40 years.

The molecular π -stack of DNA double helix shares some characteristics with solid state stacked materials, but there are also critical differences. For instance, unlike solid state π -stacked systems, DNA is a highly dynamic molecule, and undergoes dynamic motions on a timescale from picoseconds to milliseconds.⁶⁻¹² The structure of DNA is constantly modulated by the close interactions of water molecules and counterions. The electronic coupling within the π -stack, which is necessary for the conductivity of all π systems, is very sensitive to the motions of bases. Consequently, CT in DNA is highly dependent on the conformational dynamics of DNA and is much more

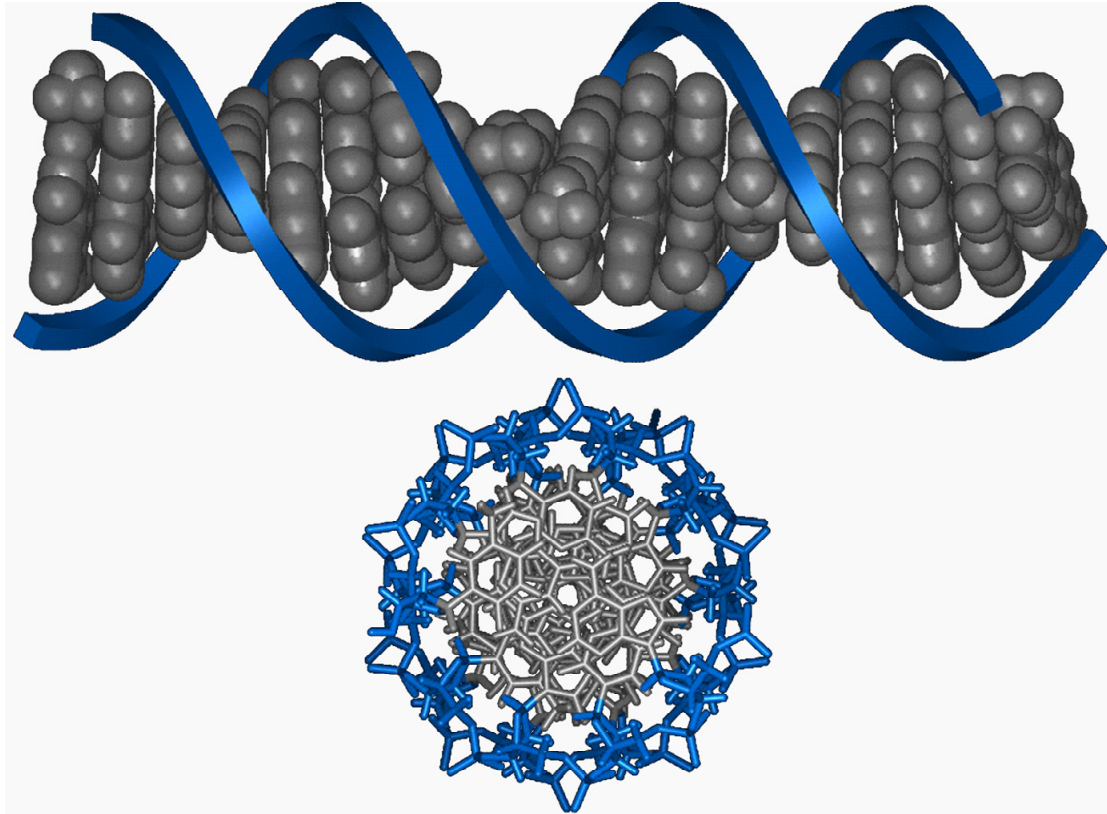


Figure 1.1. Structure of the DNA double helix (B-form), viewed from 90° to the helix axis (top) and along the helix axis (bottom). The sugar-phosphate backbone is shown in blue and the π -stack of DNA base pairs is shown in gray. This π -stack is the path of DNA-mediated charge transport.

complicated than in solid state materials.¹³ Studies on the ability of DNA to mediate charge have generated extensive debate on whether DNA is a conductor or an insulator. It is only very recently that the chemists in the field are moving towards a consensus view that DNA is an effective medium for CT and starting to discover its biological context.^{14, 15}

1.2 EXPERIMENTAL APPROACHES TO STUDIES OF DNA-MEDIATED CHARGE TRANSPORT

A variety of experimental approaches have been utilized to probe DNA's potential for charge transport. Perhaps the most direct and easiest way is to measure the conductivity of DNA. Indeed, the earliest approaches to the issue were physical measurements of current flow in DNA fibers. However, these studies led to a mixture of conclusions: some suggesting DNA as an insulator, and others indicating DNA as a quantum wire.^{1, 16-18} More recent studies involved measurements in aligned DNA films, in small collections of molecules, and even in single molecules.¹⁹⁻²² Electron conductivity was clearly demonstrated in these studies, although the results of these experiments fell into a wide spectrum of classifications. In aligned DNA films, a differential conductivity depending upon DNA orientation was observed: a large current that increased linearly with applied voltage was found along the direction parallel to the helical axis, while no current was detected in the perpendicular direction.¹⁹ Fink measured the electrical current as a function of the potential applied across a few DNA molecules which were associated into 600 nm long ropes and found a semiconductor behavior. The resistivity values derived from the measurements were comparable to those of conducting polymers.²⁰ By

contrast, Porath et al. measured the electrical transport through individual dry poly(G)-poly(C) DNA duplexes and observed a wide band-gap semiconducting behavior.²¹ In another experiments, DNA was even found to be a superconductor at very low temperature (1 kelvin).²² Although some consensus may now have been reached that electron could transport through DNA, the results of these physical studies have not yet been reconciled with each other. The origin of these large variations in experimental results is likely due to the fact that the structure and integrity of DNA used in these studies are not fully characterized under the conditions of the measurements in which DNA are usually dehydrated, in direct contact with metal electrodes, and exposed to high voltages.

Chemists have instead employed photochemical and photophysical methods to explore CT in DNA. These approaches are distinct from the physical measurements in that the former relies on well-defined oligonucleotide assemblies in physiological conditions. In these methods, oligonucleotide assemblies are prepared containing pendant redox probes (i.e., charge donors and charge acceptors) and the electron transfer rates and yields are measured through fluorescence quenching as a function of distance on DNA duplexes in solution.²³⁻²⁷ The redox probes include metallointercalators, organic intercalators, and modified bases, which are well coupled with the base pair stack of DNA (Figure 1.2). In these studies, efficient DNA-mediated CT chemistry is observed when both the charge donor and acceptor are electronically well coupled into the base stack. The CT reaction in these assemblies occurs on an extremely fast timescale ($k_{ET} > 3 \times 10^{10} \text{ s}^{-1}$)²³ and with very shallow distance dependence.²⁴ By contrast, when nonintercalating metal complexes are tethered to a DNA duplex in which the CT reactants

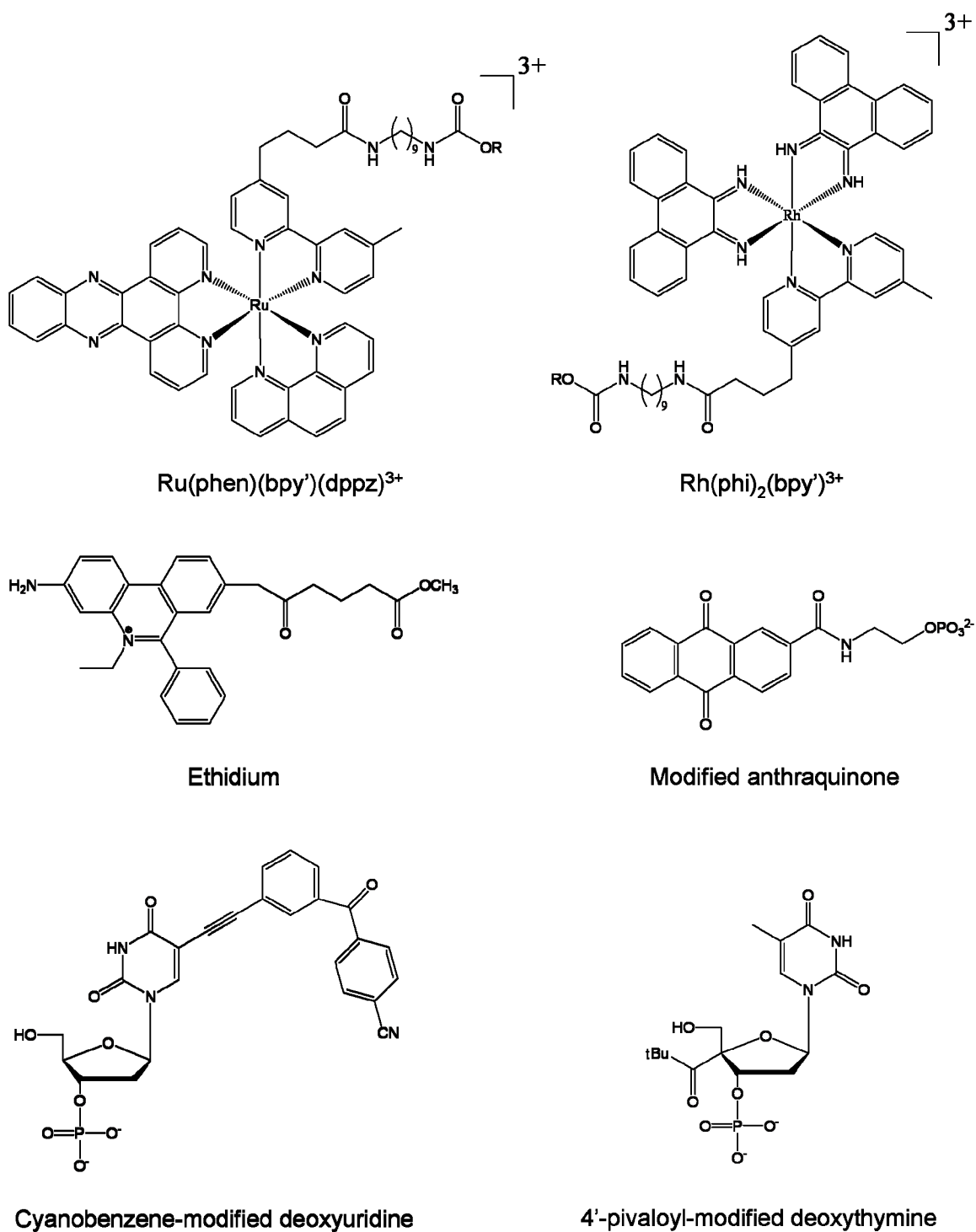


Figure 1.2. Chemical structures of some of the photooxidants that have been used in DNA charge transport studies.

are not well coupled to the DNA π -stack, efficient CT is not observed.²⁵ Moreover, local disruptions in the π -stack (i.e., an intervening mismatch) also decrease the CT yield.²⁴ These studies demonstrate that efficient CT reactions are mediated via the π -stack of DNA (Figure 1.3).

Biochemical studies, in which DNA bases (i.e., guanines doublet or triplet) are used as charge acceptors, provide another important approach to the characterization of DNA-mediated CT. This method relies on the fact that G has the lowest oxidation potential of all four bases,²⁸ and the potential of a GG doublet/triplet is even lower.²⁹ In biochemical studies, an intercalator is tethered to a DNA duplex at a given site spatially separated from guanine doublet/triplet sites, and is used as a photooxidant to oxidatively damage the guanine doublet/triplet in DNA; the yield of the oxidative damage can then be analyzed as strand breaks by gel electrophoresis. The biochemical studies have identified that DNA charge transport can proceed over long molecular distances (~ 200 Å), and established, for the first time, that the double-helical DNA can perform “chemistry at a distance”.^{30, 31} It has also been shown that DNA CT may occur *in vivo* and may be a factor leading to DNA damage within the cell.³² These studies lay the foundation for a full range of experiments using a variety of photooxidants, in which variations in distance, sequence, and structure are investigated, and the mechanism of DNA-mediated CT is explored.^{30, 33, 34}

1.3 MECHANISTIC CONSIDERATIONS

While photophysical and biochemical studies have established the DNA double helix as a medium for efficient CT, the mechanism of DNA-mediated CT remains

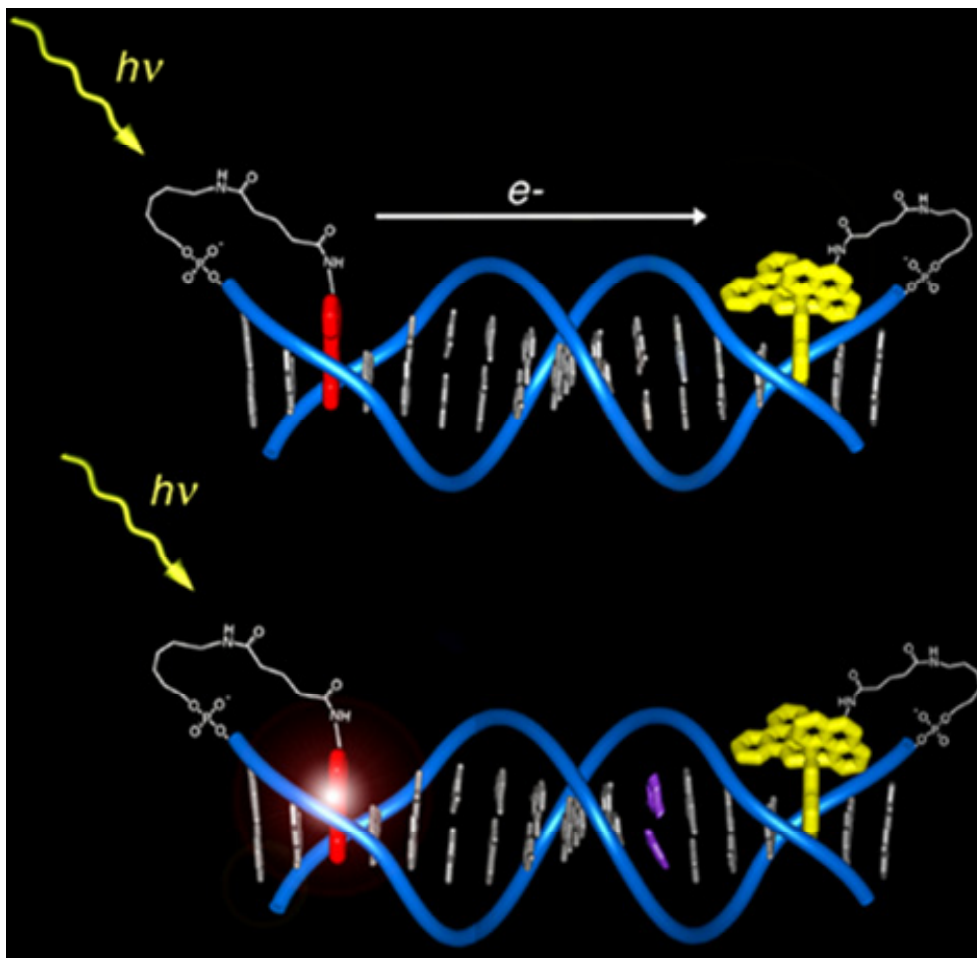


Figure 1.3. Schematic illustration of donor and acceptor tethered DNA assemblies in which long-range DNA-mediated charge transport is demonstrated. The fluorescence of a tethered ethidium intercalator (red) is quenched by a tethered rhodium(III) intercalator (yellow) located over 20 Å down the DNA helix (top). The DNA-mediated CT chemistry is exquisitely sensitive to base stack perturbations. The quenching of the ethidium is drastically diminished in the presence of an intervening base pair mismatch (bottom).

controversial, as experimental results have continuously changed our view towards the subject in the last decade. Apparently, an analogy with the σ -system in proteins is not appropriate, in which electron transfer rate shows significant distance dependence. Experimentally, a range of distance dependencies are observed in the measurement of DNA CT over short distances.³⁵⁻³⁹ On the other hand, oxidative damage studies indicate a shallow distance dependence in long range DNA CT.^{30, 31} In order to reconcile these seemingly contradictory data, Giese, Jortner, and co-workers proposed a model that combines two basic charge transport mechanisms—the tunneling (or superexchange) step and the hopping step.^{40, 41} According to this model, CT occurs by hopping between guanine bases, the energetically lower sites, and tunneling through intervening TA steps. In the hopping mechanism, charge migrates by transiently occupying the low energy sites in the π -stack and hopping one to the next and a shallow distance dependence of CT is expected. In the tunneling mechanism, the charge tunnels through high energy bases (As and Ts) without formally occupying it, the rate of which decreases exponentially with distance between the charge donor and acceptor (Figure 1.4).^{42, 43}

This guanine hopping model is supported by the observation in oxidative damage experiments that yields of guanine oxidation decrease dramatically with increasing separation between guanine “stepping stones” by TA steps.^{43, 44} However, this model does not take into account the influences of the DNA structural dynamics. For example, 5'-TA-3' steps are known to be quite flexible; the base-base coupling is significantly altered upon inserting TA steps into the bridge, which could also account for the diminished yields of oxidative damage. Indeed, oxidative damage studies by Williams et al. demonstrate that the base sequence and length are important to DNA CT. They also

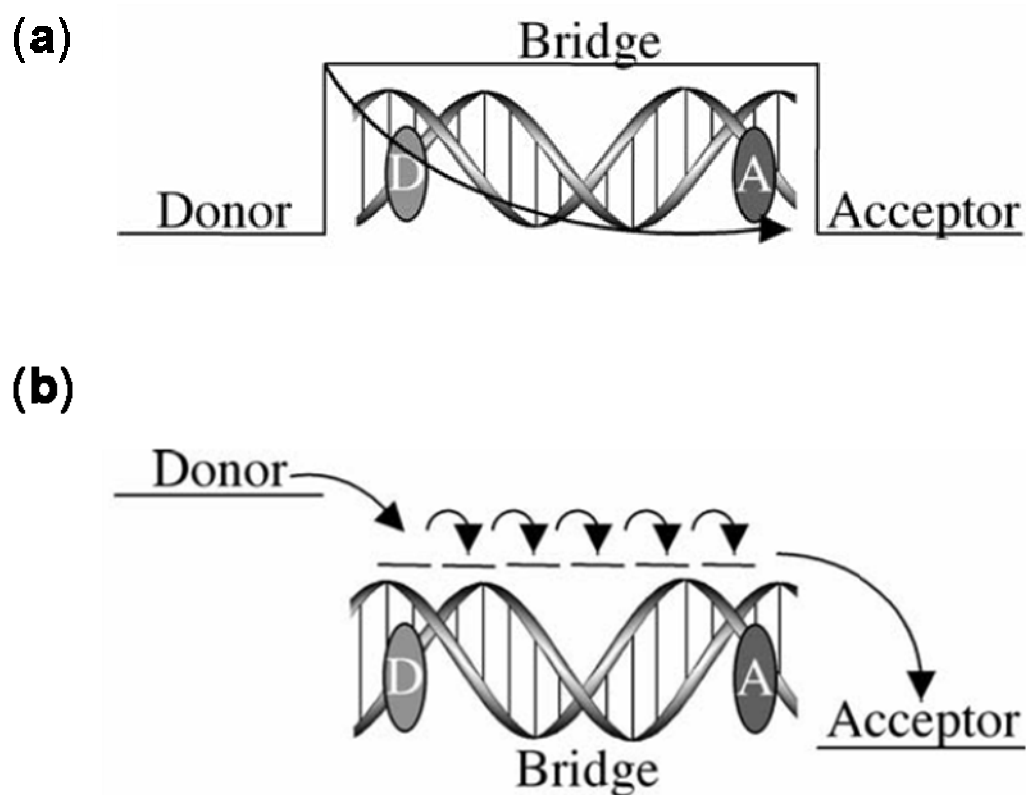


Figure 1.4. Schematic representation of possible mechanisms for charge transport through DNA. (a) Superexchange: the charge tunnels from the donor (D) to the acceptor (A) through the bridge, in which the rate of CT decreases exponentially with increasing bridge length. (b) Hopping: charge occupies the bridge hopping between discrete molecular orbitals. If hopping is faster than radical trapping, the charge should be able to migrate over long distances along the bridge.

suggest that conformational dynamics of DNA is a critical factor for long range CT in DNA.³⁴ A simple guanine hopping model is not sufficient to describe DNA CT.

Also based on yield measurements of oxidative damage, Schuster and co-workers have proposed phonon-assisted polaron hopping between guanine bases.⁴⁵ In this model, a transient polaron is formed upon the injection of charge, and the polaron migrates through DNA as a consequence of normal vibrational fluctuations (phonons). The polaron formation allows for the charge delocalization over regions of DNA sequence, and the phonon assisted polaron hopping occurs by a superexchange mechanism between the regions, and is sensitively gated in a correlated manner by the thermal motions of the hydrated counterions.⁴⁶ This model accommodates the fact that DNA is a dynamic structure on the time scale of CT, and indicates the distortion of the DNA as a mean for charge migration. It also implies that the injected charge is the cause of such distortion.

The critical importance of DNA dynamics is underscored by ultrafast spectroscopic studies on CT between covalently bound ethidium (Et) and a modified base, 7-deazaguanine (zG).³⁸ The CT reaction in these assemblies occurs on the femtosecond time scale with a very shallow distance dependence, but is sensitive to intervening sequence and mismatches.^{37, 38} These experiments strongly suggest that DNA-mediated CT is gated by dynamical motions within the base pair assembly and the orientation of the Et intercalator. This is further confirmed by the experiments using photoexcited 2-aminopurine (Ap*), a fluorescent nucleobase analog, in combination with time-resolved and steady-state fluorescence quenching.^{13, 47} In these experiments, the yield of CT through duplex DNA increases with increasing temperature governed by the

length and sequence of the DNA bridge; the distance dependence of CT is regulated by temperature, and at all temperatures in the studies, the yield of CT does not exhibit a simple distance dependence, but shows an oscillatory behavior, with a period of 4–5 base pairs.⁴⁷ These data can not be rationalized by superexchange, charge hopping, or by phonon-assisted polaron hopping.

Based on these observations, Barton and coworkers have proposed a domain-hopping model in which charge migrates through the DNA bridge among delocalized domains.^{30, 34, 47, 48} These DNA domains can be described as extended π -orbitals formed transiently, depending on DNA sequences and dynamics (Figure 1.5). In contrast to the polaron model in which a structurally distorted domain forms in response to the injected charge, the delocalized domain in the domain hopping model forms transiently, irrespective of the charge, with a size of ~ 4 base pairs.^{47, 48} This model is supported by recent experiments using kinetically fast electron hole traps, N⁴-cyclopropylcytosine (^{cp}C) and N²-cyclopropylguanine (^{cp}G).⁴⁸ In these experiments, the efficiency in hole trapping at higher-energy pyrimidines (^{cp}C) is equivalent to that at lower-energy purines (^{cp}G). These observations strongly suggest that DNA CT is not simply a function of the relative energies of the isolated bases, but instead requires orbital mixing among neighboring bases.

To date, DNA CT is still not well understood mechanistically. Many variations seen with different oxidants cannot yet be reconciled by one model. However, it is clear that DNA CT is dependent on the structure and dynamics of nucleic acids. It is this dependence that is required for DNA-mediated CT to be exploited in molecular electronics and sensors, as well as to discover its biological significance in cells.

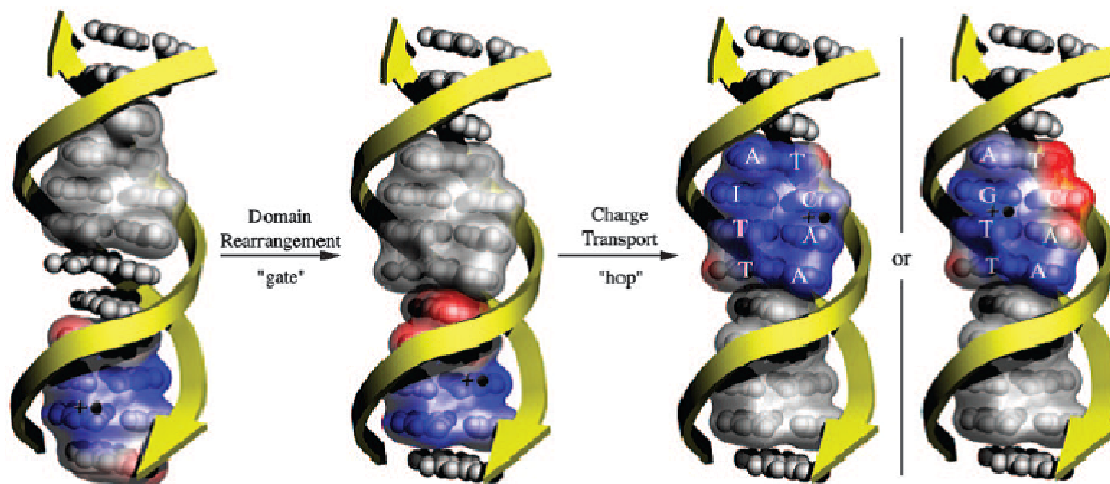


Figure 1.5. Schematic illustration of delocalized domain model for DNA CT. Charge migrates through the DNA bridge by hopping among domains: Extended π -orbitals formed transiently in a manner governed by DNA sequence and dynamics. DNA domains form transiently, irrespective of charge. Base motion causes domains to form and break up, and consequently, migration of charge among domains is conformationally gated. In duplex DNA, hole density is distributed through the domain (high–low, blue–white–red) in a sequence-dependent fashion, as shown, for instance, when an I–C base pair is replaced by a G–C base pair. Here, hole density distribution in the domains is shown schematically by static snapshots, but it will fluctuate in time with the dynamic motion of the DNA bases. (Adapted from reference 48.)

1.4 DNA-MEDIATED ELECTRON TRANSFER ON SURFACES

While photophysical and biochemical methods provide powerful tools to studies of DNA CT in solution, DNA-mediated electron transfer (ET) on surfaces are investigated electrochemically. Electrochemistry has been used extensively to measure heterogeneous electron transfer kinetics in self-assembled monolayers on solid surfaces.⁴⁹⁻⁵³ In a typical system, redox-active head groups are attached to aliphatic alkanethiols or conjugated linkers of variable length, and are subsequently self-assembled into well-ordered monolayers on a solid surface. Electrochemical studies on these systems have yielded important information regarding the ability of different media to promote long-range electronic coupling. In order to investigate ET in DNA films, we have developed analogous methods for preparing DNA-modified surfaces in which redox-active DNA intercalators are used as the “head groups” located at defined positions along the base stack of individual DNA helices on the surface (Figure 1.6).^{54, 55} The reduction of the intercalators is therefore conjugated to ET events in the DNA film, and can be monitored electrochemically.

A variety of redox-active species have been used in the electrochemical studies of ET in DNA film, among which methylene blue (MB) and daunomycin (DM) have been shown to be most proficient (Figure 1.7). MB and DM are organic intercalators that bind to DNA with a relatively high binding constant ($k \sim 10^6 \text{ M}^{-1}$ for MB and $\sim 10^7$ for DM).⁵⁶⁻⁶⁰ The reduction of MB is reversible, with a redox potential of $\sim 0 \text{ V}$ (vs. NHE) which is slightly lower than that of $[\text{Fe}(\text{CN})_6]^{3-}$. This makes MB a perfect noncovalent-tethered probe for electrocatalytic studies.⁶¹ On the other hand, with a redox potential of $\sim -0.4 \text{ V}$ (vs. NHE), DM is readily cross-linked to the guanine residues in

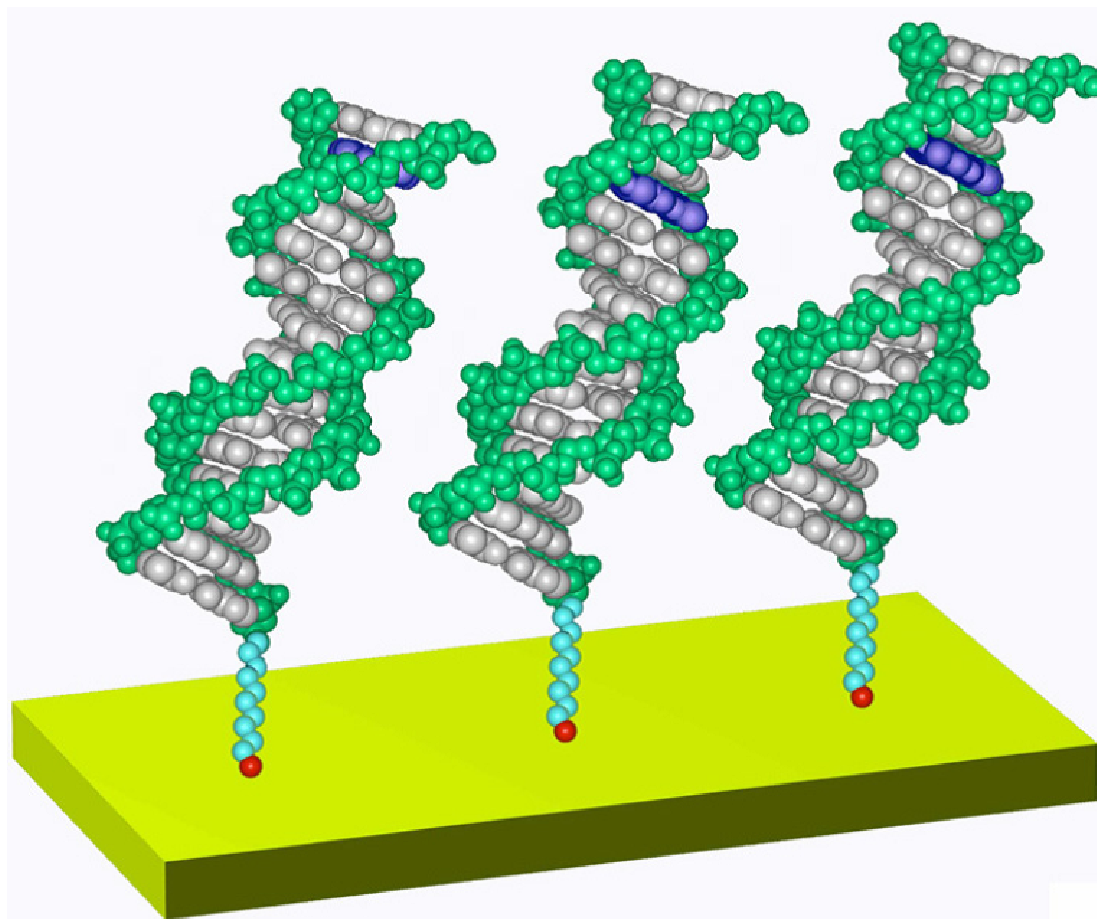


Figure 1.6. Schematic illustration of alkanethiol functionalized DNA duplexes immobilized on a gold surface for use in electrochemical assays. An intercalator (blue) bound near the top of the DNA monolayer, is reduced by electron transfer from the electrode surface through the π -stack of DNA.

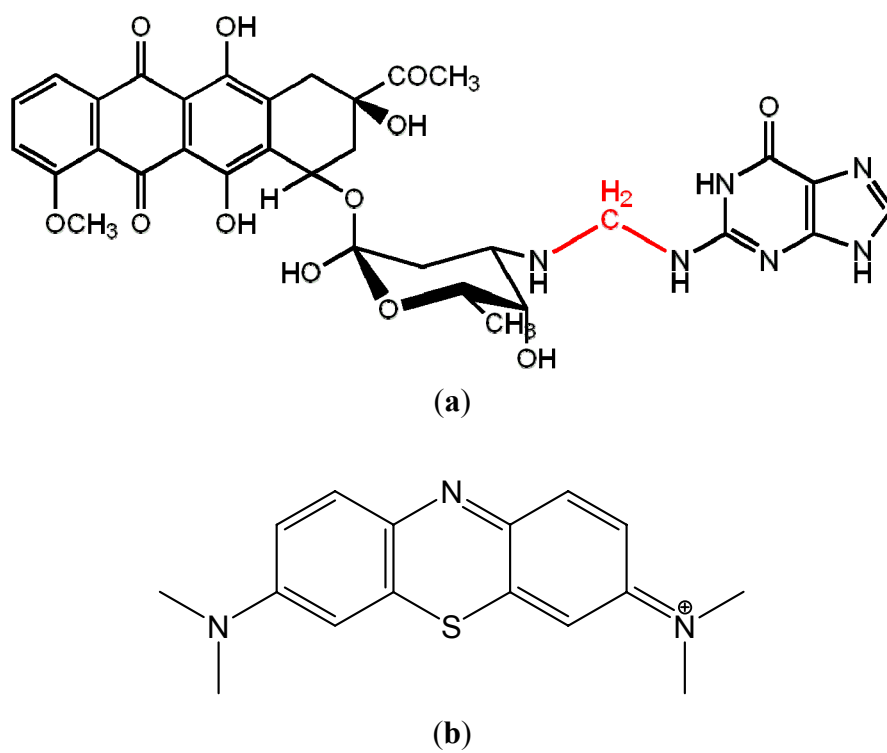


Figure 1.7. (a) Chemical structure of daunomycin cross-linked to the exocyclic amine of guanine. (b) Chemical structure of methylene blue.

double stranded DNA in the presence of formaldehyde, and the structure of DNA-DM conjugate has been well characterized by crystallography (Figure 1.7).^{62, 63} Therefore, DM is usually used as a covalently tethered probe in which site-specific cross-linking is required.

We have first examined electron transfer in densely packed DNA films with daunomycin crosslinked to various sites along the base stack. Remarkably, efficient reduction of DM is observed regardless of its position along the 15-base pair sequence. Both the intensity of the DM signal and electron transfer rate constant are found to be independent of the position of DM in the film.⁵⁴ Furthermore, the reduction of DM is shut off in the presence of an intervening CA mismatch between the electrode and the DM. This experiment establishes that, similar to DNA in solution, the pathway for ET in DNA films is through the base pair stack. Importantly, it also shows that ET in DNA films is sensitive to perturbations in base stacking, which indicates that a single-base mismatch in DNA can be detected electrochemically.

The sensitivity of ET in DNA films to an intervening single base mismatch is further explored by electrocatalytic studies with noncovalent intercalator MB.^{61, 64} In these studies, the reduction of the intercalating MB is coupled to an electrocatalytic cycle involving freely diffusing ferricyanide, which significantly enhances its sensitivity and selectivity to the changing of electron transfer in the DNA film (Figure 1.8). With this method, all single base mismatches, including thermodynamically stable GT and GA mismatches, have been detected by cyclic voltammetry and chronocoulometry.⁶⁴ These studies again underscore the sensitivity of DNA-mediated CT to perturbations in the π -stack of double helical DNA, and demonstrate that DNA CT provides a novel approach

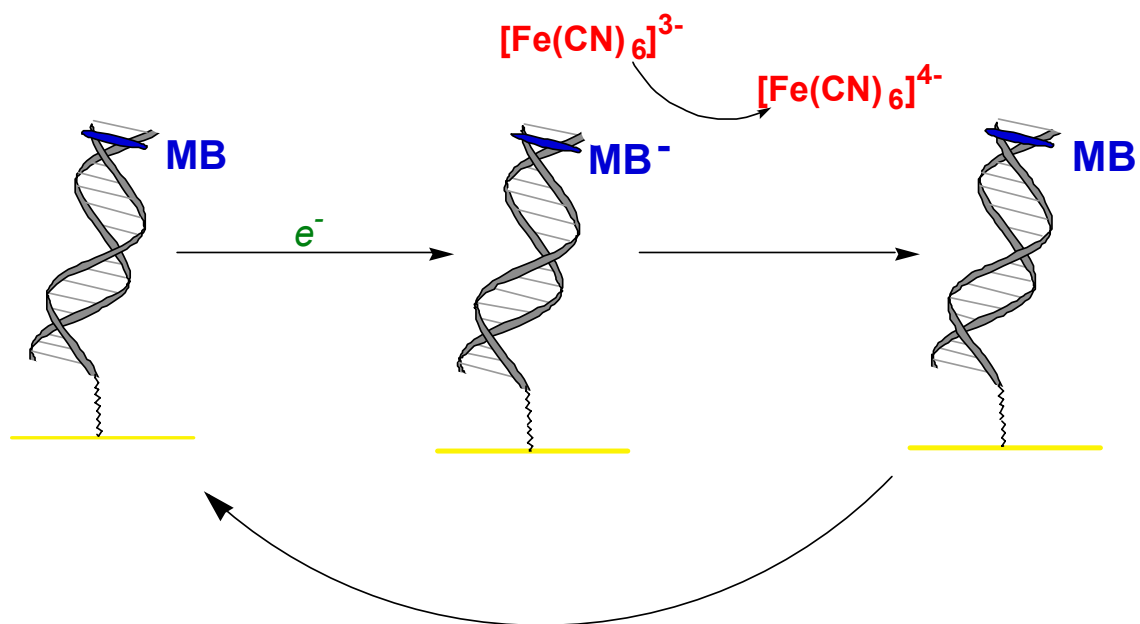


Figure 1.8. Schematic representation of electrocatalytic reduction of $[\text{Fe}(\text{CN})_6]^{3-}$ by MB at a DNA-modified electrode.

to the development of DNA sensors for mutation detection.

While ET in DNA films is sensitive to structural dynamics of base stack, it shows little dependence on base sequence, which is otherwise obvious for DNA CT in solution.⁶¹ This is probably due to the fact that the electrochemical studies report on events that occur on a much longer time scale than the photophysical and biochemical experiments. Indeed, experiments with covalent-tethered DM have shown that the rate limiting step for CT in DNA film is the CT through σ -bonds of the aliphatic linker.⁶⁵

DNA-mediated ET holds a great promise for applications in DNA sensing. However, there is still much to be explored before we can make a practical detection system based on DNA-mediated ET on surface. In this thesis, we investigate ET in different DNA films with various covalent-tethered DNA intercalators. The advantage of a covalent-tethered intercalator is that it eliminates the need for tightly packing of DNA film as required by noncovalent intercalator (i.e., MB). Consequently, ET in a loosely packed DNA film can be studied with covalent-tethered intercalators. In chapter 2, we investigate the influence of the sugar-phosphate backbone on ET in DNA film with crosslinked DM. This study confirms that it is through the base stack, not the sugar-phosphate backbone, that ET occurs, and the nicks in the sugar-phosphate backbone do not affect ET in DNA film. Based on this discovery, we electrochemically monitored the trapping of duplex DNA with overhangs on DNA modified gold electrode, which is described in Chapter 3.

The electronic coupling between an intercalator and the π -stack of DNA is important for the intercalator to be reduced by DNA-mediated CT.⁶⁶ In Chapter 4, we investigate the influence of the interaction of the intercalator with the DNA π -stack to the

intercalator reduction, using covalently tethered anthraquinone derivatives as the redox probe. This study underscores the importance of direct interaction between the intercalator with the π -stack in order to observe efficient DNA-mediated electrochemistry through DNA films.

We have been looking for a covalent intercalator that can substitute for DM with a more stable linkage to DNA and a redox potential that is more suitable for electrochemical studies on gold electrodes modified with thiol-terminated DNA. Nile blue (NB), a cationic phenoxazine dye that features a heterocyclic, planar and rigid structure, appears to be a competent candidate.^{67, 68} In Chapter 5, we describe the synthesis of DNA-NB conjugate and explore the reduction of covalently-tethered NB by ET in DNA films. Based on these studies, we develop a label-free method for mismatch detection based on DNA-mediated ET which is also described in Chapter 5. The results of these experiments provide further insight into ET in DNA films and the development of a practical sensing system employing DNA-mediated CT.

1.5 REFERENCES

1. Eley, D. D., Semiconductivity of Organic Substances .9. Nucleic Acid in Dry State. *Transactions of the Faraday Society* **1962**, 58, (470), 411.
2. Miller, J. S.; Epstein, A. J., Organic and Organometallic Molecular Magnetic Materials—Designer Magnets. *Angewandte Chemie International Edition in English* **1994**, 33, (4), 385-415.
3. Fox, M. A., Polymeric and Supramolecular Arrays for Directional Energy and Electron-Transport over Macroscopic Distances. *Accounts of Chemical Research* **1992**, 25, (12), 569-574.
4. Marks, T. J., Electrically Conductive Metallomacrocyclic Assemblies. *Science* **1985**, 227, (4689), 881-889.
5. Szentgyorgyi, A., On The Electron Donating Properties of Carcinogens. *Proceedings of the National Academy of Sciences of the United States of America* **1960**, 46, (11), 1444-1449.
6. Borer, P. N., C-13-NMR Relaxation in 3 DNA Oligonucleotide Duplexes—Model-Free Analysis of Internal and Overall Motion. *Biochemistry* **1994**, 33, (9), 2441-2450.
7. Brauns, E. B., Local dynamics in DNA by temperature-dependent Stokes shifts of an intercalated dye. *Journal of the American Chemical Society* **1998**, 120, (10), 2449-2456.
8. Cheatham, T. E.; Kollman, P. A., Molecular dynamics simulation of nucleic acids. *Annual Review of Physical Chemistry* **2000**, 51, 435-471.
9. Georghiou, S., Large-amplitude picosecond anisotropy decay of the intrinsic fluorescence of double-stranded DNA. *Biophysical journal* **1996**, 70, (4), 1909-1922.
10. Giudice, E., Simulations of nucleic acids and their complexes. *Accounts of chemical research* **2002**, 35, (6), 350-357.
11. Liang, Z. C.; Freed, J. H.; Keyes, R. S.; Bobst, A. M., An electron spin resonance study of DNA dynamics using the slowly relaxing local structure model. *Journal of Physical Chemistry B* **2000**, 104, (22), 5372-5381.
12. Nordlund, T. M.; Andersson, S.; Nilsson, L.; Rigler, R.; Graslund, A.; McLaughlin, L.

W., Structure and Dynamics of a Fluorescent DNA Oligomer Containing the EcorI Recognition Sequence - Fluorescence, Molecular-Dynamics, and Nmr-Studies. *Biochemistry* **1989**, 28, (23), 9095-9103.

13. O'Neill, M. A.; Becker, H. C.; Wan, C. Z.; Barton, J. K.; Zewail, A. H., Ultrafast dynamics in DNA-mediated electron transfer: Base gating and the role of temperature. *Angewandte Chemie-International Edition* **2003**, 42, (47), 5896-5900.

14. Treadway, C. R.; Hill, M. G.; Barton, J. K., Charge transport through a molecular pi-stack: Double helical DNA. *Chemical Physics* **2002**, 281, (2-3), 409-428.

15. Dekker, C.; Ratner, M. A., Electronic properties of DNA. *Physics World* **2001**, 14, (8), 29-33.

16. Warman, J. M.; deHaas, M. P.; Rupprecht, A., DNA: A molecular wire? *Chemical Physics Letters* **1996**, 249, (5-6), 319-322.

17. Snart, R. S., Photoelectric Effects of Deoxyribonucleic Acid. *Biopolymers* **1968**, 6, (3), 293.

18. Liang, C. Y.; Scalco, E. G., Electrical Conduction of High Polymerized Sample of Sodium Salt of Deoxyribonucleic Acid. *Journal of Chemical Physics* **1964**, 40, (4), 919.

19. Okahata, Y.; Kobayashi, T.; Tanaka, K.; Shimomura, M., Anisotropic electric conductivity in an aligned DNA cast film. *Journal of the American Chemical Society* **1998**, 120, (24), 6165-6166.

20. Fink, H. W., Electrical conduction through DNA molecules. *Nature* **1999**, 398, (6726), 407-410.

21. Porath, D.; Bezryadin, A.; de Vries, S.; Dekker, C., Direct measurement of electrical transport through DNA molecules. *Nature* **2000**, 403, (6770), 635-638.

22. Kasumov, A. Y.; Kociak, M.; Gueron, S.; Reulet, B.; Volkov, V. T.; Klinov, D. V.; Bouchiat, H., Proximity-induced superconductivity in DNA. *Science* **2001**, 291, (5502), 280-282.

23. Arkin, M. R.; Stemp, E. D. A.; Holmlin, R. E.; Barton, J. K.; Hormann, A.; Olson, E. J. C.; Barbara, P. F., Rates of DNA-mediated electron transfer between metallointercalators. *Science* **1996**, 273, (5274), 475-480.

24. Kelley, S. O.; Holmlin, R. E.; Stemp, E. D. A.; Barton, J. K., Photoinduced electron transfer in ethidium-modified DNA duplexes: Dependence on distance and base stacking. *Journal of the American Chemical Society* **1997**, 119, (41), 9861-9870.
25. Meade, T. J.; Kayyem, J. F., Electron-Transfer through DNA - Site-Specific Modification of Duplex DNA with Ruthenium Donors and Acceptors. *Angewandte Chemie-International Edition in English* **1995**, 34, (3), 352-354.
26. Murphy, C. J.; Arkin, M. R.; Jenkins, Y.; Ghatlia, N. D.; Bossmann, S. H.; Turro, N. J.; Barton, J. K., Long-Range Photoinduced Electron-Transfer through a DNA Helix. *Science* **1993**, 262, (5136), 1025-1029.
27. Lewis, F. D.; Wu, T. F.; Zhang, Y. F.; Letsinger, R. L.; Greenfield, S. R.; Wasielewski, M. R., Distance-dependent electron transfer in DNA hairpins. *Science* **1997**, 277, (5326), 673-676.
28. Steenken, S.; Jovanovic, S. V., How easily oxidizable is DNA? One-electron reduction potentials of adenosine and guanosine radicals in aqueous solution. *Journal of the American Chemical Society* **1997**, 119, (3), 617-618.
29. Prat, F.; Houk, K. N.; Foote, C. S., Effect of guanine stacking on the oxidation of 8-oxoguanine in B-DNA. *Journal of the American Chemical Society* **1998**, 120, (4), 845-846.
30. Nunez, M. E.; Hall, D. B.; Barton, J. K., Long-range oxidative damage to DNA: effects of distance and sequence. *Chemistry & Biology* **1999**, 6, (2), 85-97.
31. Ly, D.; Sani, L.; Schuster, G. B., Mechanism of charge transport in DNA: Internally-linked anthraquinone conjugates support phonon-assisted polaron hopping. *Journal of the American Chemical Society* **1999**, 121, (40), 9400-9410.
32. Rajski, S. R.; Jackson, B. A.; Barton, J. K., DNA repair: models for damage and mismatch recognition. *Mutation Research-Fundamental and Molecular Mechanisms of Mutagenesis* **2000**, 447, (1), 49-72.
33. Giese, B.; Amaudrut, J.; Kohler, A. K.; Spormann, M.; Wessely, S., Direct observation of hole transfer through DNA by hopping between adenine bases and by tunnelling. *Nature* **2001**, 412, (6844), 318-320.
34. Williams, T. T.; Odom, D. T.; Barton, J. K., Variations in DNA charge transport with nucleotide composition and sequence. *Journal of the American Chemical Society* **2000**,

122, (37), 9048-9049.

35. Lewis, F. D.; Liu, X. Y.; Liu, J. Q.; Hayes, R. T.; Wasielewski, M. R., Dynamics and equilibria for oxidation of G, GG, and GGG sequences in DNA hairpins. *Journal of the American Chemical Society* **2000**, 122, (48), 12037-12038.

36. Lewis, F. D.; Letsinger, R. L.; Wasielewski, M. R., Dynamics of photoinduced charge transfer and hole transport in synthetic DNA hairpins. *Accounts of Chemical Research* **2001**, 34, (2), 159-170.

37. Kelley, S. O.; Barton, J. K., DNA-mediated electron transfer from a modified base to ethidium: pi-stacking as a modulator of reactivity. *Chemistry & Biology* **1998**, 5, (8), 413-425.

38. Wan, C. Z.; Fiebig, T.; Kelley, S. O.; Treadway, C. R.; Barton, J. K.; Zewail, A. H., Femtosecond dynamics of DNA-mediated electron transfer. *Proceedings of the National Academy of Sciences of the United States of America* **1999**, 96, (11), 6014-6019.

39. Hess, S.; Gotz, M.; Davis, W. B.; Michel-Beyerle, M. E., On the apparently anomalous distance dependence of charge-transfer rates in 9-amino-6-chloro-2-methoxyacridine-modified DNA. *Journal of the American Chemical Society* **2001**, 123, (41), 10046-10055.

40. Bixon, M.; Jortner, J., Long-range and very long-range charge transport in DNA. *Chemical Physics* **2002**, 281, (2-3), 393-408.

41. Jortner, J.; Bixon, M.; Voityuk, A. A.; Rosch, N., Superexchange mediated charge hopping in DNA. *Journal of Physical Chemistry A* **2002**, 106, (33), 7599-7606.

42. Marcus, R. A.; Sutin, N., Electron Transfers in Chemistry and Biology. *Biochimica et Biophysica Acta* **1985**, 811, (3), 265-322.

43. Bixon, M.; Giese, B.; Wessely, S.; Langenbacher, T.; Michel-Beyerle, M. E.; Jortner, J., Long-range charge hopping in DNA. *Proceedings of the National Academy of Sciences of the United States of America* **1999**, 96, (21), 11713-11716.

44. Giese, B.; Wessely, S.; Spormann, M.; Lindemann, U.; Meggers, E.; Michel-Beyerle, M. E., On the mechanism of long-range electron transfer through DNA. *Angewandte Chemie-International Edition* **1999**, 38, (7), 996-998.

45. Henderson, P. T., Long-distance charge transport in duplex DNA: The

phonon-assisted polaron-like hopping mechanism. *Proceedings of the National Academy of Sciences of the United States of America* **1999**, 96, (15), 8353-8358.

46. Barnett, R. N.; Cleveland, C. L.; Joy, A.; Landman, U.; Schuster, G. B., Charge migration in DNA: Ion-gated transport. *Science* **2001**, 294, (5542), 567-571.

47. O'Neill, M. A.; Barton, J. K., DNA charge transport: Conformationally gated hopping through stacked domains. *Journal of the American Chemical Society* **2004**, 126, (37), 11471-11483.

48. Shao, F. W.; O'Neill, M. A.; Barton, J. K., Long-range oxidative damage to cytosines in duplex DNA. *Proceedings of the National Academy of Sciences of the United States of America* **2004**, 101, (52), 17914-17919.

49. Li, T. T. T.; Weaver, M. J., Intramolecular Electron-Transfer at Metal-Surfaces .4. Dependence of Tunneling Probability Upon Donor-Acceptor Separation Distance. *Journal of the American Chemical Society* **1984**, 106, (20), 6107-6108.

50. Chidsey, C. E. D.; Bertozzi, C. R.; Putvinski, T. M.; Mujisce, A. M., Coadsorption of Ferrocene-Terminated and Unsubstituted Alkanethiols on Gold - Electroactive Self-Assembled Monolayers. *Journal of the American Chemical Society* **1990**, 112, (11), 4301-4306.

51. Finklea, H. O.; Hanshew, D. D., Electron-Transfer Kinetics in Organized Thiol Monolayers with Attached Pentaammine(Pyridine)Ruthenium Redox Centers. *Journal of the American Chemical Society* **1992**, 114, (9), 3173-3181.

52. Weber, K.; Creager, S. E., Voltammetry of Redox-Active Groups Irreversibly Adsorbed onto Electrodes - Treatment Using the Marcus Relation between Rate and Overpotential. *Analytical Chemistry* **1994**, 66, (19), 3164-3172.

53. Sachs, S. B.; Dudek, S. P.; Hsung, R. P.; Sita, L. R.; Smalley, J. F.; Newton, M. D.; Feldberg, S. W.; Chidsey, C. E. D., Rates of interfacial electron transfer through pi-conjugated spacers. *Journal of the American Chemical Society* **1997**, 119, (43), 10563-10564.

54. Kelley, S. O.; Jackson, N. M.; Hill, M. G.; Barton, J. K., Long-range electron transfer through DNA films. *Angewandte Chemie-International Edition* **1999**, 38, (7), 941-945.

55. Sam, M.; Boon, E. M.; Barton, J. K.; Hill, M. G.; Spain, E. M., Morphology of 15-mer duplexes tethered to Au(111) probed using scanning probe microscopy. *Langmuir*

2001, 17, (19), 5727-5730.

56. Bradley, D. F.; Stellwag, N.; Paulson, C. M.; Okonski, C. T., Electric Birefringence and Dichroism of Acridine-Orange and Methylene-Blue Complexes with Polynucleotides. *Biopolymers* **1972**, 11, (3), 645.

57. Norden, B.; Tjerneld, F., Structure of Methylene-Blue DNA Complexes Studied by Linear and Circular-Dichroism Spectroscopy. *Biopolymers* **1982**, 21, (9), 1713-1734.

58. Tuite, E.; Norden, B., Sequence-Specific Interactions of Methylene-Blue with Polynucleotides and DNA - a Spectroscopic Study. *Journal of the American Chemical Society* **1994**, 116, (17), 7548-7556.

59. Tuite, E.; Kelly, J. M., The Interaction of Methylene-Blue, Azure-B, and Thionine with DNA - Formation of Complexes with Polynucleotides and Mononucleotides as Model Systems. *Biopolymers* **1995**, 35, (5), 419-433.

60. Chen, Y. Z.; Zhang, Y. L., Calculation of the binding affinity of the anticancer drug daunomycin to DNA by a statistical mechanics approach. *Physical Review E* **1997**, 55, (6), 7390-7395.

61. Kelley, S. O.; Boon, E. M.; Barton, J. K.; Jackson, N. M.; Hill, M. G., Single-base mismatch detection based on charge transduction through DNA. *Nucl. Acids Res.* **1999**, 27, (24), 4830-4837.

62. Wang, A. H. J.; Gao, Y. G.; Liaw, Y. C.; Li, Y. K., Formaldehyde Cross-Links Daunorubicin and DNA Efficiently - Hplc and X-Ray-Diffraction Studies. *Biochemistry* **1991**, 30, (16), 3812-3815.

63. Leng, F. F.; Savkur, R.; Fokt, I.; Przewloka, T.; Priebe, W.; Chaires, J. B., Base specific and regioselective chemical cross-linking of daunorubicin to DNA. *Journal of the American Chemical Society* **1996**, 118, (20), 4731-4738.

64. Boon, E. M.; Ceres, D. M.; Drummond, T. G.; Hill, M. G.; Barton, J. K., Mutation detection by electrocatalysis at DNA-modified electrodes. *Nature Biotechnology* **2000**, 18, (10), 1096-1100.

65. Drummond, T. G.; Hill, M. G.; Barton, J. K., Electron Transfer Rates in DNA Films as a Function of Tether Length. *J. Am. Chem. Soc.* **2004**, 126, (46), 15010-15011.

66. Boon, E. M.; Jackson, N. M.; Wightman, M. D.; Kelley, S. O.; Hill, M. G.; Barton, J.

K., Intercalative stacking: A critical feature of DNA charge-transport electrochemistry. *Journal of Physical Chemistry B* **2003**, 107, (42), 11805-11812.

67. Gurr, E., *Synthetic Dyes in Biology, Medicine and Chemistry*. Academic Press: London, England, 1971.

68. Lillie, R. D., *Conn's Biological Stains*. Williams & Wilkins: Baltimore, MD., 1977.

CHAPTER 2

DNA Electrochemistry through the Base Pairs Not the Sugar-phosphate Backbone

Adapted from Liu, T. and Barton, J. K. *Journal of the American Chemical Society* **2005**,
127, 10160.

2.1 INTRODUCTION

Charge transport (CT) mediated by double helical DNA has now been demonstrated in a variety of contexts, ranging from spectroscopic assays to electrochemical sensors and biochemical experiments.¹⁻⁴ Mechanistic studies of DNA CT have focused on photoinduced hole transport experiments to measure oxidative DNA damage and have led to models involving incoherent transport through delocalized or partially localized domains of the DNA duplex.⁵⁻⁹ Our mechanistic understanding of ground state transport through DNA films is less developed,¹⁰ but both in transport experiments in films¹¹⁻¹³ and photoinduced reactions in solution,^{14, 15} it is clear that the integrity of base pair stacking is critical; small perturbations in base stacking can lead to a significant loss in CT efficiency. The role of the sugar-phosphate backbone in DNA CT has been less clear. Recent polaron models for DNA CT that depend upon ion polarization effects in the surrounding medium underscore the need to explore how changes in the sugar-phosphate backbone affect CT.¹⁶⁻¹⁸ Here we therefore compare directly the effects on ground state CT of perturbations in DNA duplex base pair stacking in comparison to breaks in the sugar-phosphate backbone.

Electrochemistry has been used extensively to examine the kinetics of electron transfer in self-assembled monolayers.¹⁹⁻²¹ We have developed methodology to assemble DNA duplexes onto gold surfaces with alkane thiols as linkers.¹¹⁻¹³ These films have been characterized through methods including AFM, STM, and radioactive tagging.²²⁻²⁴ These DNA-modified electrodes are valuable in probing DNA mismatches, lesions, as well as protein/DNA interactions and reactions.^{11-13, 25} Daunomycin (DM), an intercalator that can covalently crosslink to guanine residues,²⁶⁻²⁸ has been used commonly as the

site-specific redox reporter; indeed an intercalating probe is essential to monitor a DNA-mediated reaction in the films.²⁹ In our previous studies, the electrochemical response of DM showed no dependence on its position in the DNA duplex, but a well-behaved sensitivity to the length of the intervening alkane-thiol linker.¹⁰⁻¹³

Here in DNA films containing covalent DM, we compare CT with breaks in the sugar-phosphate backbone versus CT with an intervening DNA mismatch. We have constructed a series of DM-labeled DNA assemblies: a Watson-Crick base paired DNA duplex (**TA**), a duplex with a nick in the backbone (**TA-n**), a duplex containing both a nick and a CA mismatch (**CA-n**), and a duplex containing perfectly matched DNA with a nick on both strands (**TA-n2**) (Figure 2.1.). These duplexes each contain two attachment sites for DM and are 30 base pairs in length. Thus with DM bound and the DNA-modified electrode assembled, the CT distance through DNA of 82 Å (to the first DM) is significantly longer than in previous studies (45 Å)¹¹⁻¹³ and comparable to the longer distances in photoinduced CT experiments.^{30, 31}

2.2 MATERIALS AND METHODS

2.2.1 Materials

All reagents for DNA synthesis were obtained from Glen research. Daunomycin, mercaptohexanol (MCH) were purchased from Fluka in the highest available purity. All buffers were prepared with Milli-Q water and filtered with a sterile 0.2 µM filter.

2.2.2 Synthesis of thiol-terminated oligonucleotides

The synthesis of thiol-terminated oligonucleotides (DNA-5'-SH) employed

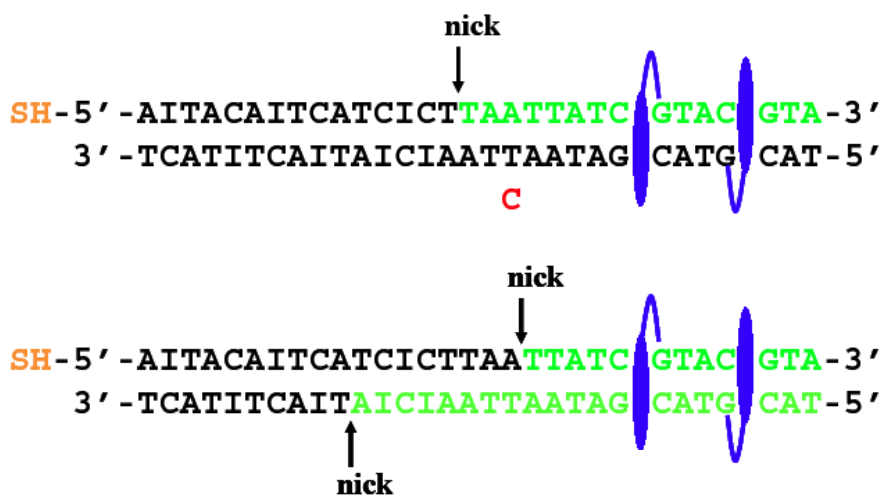
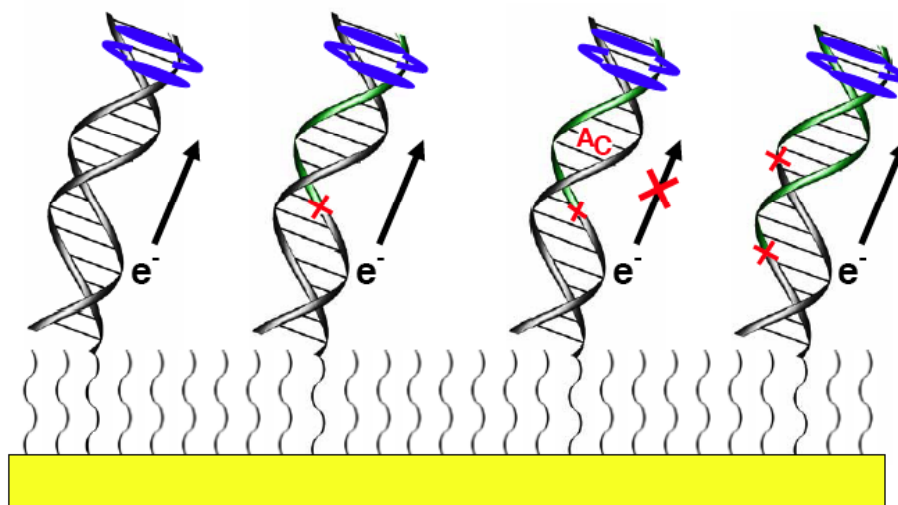


Figure 2.1. Schematic representation of the different DNA-DM adducts on the gold electrode (left to right): **TA**, the intact, well matched 30mer duplex; **TA-n**, the 30mer containing a single nick; **CA-n**, the nicked 30mer containing a CA mismatch; and **TA-n2** the 30mer containing a nick on both strands. The position of the nick is indicated by the arrow. Also shown is the sequence of the duplexes. The tether used is HS-CH₂CH₂-CONH(CH₂)₆NHCO-5'-DNA. The CA mismatch is indicated in red. Each duplex also contains two DM adducts; likely binding sites are indicated (blue).

follows a protocol that was developed by adaptation of a literature procedure.³² A schematic illustration of the synthesis is shown in Figure 2.2. Oligonucleotides were synthesized by standard solid phase phosphoramidite techniques with an ABI 392 model DNA/RNA synthesizer. Prior to being detached from the controlled pore glass (CPG) resin (Glen Research), the oligonucleotides were treated with carbonyl diimidazole (CDI, Fluka) and 1,6-diaminohexane (Aldrich) successively to couple the 5'-terminal ribose sugar to the hexylamine via amide bond formation which introduced a primary amine group to the 5'-terminus of the oligonucleotides (DNA-5'-NH₂).

The DNA-5'-NH₂ was cleaved from CPG and the cyanoethyl protecting groups were removed by heating in concentrated ammonium hydroxide at 60°C for 10 to 12 hours. The DNA-5'-NH₂ product was then cooled and evaporated to dryness *in vacuo*. This product is purified by reverse phase HPLC on a C-18 300 Å column with a gradient of 3.7%-13% acetonitrile in 25 minutes 13%-50% acetonitrile in 40 minutes, with 50 mM NH₄OAc, pH 7 as the aqueous phase (monitored at 260 and 290 nm). The purified oligonucleotides were treated with 2-pyridyldithiopropionic acid N-succinimide ester (PDSP, Pierce) to produce a disulfide containing tether. After another HPLC purification (analogously to DNA-5'-NH₂), the disulfide bond was cleaved by treatment with dithiothreitol (DTT, ICN Pharmocopia) to produce the free thiol (DNA-SH). After the third HPLC purification, the derivative oligonucleotides were characterized by Electrospray Ionization mass spectrometry (ESI-MS).

The non-thiolated strands were synthesized by standard techniques and purified by reverse phase HPLC (same condition as described previously). The purified oligonucleotides were dissolved in 50mM, pH 7.1 sodium phosphate buffer. The

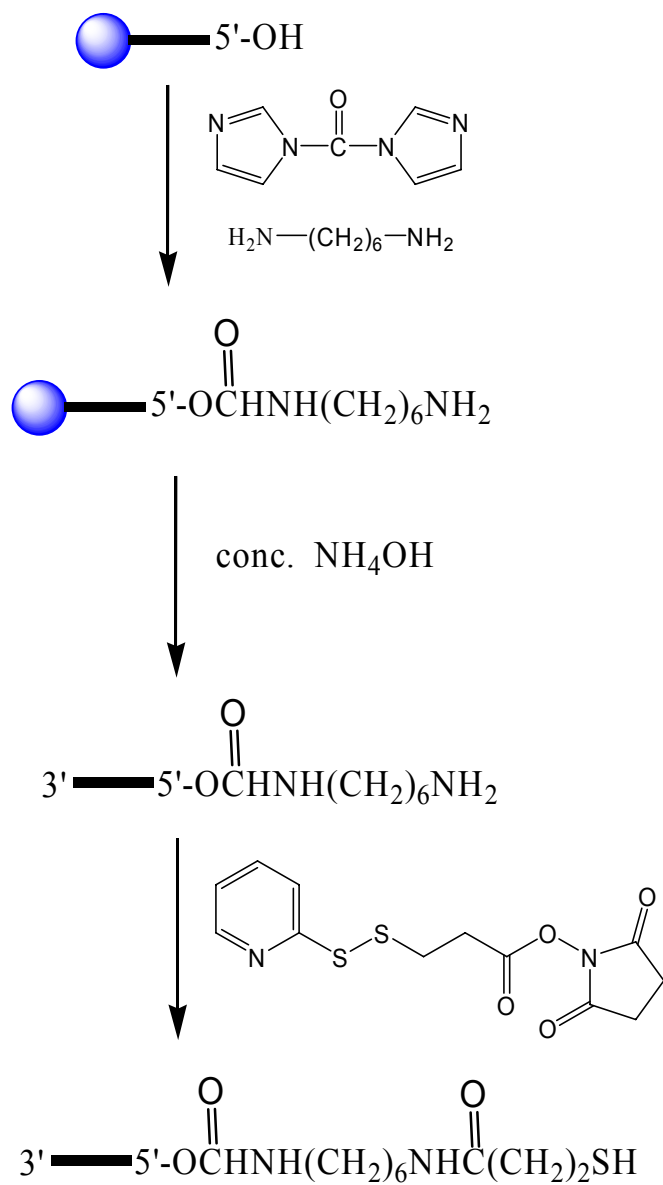


Figure 2.2. Synthesis of a thiol-modified oligonucleotide.

concentration of each oligonucleotide solution was quantified by UV-Vis spectroscopy ($\lambda_{\text{max}} = 260 \text{ nm}$, $\epsilon \text{ (M}^{-1}\cdot\text{cm}^{-1}\text{)}$). The extinction coefficients of single strands were calculated by OligoAnalyzer 3.0 provided by Integrated DNA Technologies.³³

2.2.3 Synthesis of DNA-daunomycin conjugates

A schematic representation of DNA-DM conjugate is showed in Figure 2.3. Equimolar amounts of thiol-modified DNA and the appropriate corresponding strand were mixed in 50 mM sodium phosphate, pH 7.1 for a final solution of 100 μM duplex. This solution was degassed and blanketed with argon, heated to 90 $^{\circ}\text{C}$ for 5 minutes and then cooled slowly to 20 $^{\circ}\text{C}$ in 90 minutes. The resulting duplexes were incubated with 0.4 mM DM and 0.05% formaldehyde at pH 7.1 at room temperature for 5-6 hours. Excess DM was removed by extraction with chloroform. The stoichiometry of the cross-linking reaction was assayed by comparing the absorbance of DM at 480nm before and after extraction ($\epsilon_{480\text{nm}} = 7.5 \times 10^3 \text{ M}^{-1}\cdot\text{cm}^{-1}$). As expected given two 5'-CG-3' sites for crosslinking, the stoichiometry determined by UV-visible absorption reveals consistently a DNA : DM ratio of 1 : 2.

2.2.4 Preparation of DNA-modified electrodes

Bulk gold electrodes were polished sequentially by 1.0 μm , 0.3 μm , and 0.05 μm alumina and etched in 1.0 M H_2SO_4 by cyclic voltammetry from +1625 mV to -200 mV (vs. Ag/AgCl). The synthesized DNA-DM adducts (50 μM) are then self-assembled overnight on the prepared gold electrodes in 50 mM sodium phosphate, pH 7.1, with subsequent backfilling using 1 mM mercaptohexanol (MCH) for 5 minutes. The surface

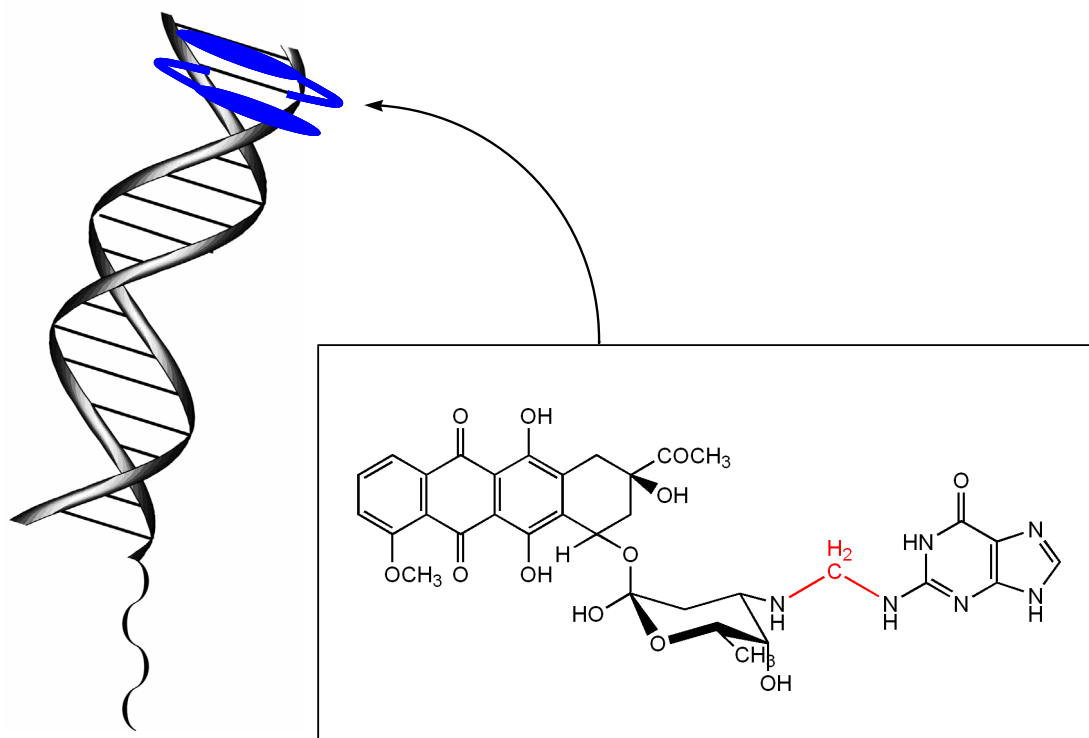


Figure 2.3. Schematic representation of a DNA-daunomycin conjugate. The linkage between daunomycin and guanine is highlighted in red.

coverage of DNA-DM ranges from 3 to 5 pmol/cm² on these films as determined both by ruthenium hexammine assay³⁴ and by integration of the DM reduction (at pH > ~7.0, each DM undergoes a 1 e⁻ reduction).

2.2.5 Electrochemical measurements

Cyclic voltammetry (CV) and square wave voltammetry (SWV) experiments were carried out on a BAS CV50W model electrochemical analyzer. Experiments were conducted in 50 mM sodium phosphate, pH 7.1 at room temperature under argon. A two-compartment cell was used with a Pt wire as auxiliary electrode, and saturated calomel electrode (SCE) as reference. The surface area of the gold working electrode was 0.02-0.03 cm².

2.3 RESULTS AND DISCUSSION

We constructed four types of DNA duplexes: a Watson-Crick base paired DNA duplex (**TA**), a duplex with a nick in the backbone (**TA-n**), a duplex containing both a nick and a CA mismatch (**CA-n**), and a duplex containing well matched DNA with a nick on both strands (**TA-n2**). The sequence of the duplexes is shown in Table 2.1. Duplex containing one nick (**TA-n**) in the phosphate backbone was made by annealing a 30mer strand to a 5'-thiolated 15mer strand (DNA-5'-SH) and an unmodified 15mer strand (DNA-5'-OH). To make the duplex containing two nicks (**TA-n2**) in the backbone, two sticky-ended DNA duplexes were annealed to each other through 8-base overhang on each duplex. These duplexes were then covalently coupled with DM by the method described before. The resulting DNA-DM adducts were self-assembled into monolayers

Table 2.1. DNA sequences *

TA	5' -AITACAITCATCICCTTAATTATCGTACGTA-3' † 3' -TCATITCAITAICIAATTAATAGCATGCAT-5'
TA-n	5' -AITACAITCATCICCT TAATTATCGTACGTA -3' 3' -TCATITCAITAICIAATTAATAGCATGCAT-5'
CA-n	<div style="text-align: center;">↓</div> 5' -AITACAITCATCICCT TAATTATCGTACGTA -3' 3' -TCATITCAITAICIAAT CA ATAGCATGCAT-5'
TA-n2	<div style="text-align: center;">↓</div> 5' -AITACAITCATCICCT TAATTATCGTACGTA -3' 3' -TCATITCAIT AICIAATTAATAGCATGCAT -5' <div style="text-align: center;">↑</div>

* The position of the CA mismatch is highlighted in bold and italics. The arrows indicate the positions of nicks, and the strand above the nicks is highlighted in green.

† “I” stands for inosine.

on gold electrodes and backfilled with 1mM mercaptohexanol for 5min. The backfilling process is necessary to remove nonspecifically absorbed DNA duplexes on the electrode surface.¹³ These DNA-modified electrodes were then investigated by cyclic voltammetry and square wave voltammetry. DNA mediated CT events were monitored by the reduction signal of DM.¹¹

As is evident in Figure 2.4, remarkably efficient reduction of DM is observed for the well matched duplexes, either with an intact sugar-phosphate backbone or with a backbone containing one or even two nicks. The DM reduction intensities are equivalent, and potentials vary by <15 mV. In contrast, with the CA mismatch, the intensity of DM reduction is diminished.^{11, 12} Integration of the charge (by integrating the cathodic peak current in CV) confirms that there is no significant difference in reduction efficiency between the intact, well matched duplex and the matched DNA with nick(s). The single base CA mismatch, however, significantly attenuates DM reduction.

We can also estimate the electron transfer rates through analysis of the characteristic splittings of anodic and cathodic peaks as a function of scan rate.^{35, 36} Earlier studies, where the alkane linker length was varied, showed tunneling through the linker to be rate limiting, with no apparent variation in rate with change in DM position within a 15mer duplex.^{10, 11} Here we estimate a rate of 30 s^{-1} for the intact 30mer duplex, equivalent to that measured earlier for the 15mer. Importantly, the estimated rates are also essentially the same for **TA**, **TA-n** and **TA-n2** (Figure 2.5). For the **CA-n** duplex, the peaks are too small for an accurate measurement of the rate. Clearly, perturbations in the sugar-phosphate backbone do not substantially affect the electron transfer rate. Note that a single nick corresponds to a local decrease in formal negative charge (0 for two

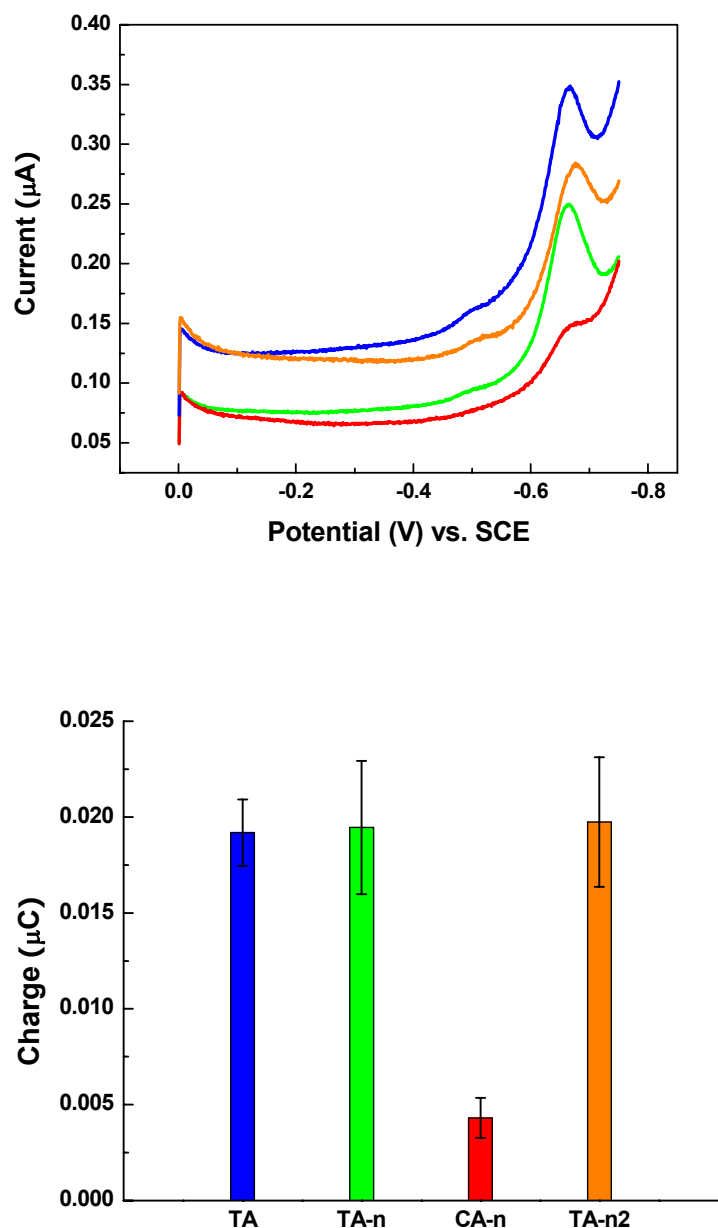


Figure 2.4. DM reduction of TA, TA-n, CA-n, and TA-n2 duplex films in 50 mM sodium phosphate, pH 7.1. Square wave voltammograms of DNA-DM films (top) and the quantification of charge integration from cyclic voltammetry (bottom) show that the intact matched duplex (blue), duplex with one nick (green), and duplex with two nicks (orange) lead to a similar yield of DM reduction. The incorporation of a CA mismatch (red), however, significantly attenuates the intensity of the reduction response. Potentials are given versus SCE. At least five electrodes were measured with each DNA assembly. For square wave voltammetry, step height = 0.001 V, pulse amplitude = 0.01 V, and frequency = 15 Hz.

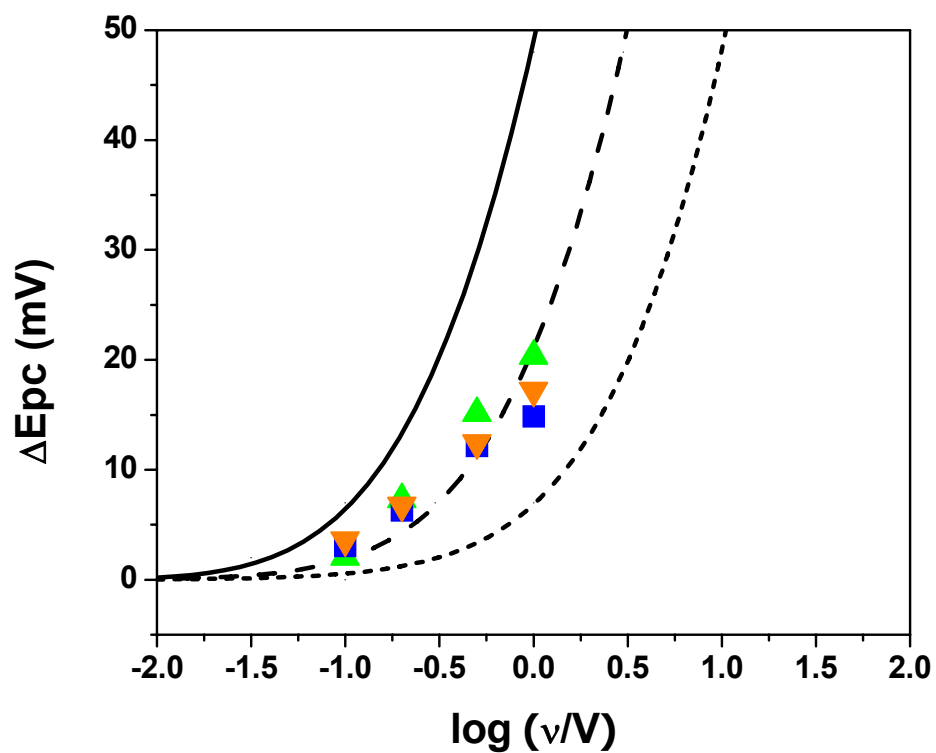


Figure 2.5. Plot of peak splitting ΔE_{pc} (where $\Delta E_{pc} = E_{pc} - E^\circ$) versus $\log(v)$ (where $v = \text{scan rate}$) for the intact **TA** duplex (blue square) from cyclic voltammetry, **TA-n** duplex with one nick (green triangle), and **TA-n2** duplex with two nicks (orange triangle). Simulated curves corresponding to rate constants of 10 s^{-1} (—), 30 s^{-1} (- - -), and 100 s^{-1} (· · ·) are shown for comparison.³⁶

terminal hydroxyls versus -1 for the phosphodiester linkage). One might have expected that if CT depends upon the ion polarization in the medium surrounding the DNA, some effect of this change in localized charge would have been seen.

These results demonstrate that in these electrochemical studies, as in solution, the pathway for DNA mediated charge transfer is necessarily through the base pair stack, not the sugar-phosphate backbone. No effect of the change in localized charge or the loss of integrity of the backbone are apparent, yet, as in solution, exquisite sensitivity to base pair stacking is seen. Mechanistic descriptions of CT in DNA films must take into account these results, and applications in DNA sensor development may exploit these findings.

2.4 SUMMARY

Using intercalated, covalently bound daunomycin as a redox probe, we have examined ground state charge transport in DNA films with a perturbation in base pair stacking in comparison with breaks in the sugar-phosphate backbone. While the introduction of one or even two nicks in the sugar-phosphate backbone yields no detectable effect on electron transfer, a CA mismatch significantly attenuates the electron transfer yield. These results confirm that the base pair stack is the pathway for DNA mediated charge transfer, not the sugar-phosphate backbone.

2.5 REFERENCES

1. Murphy, C. J.; Arkin, M. R.; Jenkins, Y.; Ghatlia, N. D.; Bossmann, S. H.; Turro, N. J.; Barton, J. K., Long-Range Photoinduced Electron-Transfer through a DNA Helix. *Science* **1993**, 262, (5136), 1025-1029.
2. Kelley, S. O.; Barton, J. K., Electron transfer between bases in double helical DNA. *Science* **1999**, 283, (5400), 375-381.
3. Delaney, S.; Barton, J. K., Long-range DNA charge transport. *Journal of Organic Chemistry* **2003**, 68, (17), 6475-6483.
4. Drummond, T. G.; Hill, M. G.; Barton, J. K., Electrochemical DNA sensors. *Nature Biotechnology* **2003**, 21, (10), 1192-1199.
5. Bixon, M.; Giese, B.; Wessely, S.; Langenbacher, T.; Michel-Beyerle, M. E.; Jortner, J., Long-range charge hopping in DNA. *Proceedings of the National Academy of Sciences of the United States of America* **1999**, 96, (21), 11713-11716.
6. Giese, B.; Amaudrut, J.; Kohler, A. K.; Spormann, M.; Wessely, S., Direct observation of hole transfer through DNA by hopping between adenine bases and by tunnelling. *Nature* **2001**, 412, (6844), 318-320.
7. Schuster, G. B., Long-range charge transfer in DNA: Transient structural distortions control the distance dependence. *Accounts of Chemical Research* **2000**, 33, (4), 253-260.
8. O'Neill, M. A.; Barton, J. K., DNA-mediated charge transport requires conformational motion of the DNA bases: Elimination of charge transport in rigid glasses at 77 K. *Journal of the American Chemical Society* **2004**, 126, (41), 13234-13235.
9. Shao, F. W.; O'Neill, M. A.; Barton, J. K., Long-range oxidative damage to cytosines in duplex DNA. *Proceedings of the National Academy of Sciences of the United States of America* **2004**, 101, (52), 17914-17919.
10. Drummond, T. G.; Hill, M. G.; Barton, J. K., Electron transfer rates in DNA films as a function of tether length. *Journal of the American Chemical Society* **2004**, 126, (46), 15010-15011.
11. Kelley, S. O.; Jackson, N. M.; Hill, M. G.; Barton, J. K., Long-range electron transfer through DNA films. *Angewandte Chemie-International Edition* **1999**, 38, (7), 941-945.

12. Boon, E. M.; Ceres, D. M.; Drummond, T. G.; Hill, M. G.; Barton, J. K., Mutation detection by electrocatalysis at DNA-modified electrodes. *Nature Biotechnology* **2000**, *18*, (10), 1096-1100.
13. Boon, E. M.; Salas, J. E.; Barton, J. K., An electrical probe of protein-DNA interactions on DNA-modified surfaces. *Nature Biotechnology* **2002**, *20*, (3), 282-286.
14. Bhattacharya, P. K.; Barton, J. K., Influence of intervening mismatches on long-range guanine oxidation in DNA duplexes. *Journal of the American Chemical Society* **2001**, *123*, (36), 8649-8656.
15. Kelley, S. O.; Holmlin, R. E.; Stemp, E. D. A.; Barton, J. K., Photoinduced electron transfer in ethidium-modified DNA duplexes: Dependence on distance and base stacking. *Journal of the American Chemical Society* **1997**, *119*, (41), 9861-9870.
16. Henderson, P. T.; Jones, D.; Hampikian, G.; Kan, Y. Z.; Schuster, G. B., Long-distance charge transport in duplex DNA: The phonon-assisted polaron-like hopping mechanism. *Proceedings of the National Academy of Sciences of the United States of America* **1999**, *96*, (15), 8353-8358.
17. Barnett, R. N.; Cleveland, C. L.; Joy, A.; Landman, U.; Schuster, G. B., Charge migration in DNA: Ion-gated transport. *Science* **2001**, *294*, (5542), 567-571.
18. Conwell, E. M.; Rakhmanova, S. V., Polarons in DNA. *Proceedings of the National Academy of Sciences of the United States of America* **2000**, *97*, (9), 4556-4560.
19. Finklea, H. O., Electrochemistry of organized monolayers of thiols and related molecules on electrodes. In *Electroanalytical Chemistry: a Series of Advances, Vol 19*, 1996, pp 109-335.
20. Sachs, S. B.; Dudek, S. P.; Hsung, R. P.; Sita, L. R.; Smalley, J. F.; Newton, M. D.; Feldberg, S. W.; Chidsey, C. E. D., Rates of interfacial electron transfer through pi-conjugated spacers. *Journal of the American Chemical Society* **1997**, *119*, (43), 10563-10564.
21. Munge, B.; Das, S. K.; Ilagan, R.; Pendon, Z.; Yang, J.; Frank, H. A.; Rusling, J. F., Electron transfer reactions of redox cofactors in spinach Photosystem I reaction center protein in lipid films on electrodes. *Journal of the American Chemical Society* **2003**, *125*, (41), 12457-12463.
22. Kelley, S. O.; Barton, J. K.; Jackson, N. M.; Hill, M. G., Electrochemistry of

methylene blue bound to a DNA-modified electrode. *Bioconjugate Chemistry* **1997**, 8, (1), 31-37.

23. Kelley, S. O.; Barton, J. K.; Jackson, N. M.; McPherson, L. D.; Potter, A. B.; Spain, E. M.; Allen, M. J.; Hill, M. G., Orienting DNA helices on gold using applied electric fields. *Langmuir* **1998**, 14, (24), 6781-6784.

24. Ceres, D. M.; Barton, J. K., In situ scanning tunneling microscopy of DNA-modified gold surfaces: Bias and mismatch dependence. *Journal of the American Chemical Society* **2003**, 125, (49), 14964-14965.

25. Boal, A. K.; Barton, J. K., Electrochemical detection of lesions in DNA. *Bioconjugate Chemistry* **2005**, 16, (2), 312-321.

26. Arcamone, F., *Doxorubicin: Anticancer Antibiotics*. Academic Press: New York, 1981.

27. Leng, F.; Savkur, R.; Fokt, I.; Przewloka, T.; Priebe, W.; Chaires, J. B., Base Specific and Regioselective Chemical Cross-Linking of Daunorubicin to DNA. *Journal of the American Chemical Society* **1996**, 118, (20), 4731-4738.

28. Wang, A. H. J.; Gao, Y. G.; Liaw, Y. C.; Li, Y. K., Formaldehyde Cross-Links Daunorubicin and DNA Efficiently - Hplc and X-Ray-Diffraction Studies. *Biochemistry* **1991**, 30, (16), 3812-3815.

29. Boon, E. M.; Jackson, N. M.; Wightman, M. D.; Kelley, S. O.; Hill, M. G.; Barton, J. K., Intercalative stacking: A critical feature of DNA charge-transport electrochemistry. *Journal of Physical Chemistry B* **2003**, 107, (42), 11805-11812.

30. Nunez, M. E.; Hall, D. B.; Barton, J. K., Long-range oxidative damage to DNA: effects of distance and sequence. *Chemistry & Biology* **1999**, 6, (2), 85-97.

31. Hall, D. B.; Holmlin, R. E.; Barton, J. K., Oxidative DNA damage through long-range electron transfer. *Nature* **1996**, 382, (6593), 731-735.

32. Harrison, J. G.; Balasubramanian, S., A convenient synthetic route to oligonucleotide conjugates. *Bioorganic & Medicinal Chemistry Letters* **1997**, 7, (8), 1041-1046.

33. IDT, <http://www.idtdna.com/analyzer/Applications/OligoAnalyzer/>.

34. Steel, A. B.; Herne, T. M.; Tarlov, M. J., Electrochemical quantitation of DNA

immobilized on gold. *Analytical Chemistry* **1998**, 70, (22), 4670-4677.

35. Laviron, E., General Expression of the Linear Potential Sweep Voltammogram in the Case of Diffusionless Electrochemical Systems. *Journal of Electroanalytical Chemistry* **1979**, 101, (1), 19-28.

36. Tender, L.; Carter, M. T.; Murray, R. W., Cyclic Voltammetric Analysis of Ferrocene Alkanethiol Monolayer Electrode-Kinetics Based on Marcus Theory. *Analytical Chemistry* **1994**, 66, (19), 3173-3181.

CHAPTER 3

Electrochemical Studies on Electrodes Modified with DNA Duplexes Containing Base Overhangs: Capturing Duplex DNA Targets

This work was completed in collaboration with Professor Mike Hill in the Chemistry Department at Occidental College.

3.1 INTRODUCTION

3.1.1 Mutation detections by DNA-mediated charge transport

The analysis of nucleic acids has established broad applications in diagnostic testing, genetic studies, and pharmacological research. The enthusiasm for relating certain diseases to specific genes and developing customized drug design stimulated the research on DNA-based biosensors for gene mutation detection,¹ single-nucleotide polymorphisms (SNPs) discovery,²⁻⁴ and investigations of interactions between DNA and ligands such as antitumor drugs and proteins.⁵ The past decade has witnessed the development of a large variety of technologies for the analysis of oligonucleotides, and more specifically, mutation detection. Different strategies include allele-specific hybridization, primer extension, mass spectroscopy, quartz crystal microgravimetry, surface plasmon resonance, restriction-enzyme digestion, and electrochemistry, etc. In spite of their variations in detection methodology, most assays that have been proposed for mutational analysis are based, directly or indirectly, on differential hybridization. In differential hybridization, the mutation is identified by its diminished association to a probe sequence at a defined temperature, as the binding energy of a mutational strand to the single-stranded probe is less than the binding energy of a completely complementary strand. The difference in binding energy results in a difference in melting temperature between a perfect DNA sequence and one with mutations. However, this difference can be very small and can vary based on sequence context, especially for strands with a single base mutation. Therefore, this approach is necessarily limited in sensitivity and can be very complicated as it requires elaborate temperature control.

Numerous studies have shown that DNA can mediate charge transport (CT)

through its π -stack of base pairs. It has been demonstrated, both in solution and in films, that DNA mediated long-range charge transport is exceptionally sensitive to base stacking perturbations such as mismatches and base lesions.⁶⁻¹⁰ In particular, Kelley et al. modified a gold electrode with a film of DNA duplex containing a covalently tethered redox-active intercalator, daunomycin (DM), as the probe of DNA mediated CT chemistry. They found that reduction of daunomycin was accomplished with perfectly matched DNA duplexes, but was shut off in the presence of an intervening CA mismatch.¹⁰ This sensitivity depends upon the electronic coupling within the base pair stack. Other perturbations in the π -stack such as those caused by base lesions can also affect the CT efficiency in DNA films.¹¹ On the other hand, the reduction of daunomycin is independent of its intercalating position in DNA duplex,¹⁰ and nicks in the sugar phosphate backbone of DNA show no effect on charge transport in DNA films either.¹²

The remarkable sensitivity of DNA-mediated charge transport to perturbations in base pair stacking and dynamics provides a unique approach to mutational analysis. This approach exploits differences in electronic coupling within the π -stack to detect mutations, rather than differences in hybridization thermodynamics. The pioneering work by Kelley et al. showed that a duplex containing a single CA mismatch could be well differentiated from a completely matched duplex by the redox response of tethered daunomycin.¹⁰ Because this method is not based on differential hybridization, its sensitivity is no longer limited by differences in melting temperatures. Greatly enhanced sensitivity and selectivity can be achieved by coupling the DNA-mediated reduction of the intercalative redox-active probe to electrocatalytic cycle involving an oxidant in solution that can reoxidize the intercalator.¹³ Indeed, based on this methodology, Boon

et al. successfully detect eight possible single-base DNA mismatches as well as naturally occurring mutational “hot spots” from the p53 gene, using methylene blue (MB) as a probe and ferricyanide ($[\text{Fe}(\text{CN})_6]^{3-}$) as the in-solution oxidant.¹⁴ In addition to mismatches, various base damages can be detected based on DNA mediated charge transport as well.¹¹

In a typical mutational detection assay based on DNA-mediated charge transport, a test strand is annealed to a single-stranded thiol-terminated probe to form a duplex in solution. If a covalently tethered intercalator is used as the redox-active marker, the intercalator is chemically tethered to the 5'-end of the test strand. When applied to the gold electrode, the duplexes are then self-assembled into a monolayer on electrode surface with the redox-active intercalator bound near the top of the film. The reduction of the intercalator is easily monitored electrochemically if the duplex is fully Watson-Crick base paired; the reduction signal diminishes significantly if there is a mismatch in the base pair stack. The disadvantage of this method is that it usually involves tedious sample preparation and electrode modification for each test. The probe strand has to be annealed to a test strand in solution before being immobilized on the electrode. Consequently, electrode modification is time consuming and the modified electrodes are not reusable. Therefore, this assay methodology is not feasible for applications that require fast detection, simple preparation, and little or no sample modifications, and does not permit high throughput detections.

In order to simplify the assay process and make it possible for high throughput detection, we developed a detection strategy that avoids the tedious electrode modification process. A scheme of the strategy is illustrated in Figure 3.1. The gold

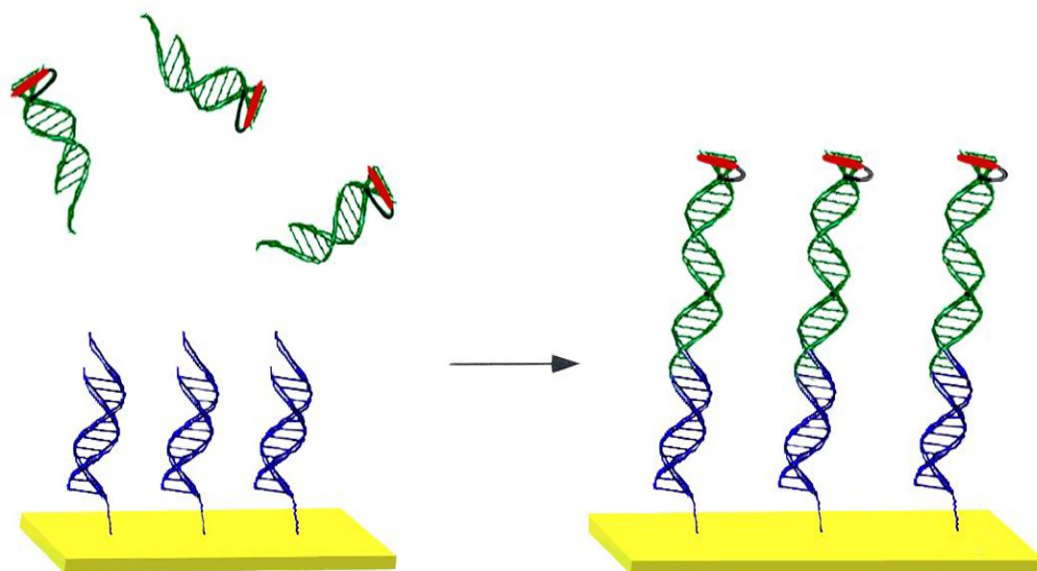


Figure 3.1. Schematic representation of the trapping of double stranded DNA target onto gold electrode. The gold electrode surface was modified with a film of thiolate double stranded DNA probe (blue) which contained an overhang of 6 bases. The modified electrode was then incubated with solution of target duplex (green) containing a 6-base overhanging sequence complementary to that of the probe duplex. As a consequence, the trapping of the target onto the electrode surface is achieved through the annealing of the two complementary overhangs of the target duplex and the probe duplex. Shown in red is the daunomycin molecule that is covalently attached to the blunt end of the target duplex.

electrode surface is modified with a monolayer of double-stranded DNA probe with a 6-base overhang (probe duplex). Another duplex (target duplex), which contains the test strand sequence, has a 6-base overhang at its 3'-end that is complementary to the overhang of the probe duplex. A redox-active intercalator, daunomycin, is covalently tethered to the target duplex near the blunt end. The modified electrode is then exposed to the target duplex solution for *in situ* hybridization of the test duplexes and the probe duplexes through their overhangs. Consequently, a monolayer of a long DNA duplex, which has a nick in sugar-phosphate backbone of each strand, is formed on the electrode. Because the nicks in sugar-phosphate backbone do not affect DNA mediated charge transport,¹² reduction of the tethered daunomycin can be observed electrochemically if the target duplex is completely Watson-Crick base paired; the presence of a mispaired base within the target duplex will significantly diminish the reduction of daunomycin. In this strategy, the thiol-terminated probe strand does not need to be complementary to test strand and the probe duplex is immobilized onto the electrode before being annealed to the target duplex. Therefore, the electrode is reusable and the target duplex can be easily removed by dehybridization. This strategy also makes high throughput detection possible as multiple targets can be addressed to the corresponding probes by simply changing the overhangs of probes.

3.1.2 Surface hybridization of DNA

Obviously, reliable hybridization of the target duplex and the probe duplex on the electrode surface is critical for this mismatch detection strategy. Although extensive studies have been reported on *in situ* hybridization of single stranded DNA on

surfaces,¹⁵⁻²⁴ little is known about surface hybridization of DNA duplexes with overhangs. Experiments on single stranded DNA reveal that the hybridization process on surfaces is very complicated and several factors are involved. The surface immobilization of probe strand leads to hybridization kinetics that is significantly altered from those found in bulk solution. In particular, the observed rates and efficiency (i.e., percentage of probes on surface that are hybridized) depend on factors such as probe density,^{16, 25-27} probe length,^{19, 28} location of the complementary sequence on the probe,^{15, 17} and rates of diffusion from bulk solution.^{25, 29} The combination of these factors makes it hard to optimize the hybridization conditions and sometimes leads to contradictory conclusions regarding experimental results.

In spite of its complexity, there are still some general rules about DNA hybridization on surfaces. For instance, because of steric effect and electrostatic repulsion force, longer probes usually lead to slower hybridization rates.¹⁹ For the same reason, hybridization rates are affected by probe density.²⁷ When the probe density is low, the steric effect is negligible and hybridization rate is proportional to the coverage of probes on surface. When the probe density is very high, both the steric effect and the electrostatic repulsions between oligonucleotides are very significant. In this case, the hybridization rate can be very slow. Temperature and ionic strength also affect the surface hybridization of DNA.²⁰ Raising the temperature usually weakens the interaction between the immobilized probes and the surface, and diminishes the nonspecific absorptions of oligonucleotides onto the surface. It also helps DNA strands to overcome the energy barrier and facilitates hybridization. Cations (such as Na⁺, K⁺, and Mg²⁺) in solution can significantly reduce the electrostatic repulsions between the polyanionic

oligonucleotides.²⁰ Hybridization rate and efficiency are remarkably higher in DNA solutions of high salt concentration.¹⁶ Although these rules are discovered in experiments with single stranded DNA, they may be applied to the DNA duplex with an overhang, because of their intrinsic polyanionic nature. One distinct difference between single stranded DNA and double stranded DNA, however, is that the nonspecific interactions between single stranded DNA and the gold surface are much more significant than that between double stranded DNA and the gold surface. Therefore, the surface hybridization of the DNA duplex with an overhang should be more efficient, as nonspecific interactions can significantly deter surface hybridization of single stranded DNA.^{27, 30}

Here we demonstrate the feasibility of the strategy of trapping duplex DNA with an overhang on an electrode and detecting an intervening CA mismatch. We modify a gold electrode with a probe duplex with a 6-base overhang, and study the *in situ* hybridization of a target duplex with a complementary 6-base overhang on the modified electrode. The temperature dependence of the reduction of an intercalating daunomycin in the target duplex is investigated. We also explore the reusability of the probed duplex-modified electrode. These studies will hopefully lead to the development of a sensitive, label-free mutational detection method with reusable electrodes based on DNA-mediated charge transport.

3.2 MATERIALS AND METHODS

3.2.1 Materials

DNA synthesis reagents were purchased from Glen research. Daunomycin, ruthenium hexamine chloride ($[\text{Ru}(\text{NH}_3)_6]\text{Cl}_3$), and reagents used in the synthesis of

thiol-terminated DNA were purchased from Fluka in the highest available purity. All buffers were prepared with Milli-Q water and filtered with a sterile 0.2 μm filter.

3.2.2 Oligonucleotides synthesis

The sequences of the oligonucleotides used in the experiments are listed in Table 3.1. Oligonucleotides were prepared using standard phosphoramidite synthesis on ABI 392 model DNA synthesizer. Oligonucleotide composition was verified by mass spectrometry. Thiol-modified strands were prepared using the synthesis method we have described previously in Chapter 2. Briefly, thiol-terminated linkers were attached to single-stranded oligonucleotides by CDI, diamine linker and PDSP, purified by reversed-phase HPLC, and hybridized to unmodified complements to form the probe duplex. The synthesis of the target duplex with covalently tethered daunomycin is similar to the process that has been previously described in Chapter 2. A 20mer single stranded DNA and one equivalent of a 14mer single stranded DNA were annealed in the thermocycler to form the target duplex containing a 6-base overhang. Because daunomycin crosslinks to guanine residues in a DNA duplex in the presence of formaldehyde, guanines in the target duplex were substituted by inosines during the oligonucleotide synthesis except for the GG at the site of crosslinking. The target duplex (0.1 mM) was incubated with daunomycin (0.2 mM) in the presence of 0.05% formaldehyde in 50 mM sodium phosphate, pH 7.1, at room temperature for 5 hours. Excess daunomycin was then removed by extractions with chloroform until the organic layer was colorless. The concentration of DNA solution and the stoichiometry of DNA-daunomycin conjugation were determined by UV-vis absorption spectroscopy. The

Table 3.1. DNA sequences*

Strand	Sequence
P1	HS-5' -GCCATCCTGCGTGGTG' -3' 3' -CGGTAGGACG-5'
P2	HS-5' -GCC <i>A</i> TCCTGCGTGGTG' -3' 3' -CGG <i>C</i> AGGACG-5'
T1	5' - TCATCTATACT <u>CCA</u> -3' 3' -CACCACAITAIATATIAGGT-5'
T2	5' - TCA <i>C</i> CTATACT <u>CCA</u> -3' 3' -CACCACAIT <i>A</i> IATATIAGGT-5'

*The position of the CA mismatch is highlighted in bold and italics. "I" stands for inosine. The cross-linking site for daunomycin is underscored. Only one daunomycin molecule crosslinks to the double GG site in each **T1** (or **T2**) duplex because of the steric limitation.

extinction coefficient of DNA ($\lambda_{\max} = 260 \text{ nm}$, $\epsilon(\text{M}^{-1}\cdot\text{cm}^{-1})$) was calculated by OligoAnalyzer 3.0 provided by IDT. The ratio of daunomycin and DNA after extraction was 1:1 according to the UV-vis absorption measurement (For intercalated daunomycin, $\lambda_{\max} = 480 \text{ nm}$, $\epsilon = 7.5 \times 10^3 \text{ M}^{-1}\cdot\text{cm}^{-1}$).

3.2.3 Preparation of DNA-modified electrodes

Polycrystalline gold electrodes (BAS) were polished sequentially with 1.0 μm , 0.3 μm , and 0.05 μm alumina and were etched in 1.0 M H_2SO_4 by cyclic voltammetry from +1625 mV to -200 mV (vs. Ag/AgCl). The probe duplexes (0.1 mM) were then deposited on etched electrodes for 12 hours. MgCl_2 (100 mM) was added to the DNA solution prior to deposition to ensure a densely packed film. To anneal the target duplex with the probe duplex on the electrode surface, the probe duplex-modified electrode was incubated with a solution containing 100 μM target duplex, 5 mM sodium phosphate, 50 mM NaCl, 100 mM MgCl_2 for 2 hours at room temperature followed by 1 hour in an ice-water bath.

3.2.4 Electrochemical measurements

Cyclic voltammetry was carried out anaerobically (bubbling with argon) on gold electrodes (0.02~0.03 cm^2) using a Bioanalytical Systems (BAS) Model CV-50W electrochemical analyzer. A normal three-electrode configuration was used, which consisted of a modified gold-disk working electrode, a platinum wire auxiliary electrode, and a saturated calomel reference electrode (SCE, Fisher Scientific). The working compartment of the electrochemical cell was separated from the reference compartment

by a modified Luggin capillary. Electrochemical measurements were carried out at 0 °C by incubating the electrochemical cell in an ice-water bath. For temperature dependence studies, the electrochemical cell was incubated in a refrigerating circulator (Fisher Scientific) at controlled temperatures.

The buffer used for electrochemical measurements was 5 mM sodium phosphate, 50 mM NaCl, pH 7.1 (Echem buffer). All buffers were filtered with sterile 0.2 µm filters prior to use. DNA modified electrodes were rinsed thoroughly in the Echem buffer before the measurements. All potentials here are reported versus SCE.

3.2.5 DNA quantification by ruthenium hexammine

The amount of DNA present on the electrode was measured by cyclic voltammetry with the three-electrode configuration aforementioned. Cyclic voltammetry was carried out in 10 mM Tris buffer (pH 7.4, room temperature) containing 10 µM $[\text{Ru}(\text{NH}_3)_6]^{3+}$ (Q-buffer) under argon at 0 °C. Before each measurement, the DNA-modified electrode was incubated in the Q-buffer for 5 minutes so that the association of $[\text{Ru}(\text{NH}_3)_6]^{3+}$ to DNA reached equilibrium. The amount of $[\text{Ru}(\text{NH}_3)_6]^{3+}$ associated with DNA was calculated from the charge accumulated in the cathodic peak by cyclic voltammetry. The amount of DNA on the electrode surface was derived from the amount of $[\text{Ru}(\text{NH}_3)_6]^{3+}$ assuming that the negative charge of DNA backbone were all compensated by $[\text{Ru}(\text{NH}_3)_6]^{3+}$.³¹

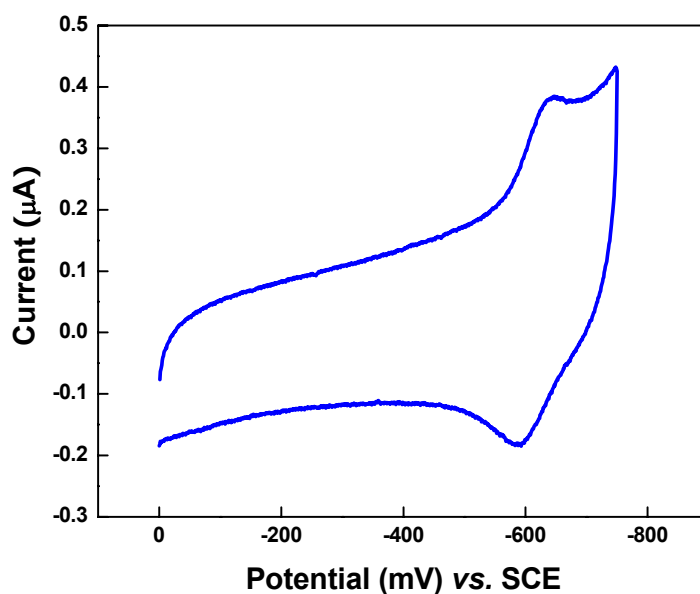
3.3 RESULTS AND DISCUSSION

3.3.1 Hybridization of DNA duplexes with overhangs on electrode

The sequences of DNA duplexes employed in the surface hybridization experiments are shown in Table 3.1. The length of the overhangs is critical to the hybridization kinetics and stability of the duplexes that form on the surface. If the overhang is too short, the hybridization is thermodynamically unfavorable; if the overhang is too long, nonspecific absorptions will be problematic since single stranded DNA has strong nonspecific interactions with gold surfaces. Additionally, increasing GC content also helps to stabilize the DNA duplexes formed. Taking these into account, we select a 6-base overhang which consists of four Gs and two Ts.

In surface hybridization experiments, gold electrodes modified with thiol-terminated probe duplexes (**P1**) are incubated with a solution containing 100 μM target duplex with crosslinked daunomycin (**T1**), 5 mM sodium phosphate, 50 mM NaCl, 100 mM MgCl_2 for 2 hours at room temperature, followed by 1 hour in ice-water bath. It is noteworthy that only one daunomycin molecule crosslinks to the GG site of each target duplex because of the steric limitation. Therefore, the stoichiometry of **T1**/daunomycin is 1:1. The modified electrodes are interrogated by cyclic voltammetry in Echem buffer in an ice-water bath. As shown in Figure 3.2, a distinct reduction peak is observed at around -650 mV, which corresponds to the reduction potential of daunomycin that intercalates to DNA.¹⁰ By varying the scan rate, the cathodic peak current is found to increase in proportion to the change in scan rate (Figure 3.3). This linear relationship between the peak current and the scan rate demonstrates that the redox-active marker is surface bound,³² which indicates that **T1** is immobilized on the electrode surface.

In our previous electrochemical studies on DNA-mediated charge transport, we have found that nicks in the sugar-phosphate do not affect electron transfer efficiency and



(a)



(b)

Figure 3.2. (a) Cyclic voltammogram of **P1** modified gold electrode after trapping of **T1**; scan rate = 100mV/s. The gold electrode was modified with a monolayer of **P1**, followed by incubation with a solution containing 100 μ M **T1**, 5 mM sodium phosphate, 50 mM NaCl and 100 mM MgCl₂, pH 7.1, for 3 hours. The cyclic voltammetry was carried out in Echem buffer (5mM phosphate, 50mM NaCl, pH 7.1) under argon. (b) The sequence of **P1** (blue) and **T1** (green). The intercalated daunomycin is shown in red with the crosslinking site highlighted in purple.

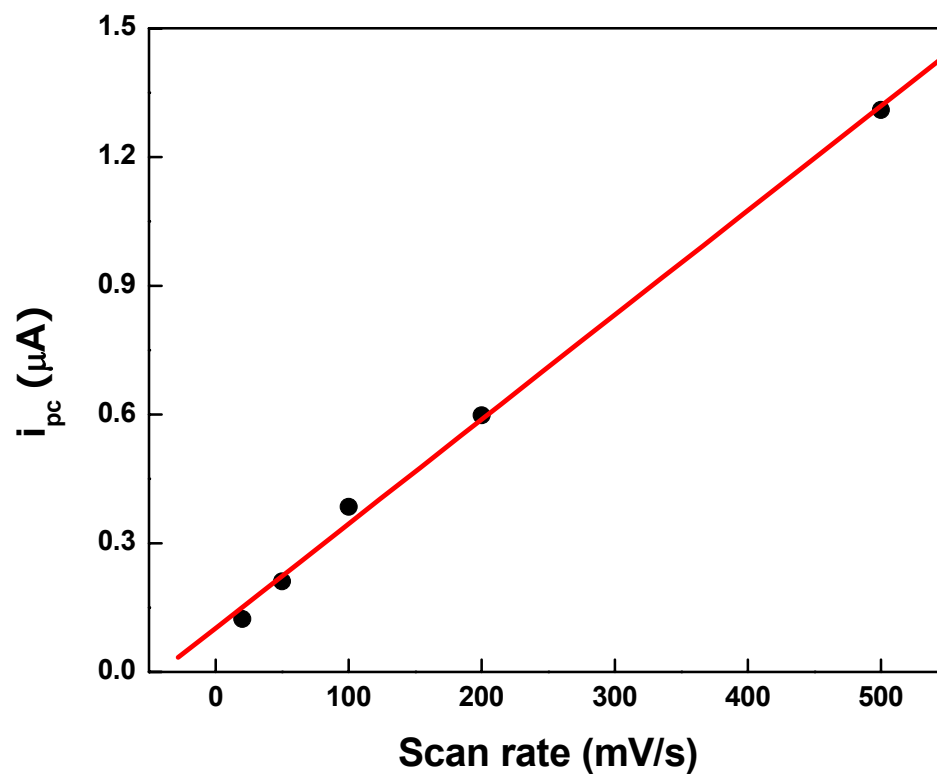


Figure 3.3. Plot of cathodic peak current vs. scan rate. Peak current is proportional to scan rate. This linearity demonstrates that the daunomycin-crosslinked target duplex (**T1**) the redox active species, is immobilized on the electrode surface.

electron transfer rate in DNA films.¹² Our experiments with DNA duplexes containing the overhang have confirmed this conclusion. By analysis of the characteristic splittings of anodic and cathodic peaks as a function of scan rate,^{33, 34} we may estimate the electron transfer rates in a DNA film that consists completely of matched probe duplex and target duplex. Here a rate of 35 s^{-1} is observed (Figure 3.4). It is consistent with the rate observed for a canonical 30mer DNA duplex, which is 30 s^{-1} (see Chapter 2). Again, it confirms the hybridization of target duplex and probe duplex on the surface and the DNA-mediated charge transport through them.

3.3.2 *Quantification of DNA duplexes immobilized on electrode*

By integrating the reduction peak in cyclic voltammetry with crosslinked daunomycin, we calculate the amount of daunomycin on the electrode from which we derive the amount of **T1** that has been immobilized. Assuming that daunomycin undergoes 1 e^- reaction in our experimental condition, the coverage of immobilized target duplexes is found to be $\sim 25 \text{ pmol/cm}^2$.

We further confirm the immobilization of **T1** by quantification with $[\text{Ru}(\text{NH}_3)_6]^{3+}$, a redox-active DNA groove binder. The DNA backbone is negatively charged and each phosphate group in the backbone contributes one negative charge to DNA strand. These negative charges are compensated by cations that electrostatically associate to the backbone of DNA. In solution, these cations are labile and readily exchange with other cations in solution.^{35, 36} The association constant between cations and DNA backbone increases with the cation charge.³⁷ When the DNA-modified electrode is placed in a low ionic strength electrolyte containing a multivalent

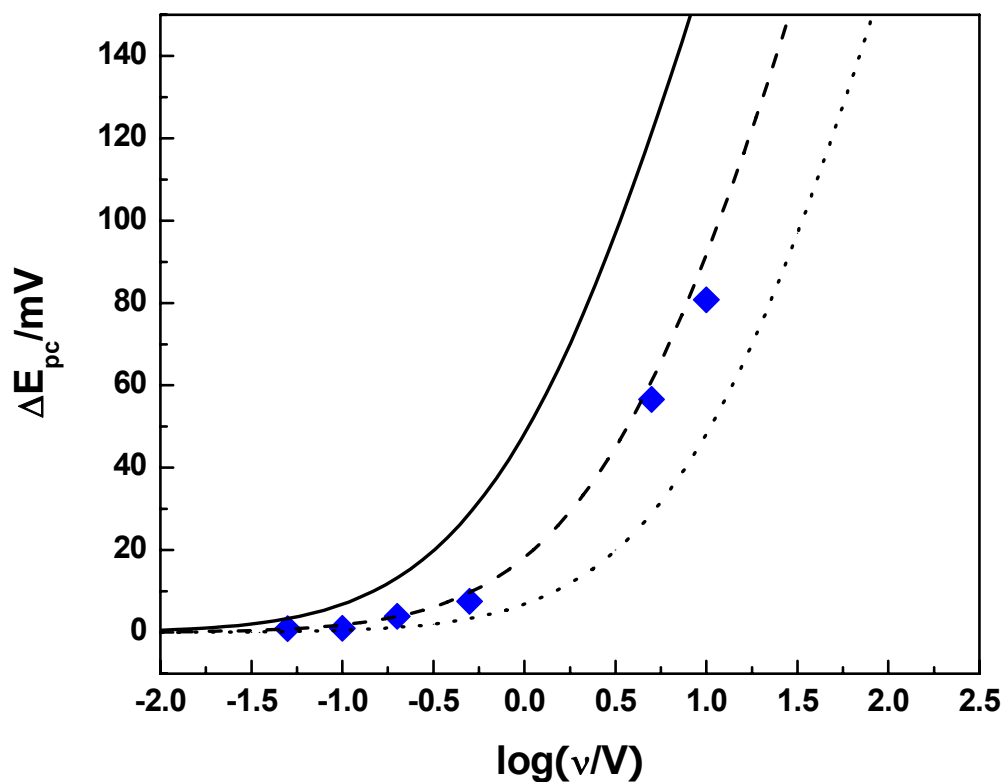


Figure 3.4. Plot of peak splitting ΔE_{pc} (where $\Delta E_{pc} = E_{pc} - E^\circ$) versus $\log(v)$ (where v = scan rate) for electrode modified **P1/T1** hybrid (\blacklozenge). For comparison, a simulated curve which corresponds to rate constants of 35 s^{-1} is shown in blue.³⁴ Simulated curves corresponding to rate constants of 10 s^{-1} (—), 35 s^{-1} (- - -), and 100 s^{-1} (\cdots) are shown for comparison. This electron transfer rate is consistent with that obtained in our studies with electrodes modified with canonical 30mer DNA duplex which is $\sim 30 \text{ s}^{-1}$.¹²

redox-active cation ($[\text{Ru}(\text{NH}_3)_6]^{3+}$ in our case), the multivalent cation replaces the native cation that associates with DNA backbone (Na^+ in our case) and is electrostatically trapped in the DNA film. The amount of the multivalent cations can be measured by cyclic voltammetry or chronocoulometry under equilibrium conditions.^{18,31}

When the concentration of $[\text{Ru}(\text{NH}_3)_6]^{3+}$ in solution is low enough ($<13 \mu\text{M}$), the disturbance by the reduction of diffusing redox species in solution is negligible in cyclic voltammetry.³¹ Therefore, the relationship between the amount of $[\text{Ru}(\text{NH}_3)_6]^{3+}$ and DNA on the electrode can be expressed by following equations:

$$\Gamma_{\text{DNA}} = z/m \cdot \Gamma_0 \quad (3.1)$$

$$\Gamma_0 = Q/(F \cdot A) \quad (3.2)$$

in which Γ_0 is the surface density of $[\text{Ru}(\text{NH}_3)_6]^{3+}$ (mol/cm^2), Γ_{DNA} is the surface density of DNA (mol/cm^2), z is the charge of $[\text{Ru}(\text{NH}_3)_6]^{3+}$ (which is 3 in this case), m is the number of residues in DNA, Q is the total charge during reduction measured by cyclic voltammetry, F is Faraday constant (C/mol), and A is the area of electrode surface (cm^2).

In 10 mM Tris, 10 μM $[\text{Ru}(\text{NH}_3)_6]^{3+}$, pH 7.4, we have quantified the amount of DNA on the electrode before and after surface hybridization, using the same duplexes (**P1** and **T1**) that have been used in the previous experiments but without crosslinked daunomycin. As shown in Figure 3.5, a remarkable growth in the reduction peak is observed after surface hybridization. By integrating the charge accumulated in the cathodic peak, we have calculated the amount of DNA on the surface. Before hybridization, the coverage of probe duplexes (**P1**) is $\sim 30 \text{ pmol}/\text{cm}^2$; after hybridization, the amount of **T1** that has annealed with **P1** on the surface is calculated to be $\sim 20 \text{ pmol}/\text{cm}^2$, obtained by subtracting the contribution of **P1** from the total charge

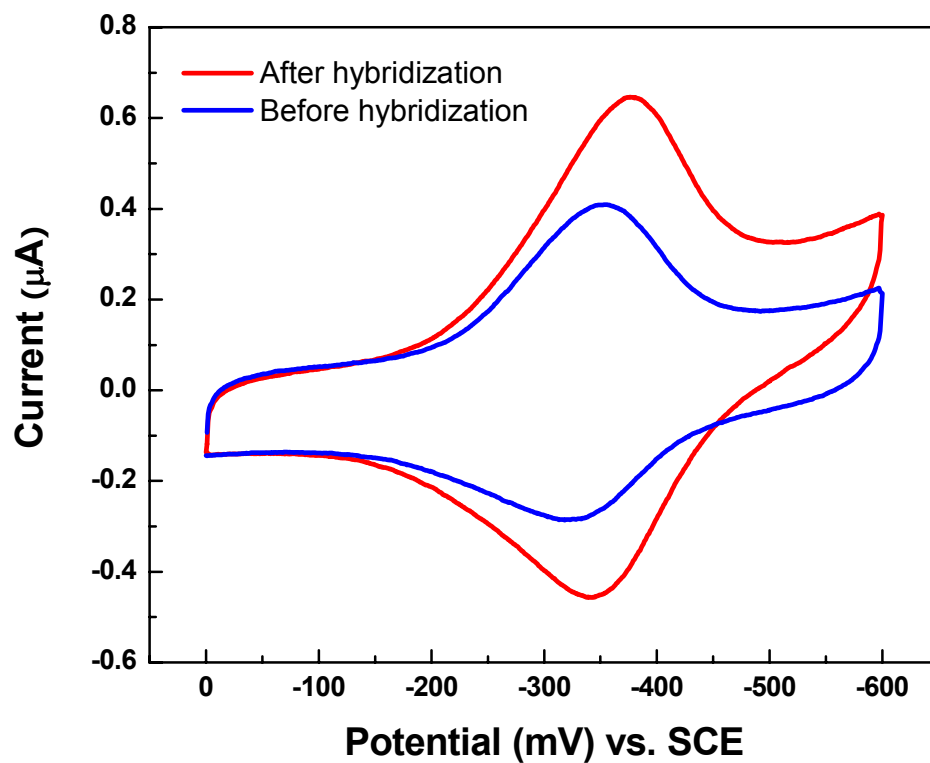


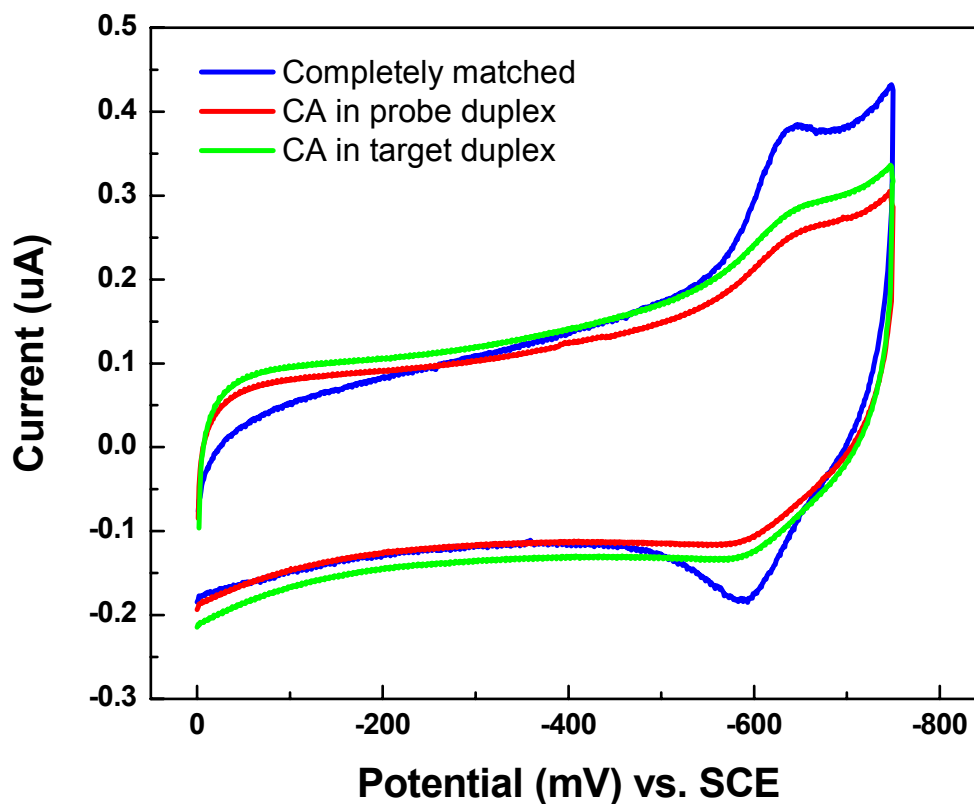
Figure 3.5. Cyclic voltammogram of **P1**-modified electrode in 10 mM Tris, 10 μM $[\text{Ru}(\text{NH}_3)_6]^{3+}$, pH 7.4 before (blue) and after (red) being incubated with 100 μM **T1** (without crosslinked daunomycin) for 3 hours; scan rate = 100 mV/s.

accumulated in the reduction of $[\text{Ru}(\text{NH}_3)_6]^{3+}$ on the electrode. This result is comparable to but a little bit smaller than the results obtained in the experiments with crosslinked daunomycin in which the coverage of immobilized **T1** is $\sim 25 \text{ pmol/cm}^2$. The discrepancy is probably due to the fact that the $[\text{Ru}(\text{NH}_3)_6]^{3+}$ quantification method underestimates the amount of DNA on the electrode when DNA is densely packed on the surface. Because in a densely packed DNA film, the exchange of cations between DNA film and bulk solution is retarded, only a portion of Na^+ ions bound to DNA backbone are replaced by $[\text{Ru}(\text{NH}_3)_6]^{3+}$.

3.3.3 Detection of a mismatch in target duplex and probe duplex

Could the immobilization of target duplex on electrode result from nonspecific absorption rather than from hybridization with probe duplex? If the immobilization is nonspecific, the reduction of daunomycin should not depend on DNA-mediated charge transport. Consequently, an intervening mismatch should not affect the reduction efficiency. On the other hand, the presence of a mismatch in either target duplex or probe duplex should diminish the reduction efficiency of daunomycin if the electron transfer is DNA mediated.

In separate experiments, a CA mismatch is incorporated into target duplex (**T2**) and probe duplex (**P2**) respectively. Indeed, a remarkable decrease in the electrochemical response is observed regardless of the position of the CA mismatch (Figure 3.6). The observation of the attenuated reduction signal in the presence of a CA mismatch strongly implicates the stacked bases of both the probe duplex and target duplex as the pathway for electron transfer. It demonstrates that the target duplex is immobilized through



(a)



(b)

Figure 3.6. (a) Cyclic voltammetry in the Echem buffer at electrodes modified with fully base-paired probe-target hybrid (**P1+T1**, blue), hybrid containing a CA mismatch in the probe (**P2+T1**, red), and hybrid containing a CA mismatch in the target (**P1+T2**, green). (b) The sequences of the probe duplex (**P1**, blue) and the target duplex (**T1**, green). The position of the CA mismatches and daunomycin are highlighted in red, and the crosslinking site is highlighted in purple. Scan rate = 100 mV/s.

hybridization with the probe duplex. Furthermore, a mismatch in the duplexes can be easily detected.

3.3.4 Temperature-dependence studies

To explore the thermostability of the DNA film after hybridization, we have studied the electrochemical response of the modified electrodes at different temperatures. In these experiments, gold electrodes were modified with densely packed probe duplexes (**P1**), followed by incubation with 100 μM target duplex (**T1**) and 100 mM MgCl_2 under the hybridization conditions as has been described in the experimental section. After hybridization, the modified electrodes were interrogated by cyclic voltammetry in Echem buffer at temperatures from 0 $^\circ\text{C}$ to 50 $^\circ\text{C}$ which was controlled by a refrigerating circulator (Fisher Scientific). Figure 3.7 illustrates the effect of temperature on the cyclic voltammetry of the modified electrodes at 0 $^\circ\text{C}$ (blue) and 40 $^\circ\text{C}$ (red). The electrochemical response of the reduction of daunomycin in the DNA film is significantly attenuated at 40 $^\circ\text{C}$. Thermal denaturation measurements by UV-Vis spectroscopy demonstrate that the **T1**-daunomycin adduct is thermally stable in solution up to 50 $^\circ\text{C}$ (3.3 μM **T1**-daunomycin adduct, 5 mM sodium phosphate, 50 mM NaCl, pH 7.1, Figure 3.8). The environment around DNA can be significantly different in films from in solution. Consequently, DNA duplexes of the same sequence may have different thermal stability in films, especially for a densely packed DNA film. In fact, it has been reported that DNA duplexes appear to be more thermally stable in the film than in bulk solution.^{13,}
²³ Therefore, the observed decrease in the electrochemical response is likely not from the dissociation of target DNA-daunomycin adduct. Rather, it may result from the

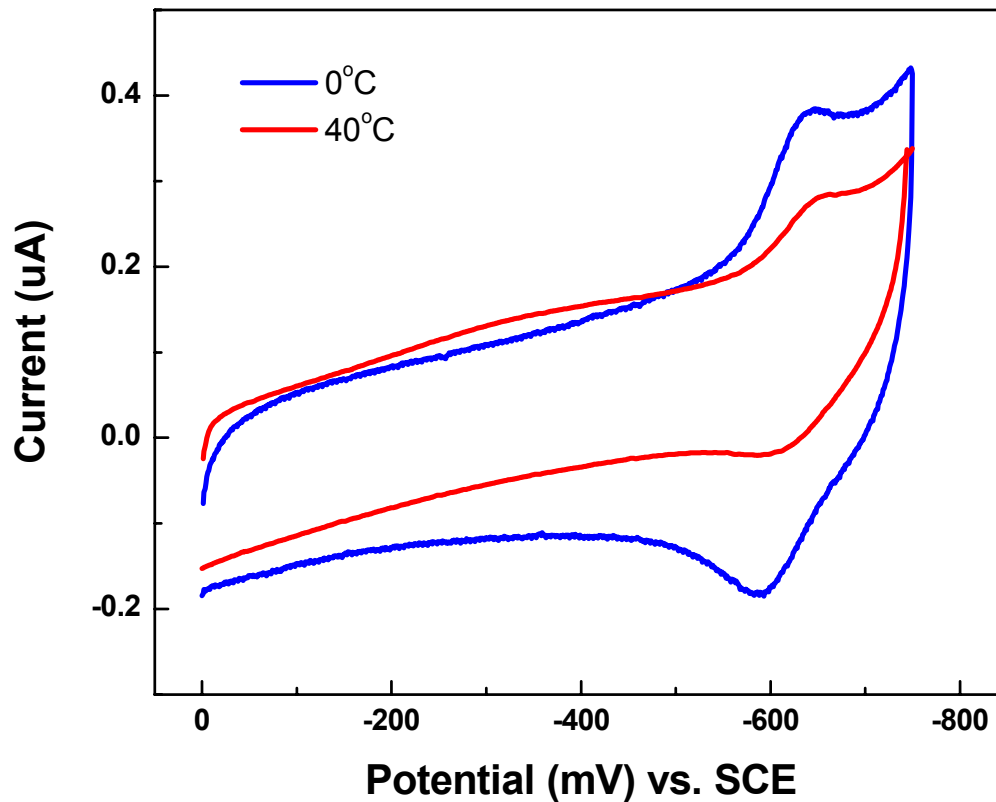
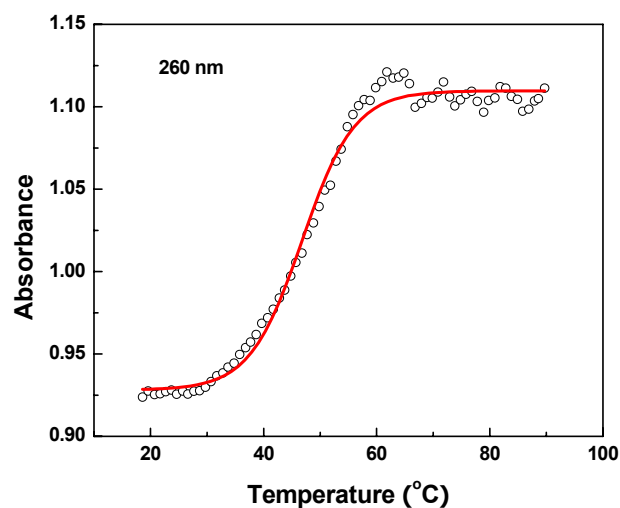
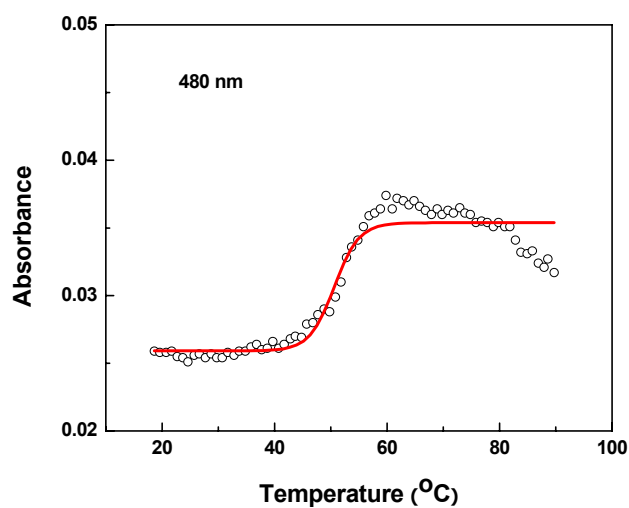


Figure 3.7. Cyclic voltammograms of electrode with fully base-paired probe-target hybrid (**P1+T1**) at 0 °C (blue) and at 40 °C (red) in the Echem buffer; scan rate = 100 mV/s. The probe-target hybrid (**P1+T1**) is less stable at high temperature and began to dissociate. Consequently, the electrochemical response decreased as temperature increases.



(a)



(b)

Figure 3.8. Melting curves of T1-daunomycin conjugates in solution monitored by UV-vis spectroscopy at (a) 260 nm and (b) 480 nm. The black circles are measured absorbance data and the red curve is the sigmoidal (Boltzmann) fit to the melting curve. Condition: 3.3 μ M DNA-daunomycin conjugate in 5 mM sodium phosphate, 50 mM NaCl, pH 7.1. According to this measurement, the DNA-daunomycin conjugate is stable up to 50 °C in solution. It is noteworthy, however, that daunomycin itself appears to be unstable above 70 °C, as its absorption changes significantly above 70 °C. A reverse experiment shows that no daunomycin binds to DNA when temperature decreases from 90 °C to room temperature.

dehybridization of the target duplex from the probe duplex on the electrode as the interaction between the overhangs is much less stable.

The integration of cathodic charge (background subtracted and normalized to the charge obtained at 0 °C) versus temperature is plotted in Figure 3.9. It demonstrates that the duplex hybrid is stable below 20 °C. The electrochemical response decreases gradually when the temperature is above 20 °C, which implicates the temperature at which the target duplex (**T1**) begins to dissociate from the probe duplex (**P1**) on the electrode. When the temperature is above 45 °C, the reduction signal is hardly observable. The “melting temperature” of our DNA film is 32 °C, at which the electrochemical signal is 50% that of the original signal. For a 6mer oligonucleotide that has the same sequence as the overhang (5'-GTGGTG-3'), the melting temperature is 17 °C (10 μM DNA, 55 mM Na⁺, pH 7.1) in solution. This discrepancy in melting temperature implicates that the target-probe hybrid is densely packed in film which is stabilized by strong electrostatic interactions between the negative DNA sugar-phosphate backbone and the compensative cations. Furthermore, the hybridization and dehybridization process is highly reversible, which is explored in the reversibility studies.

3.3.5 Reversibility studies

As would be required in an oligonucleotide array, the hybridization of target duplex and probe duplex can be achieved reversibly *in situ* at the electrode surface without compromising the sensitivity for mismatch detection. Thiol-terminated probe duplexes can be deposited on the electrode surface, hybridized with the first target for test, then heat denatured, thoroughly rinsed and rehybridized with the second target. This

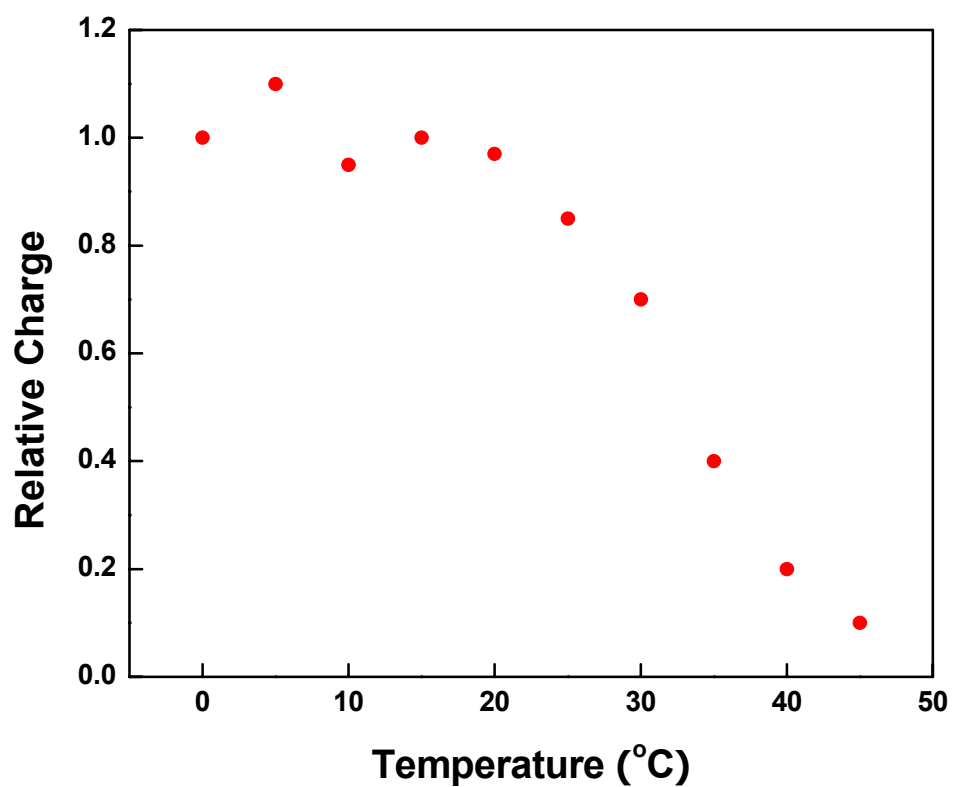
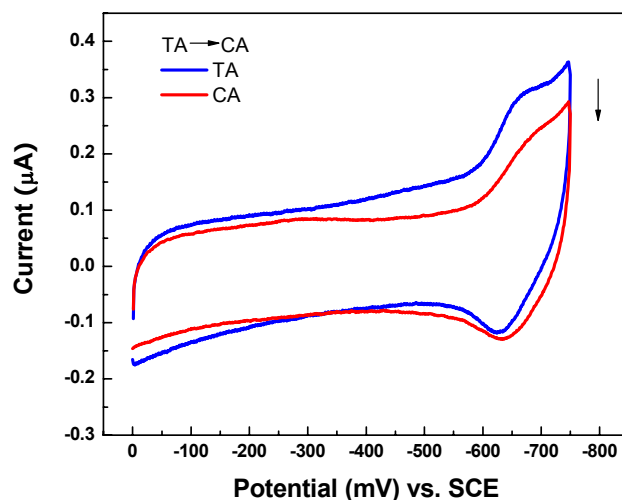


Figure 3.9. Melting curve of probe-target hybrid (**P1+T1**) on electrode. The amount of the target duplex (**T1**) trapped on the electrode is monitored by the charge accumulated in cyclic voltammetry in Echem buffer (scan rate = 100 mV/s). Since each daunomycin undergoes one electron reduction, the total charge accumulated in cyclic voltammetry corresponds to the number of the target duplex annealed to the probe duplex on electrode.

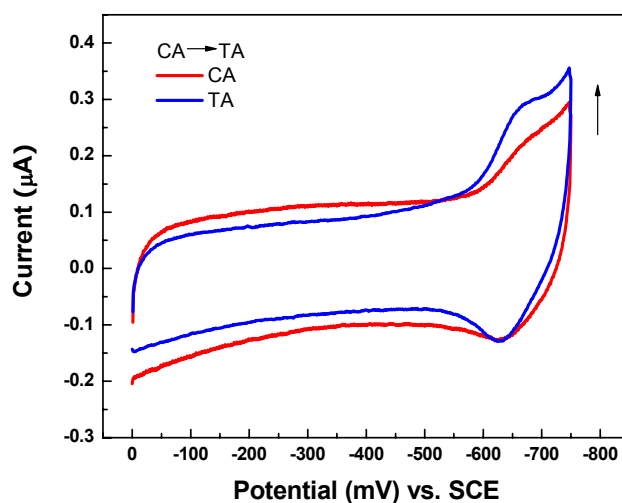
reversible assay is illustrated in Figure 3.10. Here, two separate **P1**-modified electrodes were prepared. One was hybridized with a completely matched target duplex (**T1**, Electrode-1) and the other was hybridized with a target duplex containing one CA mismatch (**T2**, Electrode-2). Being interrogated by cyclic voltammetry, the electrodes exhibit electrochemical responses characteristic of fully base-paired and CA mismatched DNA films, respectively. The target duplexes are stripped off from the electrodes by being heated in 10 mM Tris, pH 7.4, at 40 °C for 15 mins. The electrodes are then incubated with the swapped target duplexes (TA → CA, CA → TA). The new electrodes showed distinct changes in electrochemical responses expected for CA-mismatched and fully base-paired DNA films. Electrodes can be cycled through this sequence of events three times before the thiolated probe duplex film was compromised by repeated heating and incubation.

3.3.6 Implications with respect to mismatch detection based on DNA-mediated charge transport

We have shown here that two DNA duplexes with 6-base overhangs can reversibly hybridize to each other on the electrode surface and intervening mismatches in the duplexes can be detected by electron transfer through the DNA film. **P1/T1** hybrid can form reversibly *in situ* on an electrode surface. An intercalating daunomycin crosslinked to **T1** is easily reduced upon the formation of the hybrid, although there are two nicks in the backbone of the hybrid. On the other hand, a CA mismatch in either **P1** or **T1** significantly diminishes the reduction signal. These results underscore the importance of base pair stacking as the pathway for DNA-mediated charge transport, and



(a)



(b)

Figure 3.10. Cyclic voltammograms of electrodes modified with probe-target hybrid in reversible hybridization studies in Echem buffer (degassed); scan rate = 100 mV/s. **(a)** Probe duplex (**P1**) modified electrode is first incubated with 100 μM target duplex (**T1**, blue), immersed in 10 mM Tris, pH 7.4 at 40 $^{\circ}\text{C}$ for 15mins, and then rehybridized with 100 μM target duplex containing a CA mismatch (**T2**, red). **(b)** Probe duplex (**P1**) modified electrode is first incubated with 100 μM target duplex containing a CA mismatch (**T2**, red), immersed in 10 mM Tris, pH 7.4 at 40 $^{\circ}\text{C}$ for 15mins, and then rehybridized with 100 μM fully base-paired target duplex (**T1**, blue). Hybridization and rehybridization are carried out in solutions containing 100 μM DNA, 5 mM sodium phosphate, 50 mM NaCl, and 100 mM MgCl_2 , pH 7.1.

indicate that the integrity of the phosphate backbone is not crucial for the reduction of an intercalating redox-active marker.

Furthermore, the methodology presented here provides a suitable means to fabricate reusable electrodes for mutation detection based on DNA-mediated charge transport. The probe-modified electrode can be incubated with target duplex for electrochemical mismatch detection, and can be easily regenerated by heat denaturing to strip off the target duplex. The method is also useful for high throughput DNA assay, as an addressable probe array can be constructed by varying the overhangs of the probe duplexes. Consequently, our studies may provide a practical approach to the development of inexpensive but sensitive devices to detect DNA mutations on targeted genes.

However, the methodology described here also presents new challenges for the development of redox active DNA intercalators that can be covalently tethered to DNA. In our studies, we have found that the DNA-DM linkages are not very stable, especially at elevated temperatures and when being repeatedly interrogated by cyclic voltammetry. Indeed, it has been reported that the glycosidic bond in daunomycin tends to break in a two-electron reduction fashion.³⁸⁻⁴¹ Furthermore, the redox potential of daunomycin (-650 mV) is near the edge of the potential window in which thiol-terminated DNA is stable on the gold surface. In our experiments, we have found that cyclic voltammetric scans beyond -700 mV result in significant and non-reversible desorption of thiolate DNA from the gold surface. Therefore, it is necessary to develop a redox active DNA intercalator that can be covalently tethered DNA with a stable linkage and has a higher reduction potential, which will improve the sensitivity and reliability of mutation detection based on DNA-mediated charge transport.

3.4 SUMMARY

We have developed a novel method to electrochemically monitor the trapping of double stranded DNA onto modified gold electrode. Gold electrode surfaces were modified with a monolayer of double stranded DNA probes with a 6-base overhang, followed by the exposure to solution of double stranded DNA target with crosslinked daunomycin, a redox-active DNA intercalator. The target contained a 6-base overhang complementary to that of the probe. The reduction of daunomycin was observed in cyclic voltammetry as a result of the hybridization of the probe duplex and the target duplex, which provided a pathway for charge transport. The electrochemical response was significantly attenuated by CA mismatch in the probe duplex and target duplex resulted. The hybridization of probe duplex and target duplex on the surface was reversible. This method provides an alternative approach to mutation detection with reusable electrodes based on DNA-mediated charge transport.

3.5 REFERENCES

1. Drummond, T. G.; Hill, M. G.; Barton, J. K., Electrochemical DNA sensors. *Nature Biotechnology* **2003**, 21, (10), 1192-1199.
2. Brookes, A. J., The essence of SNPs. *Gene* **1999**, 234, (2), 177-186.
3. McCarthy, J. J.; Hilfiker, R., The use of single-nucleotide polymorphism maps in pharmacogenomics. *Nature Biotechnology* **2000**, 18, (5), 505-508.
4. Wang, J., Survey and summary: From DNA biosensors to gene chips. *Nucleic Acids Research* **2000**, 28, (16), 3011-3016.
5. Boon, E. M.; Salas, J. E.; Barton, J. K., An electrical probe of protein-DNA interactions on DNA-modified surfaces. *Nature Biotechnology* **2002**, 20, (3), 282-286.
6. Kelley, S. O.; Holmlin, R. E.; Stemp, E. D. A.; Barton, J. K., Photoinduced electron transfer in ethidium-modified DNA duplexes: Dependence on distance and base stacking. *Journal of the American Chemical Society* **1997**, 119, (41), 9861-9870.
7. Kelley, S. O.; Barton, J. K., Electron transfer between bases in double helical DNA. *Science* **1999**, 283, (5400), 375-381.
8. Holmlin, R. E., Charge transfer through the DNA base stack. *Angewandte Chemie* **1997**, 36, (24), 2715-2730.
9. Gasper, S. M., Three-dimensional structure and reactivity of a photochemical cleavage agent bound to DNA. *Journal of the American Chemical Society* **1998**, 120, (48), 12402-12409.
10. Kelley, S. O.; Jackson, N. M.; Hill, M. G.; Barton, J. K., Long-range electron transfer through DNA films. *Angewandte Chemie-International Edition* **1999**, 38, (7), 941-945.
11. Boal, A. K.; Barton, J. K., Electrochemical detection of lesions in DNA. *Bioconjugate Chemistry* **2005**, 16, (2), 312-321.
12. Liu, T.; Barton, J. K., DNA Electrochemistry through the Base Pairs Not the Sugar-Phosphate Backbone. *J. Am. Chem. Soc.* **2005**, 127, (29), 10160-10161.

13. Kelley, S. O.; Boon, E. M.; Barton, J. K.; Jackson, N. M.; Hill, M. G., Single-base mismatch detection based on charge transduction through DNA. *Nucleic Acids Research* **1999**, *27*, (24), 4830-4837.
14. Boon, E. M.; Ceres, D. M.; Drummond, T. G.; Hill, M. G.; Barton, J. K., Mutation detection by electrocatalysis at DNA-modified electrodes. *Nature Biotechnology* **2000**, *18*, (10), 1096-1100.
15. Peterson, A. W.; Heaton, R. J.; Georgiadis, R., Kinetic Control of Hybridization in Surface Immobilized DNA Monolayer Films. *Journal of the American Chemical Society* **2000**, *122*, (32), 7837-7838.
16. Peterson, A. W.; Heaton, R. J.; Georgiadis, R. M., The effect of surface probe density on DNA hybridization. *Nucleic Acids Research* **2001**, *29*, (24), 5163-5168.
17. Peterson, A. W.; Wolf, L. K.; Georgiadis, R. M., Hybridization of Mismatched or Partially Matched DNA at Surfaces. *J. Am. Chem. Soc.* **2002**, *124*, (49), 14601-14607.
18. Steel, A. B.; Herne, T. M.; Tarlov, M. J., Electrochemical quantitation of DNA immobilized on gold. *Analytical Chemistry* **1998**, *70*, (22), 4670-4677.
19. Steel, A. B.; Levicky, R. L.; Herne, T. M.; Tarlov, M. J., Immobilization of Nucleic Acids at Solid Surfaces: Effect of Oligonucleotide Length on Layer Assembly. *Biophysical Journal* **2000**, *79*, (2), 975-981.
20. Petrovykh, D. Y.; Kimura-Suda, H.; Whitman, L. J.; Tarlov, M. J., Quantitative Analysis and Characterization of DNA Immobilized on Gold. *Journal of the American Chemical Society* **2003**, *125*, (17), 5219-5226.
21. Wolf, L. K.; Gao, Y.; Georgiadis, R. M., Sequence-Dependent DNA Immobilization: Specific versus Nonspecific Contributions. *Langmuir* **2004**, *20*, (8), 3357-3361.
22. Hagan, M. F.; Chakraborty, A. K., Hybridization dynamics of surface immobilized DNA. *Journal of Chemical Physics* **2004**, *120*, (10), 4958-4968.
23. Flechsig, G. U.; Peter, J.; Hartwich, G.; Wang, J.; Grundler, P., DNA Hybridization Detection at Heated Electrodes. *Langmuir* **2005**, *21*, (17), 7848-7853.
24. Xu, J.; Craig, S. L., Thermodynamics of DNA Hybridization on Gold Nanoparticles. *J. Am. Chem. Soc.* **2005**, *127*, (38), 13227-13231.

25. Henry, M. R., Real-time measurements of DNA hybridization on microparticles with fluorescence resonance energy transfer. *Analytical biochemistry* **1999**, 276, (2), 204-214.
26. Zeng, J.; Almadidy, A.; Watterson, J.; Krull, U. J., Interfacial hybridization kinetics of oligonucleotides immobilized onto fused silica surfaces. *Sensors and Actuators B: Chemical* **2003**, 90, (1-3), 68-75.
27. Herne, T. M.; Tarlov, M. J., Characterization of DNA Probes Immobilized on Gold Surfaces. *Journal of the American Chemical Society* **1997**, 119, (38), 8916-8920.
28. Okahata, Y.; Kawase, M.; Niikura, K.; Ohtake, F.; Furusawa, H.; Ebara, Y., Kinetic Measurements of DNA Hybridization on an Oligonucleotide-Immobilized 27 MHz Quartz Crystal Microbalance. *Analytical Chemistry* **1998**, 70, (7), 1288-1296.
29. Georgiadis, R.; Peterlinz, K. P.; Peterson, A. W., Quantitative Measurements and Modeling of Kinetics in Nucleic Acid Monolayer Films Using SPR Spectroscopy. *Journal of the American Chemical Society* **2000**, 122, (13), 3166-3173.
30. Levicky, R.; Herne, T. M.; Tarlov, M. J.; Satija, S. K., Using Self-Assembly To Control the Structure of DNA Monolayers on Gold: A Neutron Reflectivity Study. *Journal of the American Chemical Society* **1998**, 120, (38), 9787-9792.
31. Yu, H. Z.; Luo, C. Y.; Sankar, C. G.; Sen, D., Voltammetric Procedure for Examining DNA-Modified Surfaces: Quantitation, Cationic Binding Activity, and Electron-Transfer Kinetics. *Analytical Chemistry* **2003**, 75, (15), 3902-3907.
32. Bard, A. J., Faulkner, L.R., *Electrochemical methods: fundamentals and applications*. 2nd ed.; John Wiley & Sons: New York, 2000.
33. Laviron, E., General Expression of the Linear Potential Sweep Voltammogram in the Case of Diffusionless Electrochemical Systems. *Journal of Electroanalytical Chemistry* **1979**, 101, (1), 19-28.
34. Tender, L.; Carter, M. T.; Murray, R. W., Cyclic Voltammetric Analysis of Ferrocene Alkanethiol Monolayer Electrode-Kinetics Based on Marcus Theory. *Analytical Chemistry* **1994**, 66, (19), 3173-3181.
35. Rose, D. M.; Bleam, M. L.; Record, M. T.; Bryant, R. G., ²⁵Mg NMR in DNA Solutions - Dominance of Site Binding Effects. *Proceedings of the National Academy of Sciences of the United States of America-Physical Sciences* **1980**, 77, (11), 6289-6292.

36. Su, L.; Sankar, C. G.; Sen, D.; Yu, H. Z., Kinetics of Ion-Exchange Binding of Redox Metal Cations to Thiolate-DNA Monolayers on Gold. *Analytical Chemistry* **2004**, 76, (19), 5953-5959.
37. Taquikhan, M. M., Martell, A. E., Thermodynamic Quantities Associated with the Interaction of Adenosinediphosphoric and Adenosinemonophosphoric Acids with Metal Ions. *Journal of the American Chemical Society* **1967**, 89, (22), 5585.
38. Rao, G. M.; Lown, J. W.; Plambeck, J. A., Electrochemical Studies of Anti-Tumor Antibiotics .3. Daunorubicin and Adriamycin. *Journal of the Electrochemical Society* **1978**, 125, (4), 534-539.
39. Houeelevin, C.; Gardesalbert, M.; Ferradini, C.; Faraggi, M.; Klapper, M., Pulse-Radiolysis Study of Daunorubicin Redox Cycles - Reduction by E-Aq and Coo-Free-Radicals. *Febs Letters* **1985**, 179, (1), 46-50.
40. Houeelevin, C.; Gardesalbert, M.; Rouscilles, A.; Ferradini, C.; Hickel, B., Intramolecular Semiquinone Disproportionation in DNA - Pulse-Radiolysis Study of the One-Electron Reduction of Daunorubicin Intercalated in DNA. *Biochemistry* **1991**, 30, (33), 8216-8222.
41. Taatjes, D. J.; Gaudiano, G.; Resing, K.; Koch, T. H., Redox pathway leading to the alkylation of DNA by the anthracycline, antitumor drugs adriamycin and daunomycin. *Journal of Medicinal Chemistry* **1997**, 40, (8), 1276-1286.

CHAPTER 4

DNA-Mediated Electrochemistry of Anthraquinone- DNA Conjugates

This work was completed in collaboration with Dr. Maria C. DeRosa.

4.1 INTRODUCTION

DNA-mediated charge transport (CT) chemistry has been examined using a wide variety of spectroscopic, biochemical, and biophysical methods.¹⁻¹⁰ It is now well established that CT through DNA can occur over long distances yet is remarkably sensitive to subtle perturbations in the base pair stack.¹¹⁻¹⁴ This sensitivity to base stacking provides the foundation for electrochemical assays for DNA mutations, lesions, and DNA/protein interactions.¹⁵⁻¹⁷ In these assays, thiol-modified DNA duplexes are self-assembled on a gold electrode surface and reduction of a DNA-bound redox intercalator is monitored as a direct assessment of the efficiency of CT through the intervening π -stack. A clear understanding of the redox probe/DNA interaction and how it leads to the detection of an electrochemical signal is, therefore, essential for the purposeful design and application of these sensors.

We have focused on intercalative redox probes that stack well with the base pairs, since photochemical and biochemical experiments¹⁸ have demonstrated that efficient coupling of the donor and acceptor to the π -stack via intercalation is a prerequisite for efficient DNA-mediated CT. The extent of oxidative damage caused by DNA CT, for example, can be directly correlated to the strength of intercalative binding of the oxidant.¹⁸ We have also seen that the binding mode of the redox probe affects the electrochemistry on DNA-modified electrodes. Groove binding molecules, such as $[\text{Ru}(\text{NH}_3)_6]^{3+}$, can be reduced on the electrode surface through facilitated diffusion along the groove of the immobilized duplexes, but they are not electrochemically active if the DNA-modified surfaces are passivated with polymerized naphthol; thus direct contact with the electrode is required. Intercalative species, such as methylene blue or

daunomycin, in contrast, can be reduced from a distance on the electrode through DNA-mediated electron transfer.^{19,20} This electronic access to the base pair stack, achieved by intercalation, is essential for detection schemes based on DNA-mediated CT; probes that interact with DNA purely through electrostatics do not yield appreciable differences in electrochemical signal in the presence of π -stack disruptions. Ferrocene-labeled oligomers also require direct contact with the electrode for sensitive assay.^{21,22} These observations prompt us to investigate further the significant influence of probe binding mode on the electrochemistry of DNA-modified electrodes.

Anthraquinone-modified DNA duplexes have been examined in detail in studies of DNA photooxidation^{23, 24} and for their potential utility in electrochemical DNA sensing.^{25, 26} Anthraquinone moieties tethered to DNA via two-carbon (AQ2) or five-carbon (AQ5) tethers have been used^{23, 24} primarily as covalently linked DNA photooxidants for mechanistic studies of DNA CT. It is generally considered that in AQ5 assemblies it is possible for the anthraquinone to intercalate between the first base pairs from the 5'-end of the duplex.^{25, 27} In the case of AQ2, the alkyl tether is too short to allow for intercalation; instead, access to the DNA-mediated CT pathway is proposed to occur via an end-capping interaction, where the anthraquinone stacks onto the terminal base pair.²⁵ Despite these differences in supposed binding, AQ2 and AQ5 modified duplexes exhibit similar luminescence characteristics and photoinduced DNA cleavage.

In order to further delineate the role of DNA/redox probe interactions on DNA-mediated electrochemistry, we sought to explore these AQ-DNA conjugates electrochemically. Importantly, the data presented here emphasize that electronic access

of the redox probe to the DNA π -stack is a requisite feature for efficient DNA CT in these films.

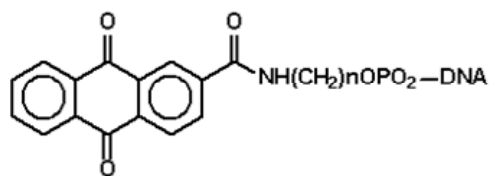
4.2 MATERIALS AND METHODS

4.2.1 Materials

DNA synthesis reagents were obtained from Glen Research. Millipore Milli Q water (18 M Ω cm) was used in all experiments. Anthraquinone-2-carboxylic acid and reagents used in synthesis of AQ2 and AQ5 were obtained from Aldrich at highest available purity and used as received.

4.2.2 Preparation of DNA-modified surfaces

The sequences of DNA strands are shown in Scheme 4.1. AQ2 and AQ5 phosphoramidites and AQ-modified oligonucleotides were prepared according to literature procedures.^{23, 24} Thiol-modified single-stranded oligonucleotides were prepared as previously described in Chapter 2. All modified oligonucleotides were purified by reverse phase HPLC and characterized by UV-visible and mass spectrometry. After HPLC purification, the thiol-modified single strands were hybridized with their AQ2- or AQ5-modified complement to yield **B1** and **B2**, respectively, by heating equimolar amounts of each strand in 5 mM sodium phosphate, 50 mM NaCl, pH 7, (final solution 0.1 mM duplex) to 90 °C followed by slow cooling to ambient temperature. The thiol-modified duplex was deposited on a gold electrode surface for 12-24 hours, backfilled with 1 mM mercaptohexanol (MCH) for 1 hour, and the electrode was thoroughly rinsed in 5 mM sodium phosphate, 50 mM NaCl, pH 7.0 before being used in



AQ2 n=2 AQ5 n=5

HS-5'-ACTTCAGCTGAGACGCA-3' 3'-TGAAGTCGACTCTGCGT-5'-AQ	B1 (with AQ2) or B2 (with AQ5)
HS-5'-GCCATCCTGCGTGGTG-3' 3'-CGGTAGGACG-5'	S1
HS-5'-GCC A TCCTGCGTGGTG-3' 3'-CGG C AGGACG-5'	S2
HS-5'-GCCATCCTGCGTGGTG-3' 3'-CGGTAGGACGCACCAC-5'	S3
5'-TCATCTATACTCCA-3' 3'-CACCACAGTAGATATGAGGT-5'-AQ	S4 (with AQ2)
5'-TCATCTA C ACTCCA-3' 3'-CACCACAGTAGAT A TGAGGT-5'-AQ	S5 (with AQ2)

Scheme 4.1. Structure of AQ2 and AQ5 DNA conjugates. The DNA sequences used in these experiments are also shown. Duplexes **B1** and **B2** were investigated with both the AQ2 and AQ5 probes tethered to the 5' end, respectively, while duplexes **S4** and **S5** were investigated with the AQ2 probe only. The position of CA mismatch is highlighted in red.

electrochemical experiments. When tightly packed monolayers were required, 0.1 M MgCl_2 was added to the duplex solution before deposition on the gold surfaces.

4.2.3 Electrochemical measurements

Cyclic voltammetry was carried out under an Ar atmosphere on 0.02 cm^2 gold electrodes using a CH Instruments electrochemical analyzer. A normal three-electrode configuration consisting of a modified gold-disk working electrode, a Ag/AgCl reference electrode, and a platinum wire auxiliary electrode was used. A modified Luggin capillary separated the working compartment of the electrochemical cell from the reference compartment. Potentials are reported versus Ag/AgCl. Polycrystalline gold electrodes were polished sequentially with 1.0, 0.3, and 0.05 micron alumina slurry, followed by etching in 1.0 M H_2SO_4 , and thorough rinsing with Milli-Q water prior to DNA deposition. DNA surface coverage measurements using $[\text{Ru}(\text{NH}_3)_6]^{3+}$ were carried out in 10 mM Tris buffer (pH 7.4, room temperature) containing $10 \mu\text{M}$ $[\text{Ru}(\text{NH}_3)_6]^{3+}$ under argon.

4.2.4 Experiments with DNA duplexes containing overhangs

Solutions ($100 \mu\text{M}$) of thiol-modified DNA duplexes containing strand overhangs were deposited on the gold electrode surface for 12-24 hours, backfilled with 1 mM mercaptohexanol for 1 hour, and thoroughly rinsed with buffer before use. The AQ2-modified sticky ended complement ($5 \mu\text{M}$) was then incubated on the electrode surface for 2 hours at 4°C .

4.3 RESULTS AND DISCUSSION

4.3.1 Electrochemistry of AQ-DNA assemblies

Anthraquinone-DNA conjugates used in these studies are shown in Scheme 4.1. Mixed sequence DNA duplexes containing either the AQ2 or AQ5 tether were prepared and characterized in parallel. Melting temperature experiments indicate that both **B1** and **B2** at 10 μM melt at 67 $^{\circ}\text{C}$ in 5 mM sodium phosphate, 50 mM NaCl, pH 7.0. AQ tethering in both cases therefore leads to a stabilization of 5 $^{\circ}\text{C}$ versus the unmodified DNA duplexes.

DNA-modified electrodes may be prepared using these DNA assemblies. The assemblies **B1** and **B2** (10 μM) are deposited onto gold electrodes to yield a loosely packed monolayer, and the surfaces are backfilled with 1-mercaptohexanol (MCH). We estimate the surface coverage of both electrodes to be ~ 10 pmol/cm² quantified using $[\text{Ru}(\text{NH}_3)_6]^{3+}$.²⁸ Figure 4.1 shows both cyclic and square wave voltammetry for the AQ-modified DNA films. **B1** yields a quasi-reversible redox couple at -450 mV versus Ag/AgCl; the redox species is determined to be surface bound based on the linear dependence of peak current on scan rate (Figure 4.2). It is noteworthy that both cathodic and anodic peaks are broad and the peak splitting is significant (~ 140 mV at scan rate of 100 mV/s). This is quite different from the electrochemistry of other redox active DNA intercalators such as daunomycin and methylene blue, in which the reduction signal is much sharper and the peak splitting is much smaller (~ 50 mV at scan rate of 100 mV/s).¹⁹
²⁹ The broad signal for AQ-modified DNA does, however, reflect slow redox kinetics or heterogeneity of redox species.

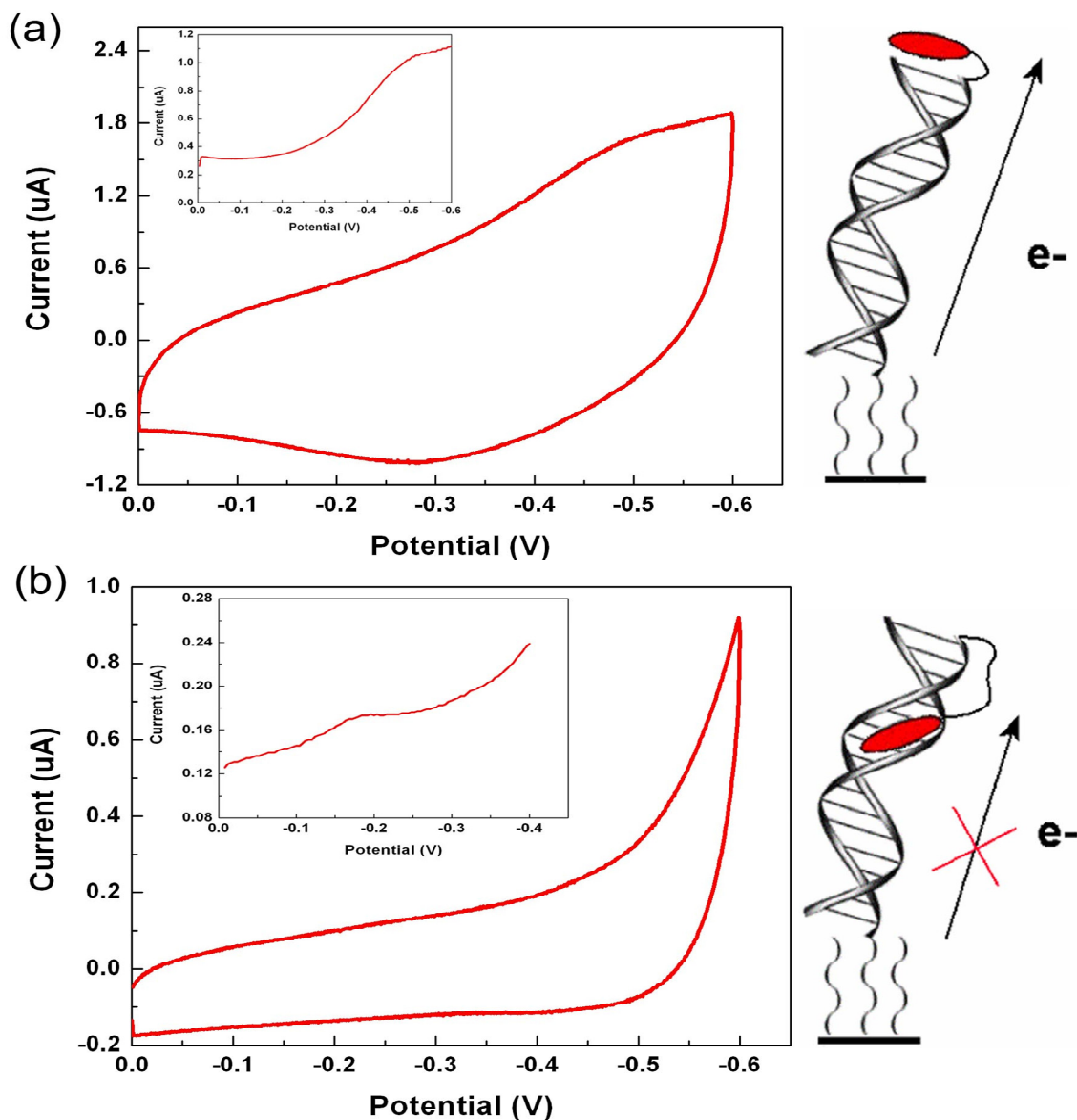


Figure 4.1. (a) Electrochemistry of a **B1**-modified electrode (vs. Ag/AgCl). The short tether precludes intercalation, but allows for the anthraquinone to interact with the DNA π -stack via endcapping. As a result, a weak but reversible redox couple at -450 mV is visible. Inset: Square wave voltammogram of **B1**-modified gold. A signal is detected at -450 mV. (b) Electrochemistry of a **B2**-modified electrode (vs. Ag/AgCl). The extra bulk of the longer tether may interfere with endcapping and the anthraquinone may be interacting with the DNA primarily through groove binding. Without the interaction with the DNA π -stack, no redox signal is seen. Inset: Square wave voltammogram of **B2** modified gold electrode. A very weak redox signal is seen at -200 mV. This signal is assigned to an intercalated AQ moiety. In both cases, films were assembled without Mg^{2+} and were backfilled with mercaptohexanol prior to the experiments. Scan rate: 200 mV/s; Buffer: 5 mM sodium phosphate, 50 mM NaCl, pH 7.0.

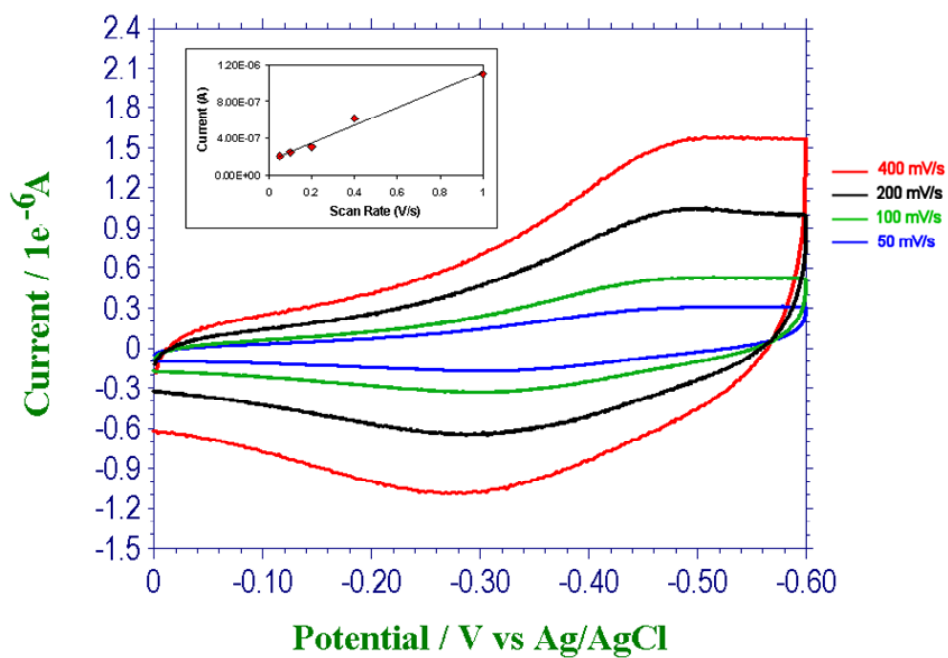


Figure 4.2. Cyclic voltammograms of **B1** at varying scan rates (vs. Ag/AgCl). Inset: Plot of current vs. scan rate for **B1**. The linear dependence is indicative of a surface bound redox species. Buffer: 5 mM phosphate buffer, 50 mM NaCl, pH 7.0.

Furthermore, the signal observed for the AQ2-DNA film is at a potential different from AQ on gold without DNA³⁰ and different from that seen earlier for an AQ-DNA conjugate where the AQ unit was covalently tethered by a long alkyl chain to the 2'-O position of a uridine nucleotide (AQ-U).³¹ In those assemblies, the AQ redox couple was observed at -570 mV (vs. Ag/AgCl) in the absence of a thiol blocking layer and after backfilling with mercaptoethanol (MCE). Interestingly for AQ-U, backfilling with MCH led to the loss of the AQ signal, suggesting that the AQ unit was being reduced directly at the electrode surface. Here we observe a signal for AQ2 despite backfilling with MCH. The electron transfer kinetics for **B1** and AQ-U are also noticeably dissimilar and highlight differences in the mechanism of AQ reduction. Qualitatively, the large peak separation between anodic and cathodic waves of **B1** is indicative of sluggish electron transfer kinetics, while for AQ-U, anodic and cathodic waves are seen at nearly coincident redox potentials. All these data suggest that the AQ moiety in **B1** is being reduced via a DNA-mediated pathway rather than directly at the electrode surface.

DNA-mediated electrochemistry is perhaps best demonstrated in comparative experiments with intervening base mismatches. We find here too that reduction of AQ2-modified DNA films containing a single CA mismatch in the intervening duplex yields a drastic attenuation in signal compared to that of the fully matched AQ2-modified DNA film (Figure 4.3).

Strikingly, while AQ2 reductions can be monitored in well-matched DNA films, gold electrodes modified with AQ5 show almost no redox activity in the electrochemical window examined (Figure 4.1(b)). Only when using square wave voltammetry, where the

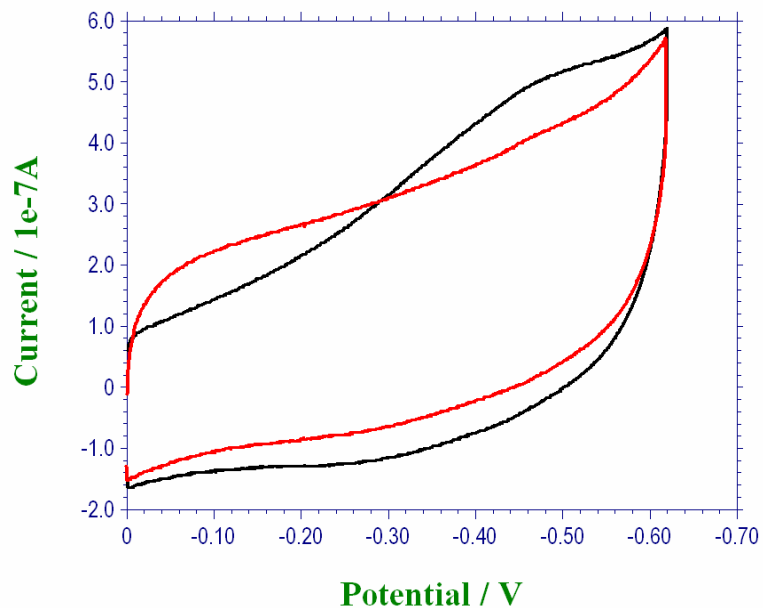


Figure 4.3. Comparison of matched (black line) and mismatched (red line) tightly packed AQ-DNA conjugates. Scan rate: 200 mV/s; Buffer: 5 mM sodium phosphate buffer, 50 mM NaCl, pH=7.0. Potential reference: Ag/AgCl. The sequences used were:

Matched	AQ2-5' -CGT CTG CGC ATC TCT-3'
	3' -GCA GAC GCG TAG AGA-5'
Mismatched	AQ2-5' -CGT CTG CGC ATC TCT-3'
	3' -GCA GAC GCA TAG AGA-5'.

capacitive current is largely eliminated allowing for greater sensitivity, can a very weak signal be observed at -200 mV (vs. Ag/AgCl). Considering the apparent equivalence of **B1** and **B2** based on melting temperature measurements, this discrepancy in electrochemical behavior is somewhat surprising.

We consider that this difference must be based upon differences in the mode of interaction of the AQ with the DNA π -stack: In **B1**, the AQ moiety is end-capped while in **B2** it may be interacting with the DNA primarily by groove-binding with a small proportion intercalated. In the groove-binding case, the lack of interaction with the base-pair stack precludes electron transfer to and from the electrode surface and, therefore, no signal is observed. We thus assign the AQ signal at \sim -200 mV (vs. Ag/AgCl) to intercalated AQ.

Other differences in electrochemical behavior for films containing **B1** versus **B2** are evident. Tightly packed films of **B2** show no change in electrochemical behavior when compared to loosely packed monolayers (data not shown). However, when duplexes of **B1** are assembled in a tightly packed monolayer and studied by square wave voltammetry, a second, weaker reduction wave at -260 mV is observed along with the stronger signal at -450 mV (vs. Ag/AgCl, Figure 4.4). The former signal is reminiscent of the weak signal seen in the case of **B2** and could be associated with a second binding mode where the AQ moiety from one duplex is intercalated into the base pair stack of a neighboring duplex.

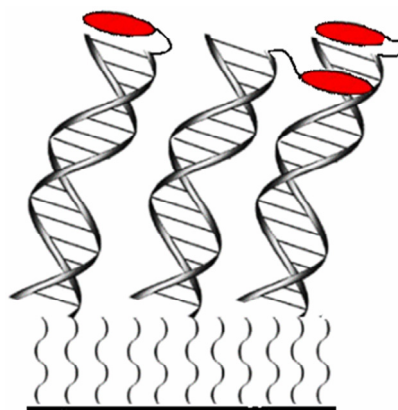
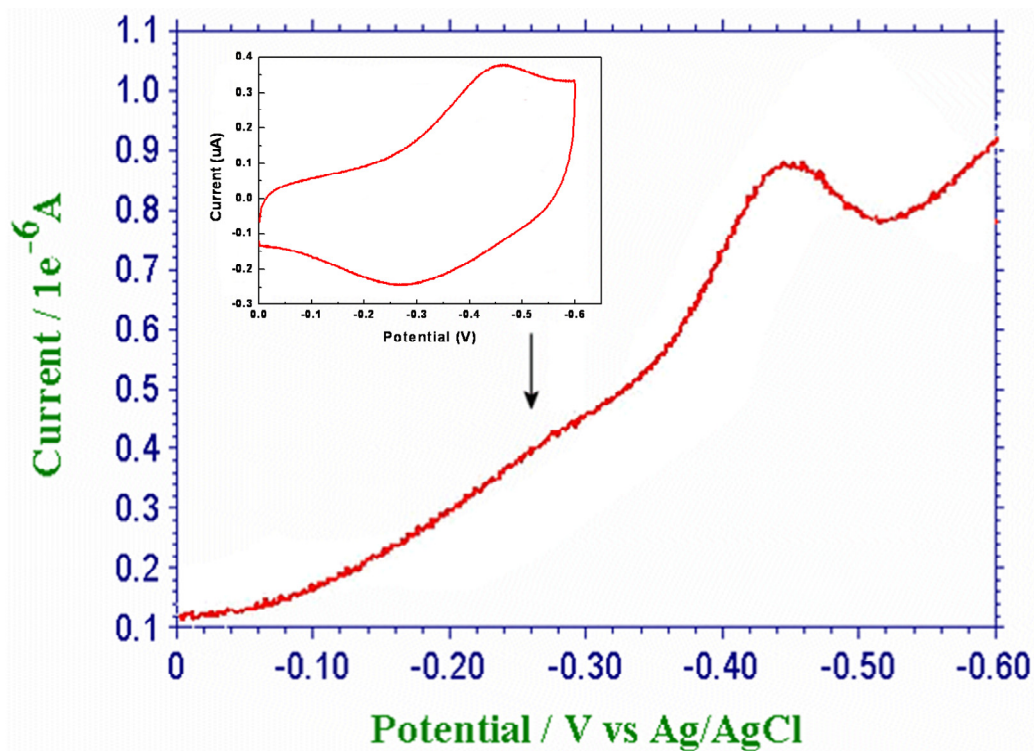


Figure 4.4. Square wave voltammogram of a **B1**-modified electrode (vs. Ag/AgCl). The electrode was prepared in the presence of Mg^{2+} , which results in a more tightly packed monolayer, and was backfilled with mercaptohexanol prior to the experiment. A very weak shoulder at -260 mV is seen as well as a large signal at -450 mV attributed to the endcapping interaction. The shoulder is the result of a second binding mode where the anthraquinone can intercalate into a neighboring duplex. Inset: Cyclic voltammogram of **B1**. (Buffer: 5 mM sodium phosphate, 50 mM NaCl, pH 7.0.)

4.3.2 Interduplex interactions among AQ-DNA assemblies

In order to confirm the identity of this redox signal, an experiment using DNA containing or lacking strand overhangs was carried out (Figure 4.5). The sequences of DNA strands in this experiment are shown in Scheme 4.1. In this experiment, a solution of AQ2-DNA **S4** containing a 6-base overhang is added to a gold surface already modified with duplex **S1** containing a 6-base overhang which is complementary to that of **S4**. Two different possible outcomes may be considered: In one case, the complementary sticky-end portions of DNA can anneal and a signal for an “end-capped” AQ (ca. -450 mV) can be observed. Alternatively, the AQ moiety can intercalate in an interduplex sense into the bottom DNA duplex modifying the gold electrode, and a signal for the intercalated AQ should be obtained (ca. -300 mV). In order to confirm the binding mode, a CA mismatch, known for its ability to disrupt DNA-mediated CT, can be incorporated into the top duplex (duplex **S5**). If the AQ unit is endcapped, then the mismatch will cause a loss of redox signal, while if the AQ is intercalated into the bottom duplex, then the mismatch will have no effect on the AQ signal.

The results of these square wave voltammetry experiments and several controls are shown in Figure 4.6. The electrochemistry of complementary sticky-end duplexes **S1** and **S4** is shown in Figure 4.6(a); a signal consistent with an intercalated AQ is detected at -300 mV when **S4** is incubated on a surface of duplex **S1** and is not seen when **S4** is incubated on MCH alone. Notably, when a mismatch is incorporated into the top duplex (duplex **S5**), no loss of the redox signal is observed (Figure 4.6(b)). Alternatively, if a mismatch is introduced into the bottom duplex (duplex **S2**), the peak current is dramatically attenuated (Figure 4.6(c)). Moreover, if the bottom sticky end duplex is

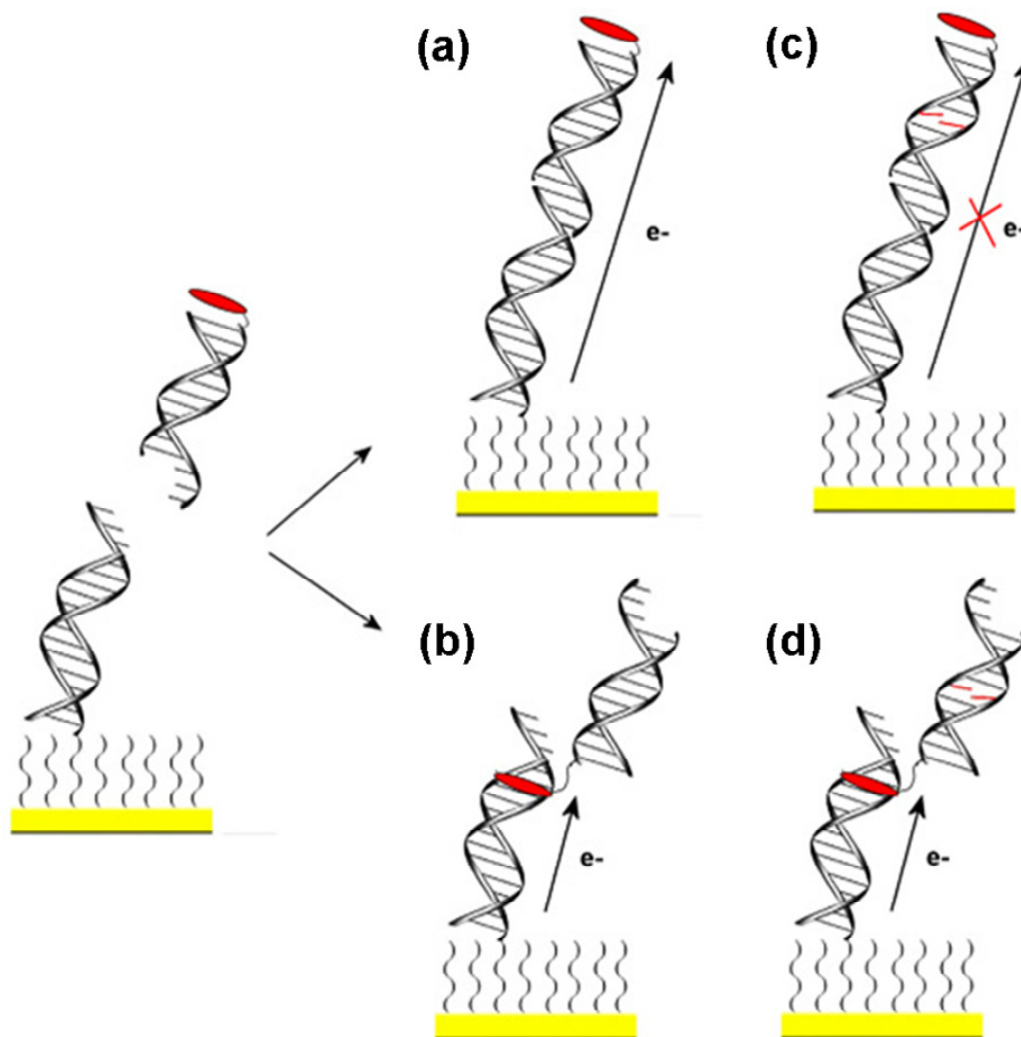


Figure 4.5. Sticky end experiment: A solution of sticky end AQ2-DNA (duplex **S4**) is added to a gold surface modified with the complementary sticky-end DNA (duplex **S1**). Two possible outcomes can be envisaged where a redox signal will be seen. **(a)** The complementary sticky-end portions of DNA anneal and a signal for an "end-capped" anthraquinone is observed. **(b)** The anthraquinone moiety intercalates into the bottom DNA duplex and a signal for the intercalated anthraquinone is observed. In order to confirm the binding mode, a mismatch can be incorporated into the top duplex (duplex **S5**). If the anthraquinone is endcapped **(c)** then the mismatch will cause a loss of redox signal. If the anthraquinone is intercalated into the bottom duplex **(d)**, then the mismatch will have no effect on the anthraquinone signal. A mismatch in the bottom duplex **S2** will attenuate either signal.

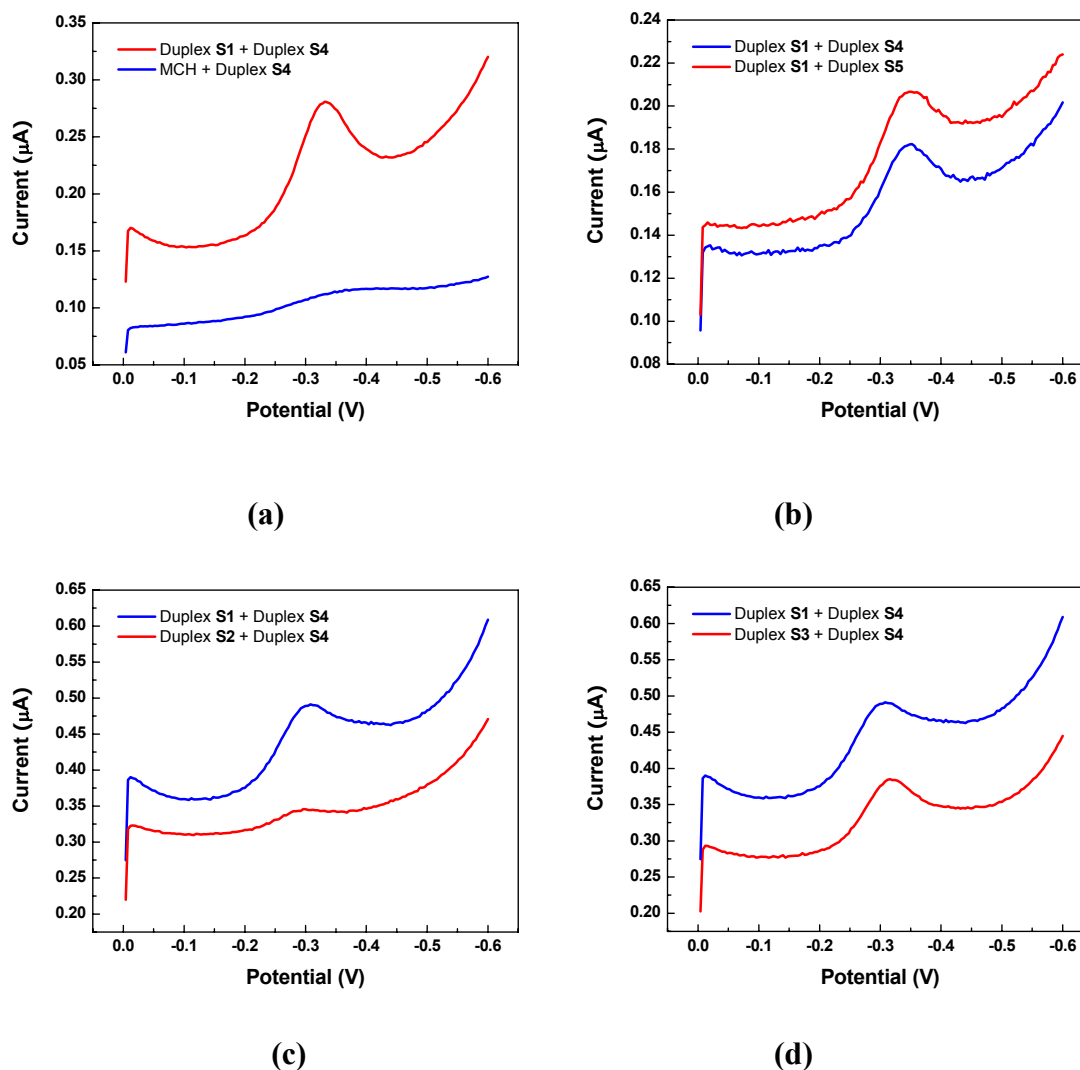


Figure 4.6. Square wave voltammetry of the sticky-end experiment (vs. Ag/AgCl). All experiments were performed in 5mM sodium phosphate, 50mM NaCl buffer at pH 7.3. **(a)** Signal from electrodes modified by sticky-ended duplex S1 and mercaptohexanol (MCH) after incubation with duplex S4. **(b)** Signals from electrodes modified with sticky-ended duplex S1 after incubation with top duplex S4 and top duplex S5 (single CA mismatch). **(c)** Signal from electrodes modified with sticky-ended bottom duplex S1 and with sticky-ended bottom duplex S2 (single CA mismatch) after incubation with fully matched top duplex S4. **(d)** Signals from electrodes modified with sticky-ended duplex S1 and blunt DNA S3 after incubation with matched top duplex S4.

replaced with a blunt end duplex (duplex **S3**), the AQ signal from duplex **S4** is unaffected. These observations all confirm that AQ is intercalated into the bottom duplex, and furthermore confirm the assignment for intercalated AQ at ~ -300 mV (vs. Ag/AgCl).

4.3.3 Redox properties as a function of DNA binding mode

This assignment for intercalated AQ indicates that a positive shift in potential is associated with base stacking. The AQ unit interacting directly with the electrode surface is instead reduced at -570 mV (AQ-U).³¹ An end-capped AQ is reduced at more positive potentials (-450 mV), while in the intercalated case, AQ is even more easily reduced (-300 mV). A positive shift of the redox couple upon intercalation in DNA has previously been observed in noncovalent AQ DNA adducts,³² and can be rationalized due to the effect of the more hydrophobic environment.

Importantly, the intensity of the redox signals also appears to be influenced by the type of interaction of the probe with the base pair stack: the peak currents associated with intercalated AQ are consistently smaller than those observed for end-capped AQ. It is difficult to discern whether this difference is solely the result of fewer probes interacting favorably with the base pair stack in the intercalative case or if the AQ moiety experiences improved coupling to the π -stack in the end capped case. Indeed, anthraquinone is known to be a relatively weak intercalator,³³ with binding constants on the order of 10^5 M⁻¹,³⁴ compared to 10^6 M⁻¹ for ethidium, a classic organic intercalator,³⁵ and 10^7 M⁻¹ for daunomycin, an anticancer drug.³⁶

Furthermore, electrochemistry of these DNA films has been demonstrated to be an effective way of distinguishing between different AQ binding modes. Redox potentials

for intercalated and end-capped AQ differ by ca. 100 mV. This potential shift may result from the change of the environment around the anthraquinone and reflect the interactions between the redox marker and DNA base stacks. Indeed, similar potential shifts have been reported for other anthraquinone derivatives and DNA intercalators. For instance, Yamana et al. tethered anthraquinone to the 2'-position of oligonucleotide and found that the reduction peak of the modified oligonucleotide shifted positively upon being hybridized with its complementary strand.³⁷ Metal complexes containing intercalative ligands have also been reported to undergo positive potential shift when interacting with double stranded DNA.³⁸

4.3.4 Implications with respect to DNA-mediated charge transport

These results underscore the importance of probe/ π stack interactions in DNA-mediated electrochemistry. **B1** and **B2** yield remarkably different electrochemical data although melting experiment shows that the AQ moiety stabilizes the double strand structure in both cases. Clearly, different interactions of the AQ moiety (endcapping, groove binding) can impart the similar thermodynamic stability on the DNA duplex, yet it is the degree of interaction with the base pair stack that ultimately determines the efficiency of DNA-mediated CT to and from the electrode surface. Significantly, endcapping has been shown to be a viable means of electronic access to the DNA π -stack as evidenced by the observation of the AQ redox couple by cyclic and square wave voltammetry. Indeed, DNA photooxidation studies with AQ2 modified DNA demonstrates that the anthraquinone group of AQ2 does have a close interaction with the

base stack of double stranded DNA (end-capping mode) and can be used to probe DNA-mediated charge transport.²³⁻²⁵

Our electrochemical studies on anthraquinone derivatives and works by Boon et al. with $[\text{Ru}(\text{NH}_3)_6]^{3+}$ and methylene blue²⁰ demonstrate that efficient charge transport to the DNA-binding moiety in DNA films requires electronic coupling between the binding moiety and DNA base stack. The binding mode can be either end-capping or base-pair intercalating. Poor interactions between the binding molecule and DNA base stack yields weak or no electron transfer between them. Thus redox markers that can well couple into the base stack of DNA is critical to mutation detection based on DNA-mediated charge transport.

4.4 SUMMARY

The electrochemistry of a series of anthraquinone-DNA conjugates is examined on DNA-modified gold electrodes. Two anthraquinone moieties prepared with tether lengths of two (AQ2) and five (AQ5) carbons are covalently attached to the 5' end of DNA oligonucleotides and were annealed to their complements to yield **B1** and **B2**, respectively. The presence of the AQ unit affords the same degree of stabilization to each duplex, as confirmed by melting temperature experiments. Despite this apparent similarity, the two conjugates show remarkably different electrochemical behavior when self-assembled onto gold electrodes. Cyclic voltammetry of **B2** shows no redox couple within the electrochemical window and only a very weak signal at -200 mV using square wave voltammetry, while **B1** shows a much stronger redox couple at -450 mV (vs. Ag/AgCl). This difference is rationalized in terms of the mode of interaction of the AQ with the DNA π -stack: in **B1**, the AQ moiety is end-capped while in **B2** it is mostly groove binding with a very small proportion intercalated. A second, weaker reduction wave is observed in **B1** at more positive potentials when the duplexes are tightly packed on the gold surface. This is consistent with the case where the AQ moiety from one duplex is intercalated into the base pair stack of a neighboring duplex. This assignment is confirmed by a series of experiments using sticky end AQ2 modified DNA. These experiments underscore the importance of direct interaction between the redox probe with the π -stack in order to observe efficient DNA-mediated electrochemistry through these films.

4.5 REFERENCES

1. Hall, D. B.; Holmlin, R. E.; Barton, J. K., Oxidative DNA damage through long-range electron transfer. *Nature* **1996**, 382, (6593), 731-735.
2. Nunez, M. E.; Hall, D. B.; Barton, J. K., Long-range oxidative damage to DNA: effects of distance and sequence. *Chemistry & Biology* **1999**, 6, (2), 85-97.
3. Henderson, P. T.; Jones, D.; Hampikian, G.; Kan, Y. Z.; Schuster, G. B., Long-distance charge transport in duplex DNA: The phonon-assisted polaron-like hopping mechanism. *Proceedings of the National Academy of Sciences of the United States of America* **1999**, 96, (15), 8353-8358.
4. Giese, B., Long-Distance Charge Transport in DNA: The Hopping Mechanism. *Acc. Chem. Res.* **2000**, 33, (9), 631-636.
5. Takada, T.; Kawai, K.; Cai, X.; Sugimoto, A.; Fujitsuka, M.; Majima, T., Charge Separation in DNA via Consecutive Adenine Hopping. *Journal of the American Chemical Society* **2004**, 126, (4), 1125-1129.
6. Nakatani, K.; Dohno, C.; Saito, I., Modulation of DNA-Mediated Hole-Transport Efficiency by Changing Superexchange Electronic Interaction. *Journal of the American Chemical Society* **2000**, 122, (24), 5893-5894.
7. Yoo, J.; Delaney, S.; Stemp, E. D. A.; Barton, J. K., Rapid Radical Formation by DNA Charge Transport through Sequences Lacking Intervening Guanines. *Journal of the American Chemical Society* **2003**, 125, (22), 6640-6641.
8. Delaney, S.; Yoo, J.; Stemp, E. D. A.; Barton, J. K., Charge equilibration between two distinct sites in double helical DNA. *Proceedings of the National Academy of Sciences of the United States of America* **2004**, 101, (29), 10511-10516.
9. O'Neill, M. A.; Barton, J. K., DNA-mediated charge transport requires conformational motion of the DNA bases: Elimination of charge transport in rigid glasses at 77 K. *Journal of the American Chemical Society* **2004**, 126, (41), 13234-13235.
10. Wan, C.; Fiebig, T.; Kelley, S. O.; Treadway, C. R.; Barton, J. K.; Zewail, A. H., Femtosecond dynamics of DNA-mediated electron transfer. *Proceedings of the National Academy of Sciences of the United States of America* **1999**, 96, (11), 6014-6019.

11. Bhattacharya, P. K.; Barton, J. K., Influence of intervening mismatches on long-range guanine oxidation in DNA duplexes. *Journal of the American Chemical Society* **2001**, 123, (36), 8649-8656.
12. O'Neill, M. A.; Becker, H. C.; Wan, C. Z.; Barton, J. K.; Zewail, A. H., Ultrafast dynamics in DNA-mediated electron transfer: Base gating and the role of temperature. *Angewandte Chemie-International Edition* **2003**, 42, (47), 5896-5900.
13. Ceres, D. M.; Barton, J. K., In situ scanning tunneling microscopy of DNA-modified gold surfaces: Bias and mismatch dependence. *Journal of the American Chemical Society* **2003**, 125, (49), 14964-14965.
14. Rajski, S. R.; Barton, J. K., How Different DNA-Binding Proteins Affect Long-Range Oxidative Damage to DNA. *Biochemistry* **2001**, 40, (18), 5556-5564.
15. Boon, E. M.; Ceres, D. M.; Drummond, T. G.; Hill, M. G.; Barton, J. K., Mutation detection by electrocatalysis at DNA-modified electrodes. *Nature Biotechnology* **2000**, 18, (10), 1096-1100.
16. Boon, E. M.; Salas, J. E.; Barton, J. K., An electrical probe of protein-DNA interactions on DNA-modified surfaces. *Nature Biotechnology* **2002**, 20, (3), 282-286.
17. Boal, A. K.; Barton, J. K., Electrochemical detection of lesions in DNA. *Bioconjugate Chemistry* **2005**, 16, (2), 312-321.
18. Delaney, S.; Pascaly, M.; Bhattacharya, P. K.; Han, K.; Barton, J. K., Oxidative Damage by Ruthenium Complexes Containing the Dipyridophenazine Ligand or Its Derivatives: A Focus on Intercalation. *Inorganic Chemistry* **2002**, 41, (7), 1966-1974.
19. Kelley, S. O.; Jackson, N. M.; Hill, M. G.; Barton, J. K., Long-range electron transfer through DNA films. *Angewandte Chemie-International Edition* **1999**, 38, (7), 941-945.
20. Boon, E. M.; Jackson, N. M.; Wightman, M. D.; Kelley, S. O.; Hill, M. G.; Barton, J. K., Intercalative stacking: A critical feature of DNA charge-transport electrochemistry. *Journal of Physical Chemistry B* **2003**, 107, (42), 11805-11812.
21. Yu, C. J.; Wan, Y.; Yowanto, H.; Li, J.; Tao, C.; James, M. D.; Tan, C. L.; Blackburn, G. F.; Meade, T. J., Electronic Detection of Single-Base Mismatches in DNA with Ferrocene-Modified Probes. *Journal of the American Chemical Society* **2001**, 123, (45), 11155-11161.

22. Immoos, C. E.; Lee, S. J.; Grinstaff, M. W., DNA-PEG-DNA Triblock Macromolecules for Reagentless DNA Detection. *Journal of the American Chemical Society* **2004**, 126, (35), 10814-10815.
23. Williams, T. T.; Dohno, C.; Stemp, E. D. A.; Barton, J. K., Effects of the Photooxidant on DNA-Mediated Charge Transport. *Journal of the American Chemical Society* **2004**, 126, (26), 8148-8158.
24. Shao, F. W.; O'Neill, M. A.; Barton, J. K., Long-range oxidative damage to cytosines in duplex DNA. *Proceedings of the National Academy of Sciences of the United States of America* **2004**, 101, (52), 17914-17919.
25. Gasper, S. M.; Schuster, G. B., Intramolecular Photoinduced Electron Transfer to Anthraquinones Linked to Duplex DNA: The Effect of Gaps and Traps on Long-Range Radical Cation Migration. *Journal of the American Chemical Society* **1997**, 119, (52), 12762-12771.
26. Kanvah, S.; Schuster, G. B., One-Electron Oxidation of DNA: The Effect of Replacement of Cytosine with 5-Methylcytosine on Long-Distance Radical Cation Transport and Reaction. *Journal of the American Chemical Society* **2004**, 126, (23), 7341-7344.
27. Veal, J. M.; Wilson, W. D., Modeling of Nucleic-Acid Complexes with Cationic Ligands - a Specialized Molecular Mechanics Force-Field and Its Application. *Journal of Biomolecular Structure & Dynamics* **1991**, 8, (6), 1119-1145.
28. Yu, H. Z.; Luo, C. Y.; Sankar, C. G.; Sen, D., Voltammetric Procedure for Examining DNA-Modified Surfaces: Quantitation, Cationic Binding Activity, and Electron-Transfer Kinetics. *Analytical Chemistry* **2003**, 75, (15), 3902-3907.
29. Kelley, S. O.; Boon, E. M.; Barton, J. K.; Jackson, N. M.; Hill, M. G., Single-base mismatch detection based on charge transduction through DNA. *Nucleic Acids Research* **1999**, 27, (24), 4830-4837.
30. Whittemore, N. A.; Mullenix, A. N.; Inamati, G. B.; Manoharan, M.; Cook, P. D.; Tuinman, A. A.; Baker, D. C.; Chambers, J. Q., Synthesis and Electrochemistry of Anthraquinone-Oligodeoxynucleotide Conjugates. *Bioconjugate Chemistry* **1999**, 10, (2), 261-270.
31. Kertesz, V.; Whittemore, N. A.; Inamati, G. B.; Manoharan, M.; Cook, P. D.; Baker, D. C.; Chambers, J. Q., Electrochemical detection of surface hybridization of

oligodeoxynucleotides bearing anthraquinone tags at gold electrodes. *Electroanalysis* **2000**, 12, (12), 889-894.

32. Yamana, K.; Kumamoto, S.; Hasegawa, T.; Nakano, H.; Sugie, Y., Electrochemistry of 2'-anthraquinone-modified oligonucleotide immobilized on gold surface: differential electron transfer efficiency between single and double helical forms. *Chemistry Letters* **2002**, (5), 506-507.

33. Tanious, F. A.; Yen, S. F.; Wilson, W. D., Kinetic and Equilibrium-Analysis of a Threading Intercalation Mode - DNA-Sequence and Ion Effects. *Biochemistry* **1991**, 30, (7), 1813-1819.

34. Breslin, D. T.; Schuster, G. B., Anthraquinone Photonucleases: Mechanisms for GG-Selective and Nonselective Cleavage of Double-Stranded DNA. *Journal of the American Chemical Society* **1996**, 118, (10), 2311-2319.

35. Baguley, B. C.; Falkenhaus, E. M., Interaction of Ethidium with Synthetic Double-Stranded Polynucleotides at Low Ionic-Strength. *Nucleic Acids Research* **1978**, 5, (1), 161-171.

36. Chen, Y. Z.; Zhang, Y. L., Calculation of the binding affinity of the anticancer drug daunomycin to DNA by a statistical mechanics approach. *Physical Review E* **1997**, 55, (6), 7390-7395.

37. Yamana, K.; Kumamoto, S.; Nakano, H.; Matsuo, Y.; Sugie, Y., Cyclic voltammetric responses in hybrid formation of 2'-anthraquinone-modified oligonucleotide with DNA. *Chemistry Letters* **2001**, (11), 1132-1133.

38. Carter, M. T.; Rodriguez, M.; Bard, A. J., Voltammetric Studies of the Interaction of Metal-Chelates with DNA .2. Tris-Chelated Complexes of Cobalt(III) and Iron(II) with 1,10-Phenanthroline and 2,2'-Bipyridine. *Journal of the American Chemical Society* **1989**, 111, (24), 8901-8911.

CHAPTER 5

DNA-Mediated Electrochemistry of DNA–Nile Blue Conjugates

5.1 INTRODUCTION

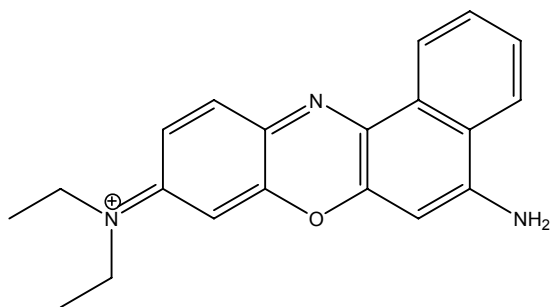
For a mutational assay based on DNA mediated CT, sensitivity is no longer limited to the differences in the melting temperature between a perfect DNA duplex and one containing a mismatch. In fact, the electronic coupling between the intercalative redox probe and the π -stack of DNA is critical to the sensitivity of an assay based on DNA mediated CT. Photochemical and biochemical experiments have demonstrated that efficient coupling of the donor and acceptor to the π -stack is a prerequisite for efficient DNA CT.¹ The extent of oxidative damage caused by CT in DNA, for example, can be directly correlated with intercalative binding of the oxidant.¹ It has also been demonstrated by electrochemical studies that effective intercalation into the π -stack by the redox active probe is necessary to differentiate DNA containing a mismatch from a perfect DNA duplex.^{2, 3} For instance, groove binding molecules, such as $[\text{Ru}(\text{NH}_3)_6]^{3+}$, are reduced on the electrode surface through facilitated diffusion along the groove of the immobilized duplexes, regardless of the presence of a mismatch.^{2, 4} On the other hand, end-capping probes, such as end-tethered anthraquinone, are poorly coupled to the π -stack and electron transfer between the probe and DNA is sluggish. The electrochemical response of such end capping probes features broad cathodic and anodic peaks and yields poor discrimination in electrochemical response between perfect and mismatched duplexes.⁵

Because of their high affinity for duplex DNA, methylene blue (MB) and daunomycin (DM) are two redox active intercalators that have been predominantly used in electrochemical assays based on DNA mediated CT. MB is usually used in a non-tethered mode in which the intercalator in solution can freely associate to and

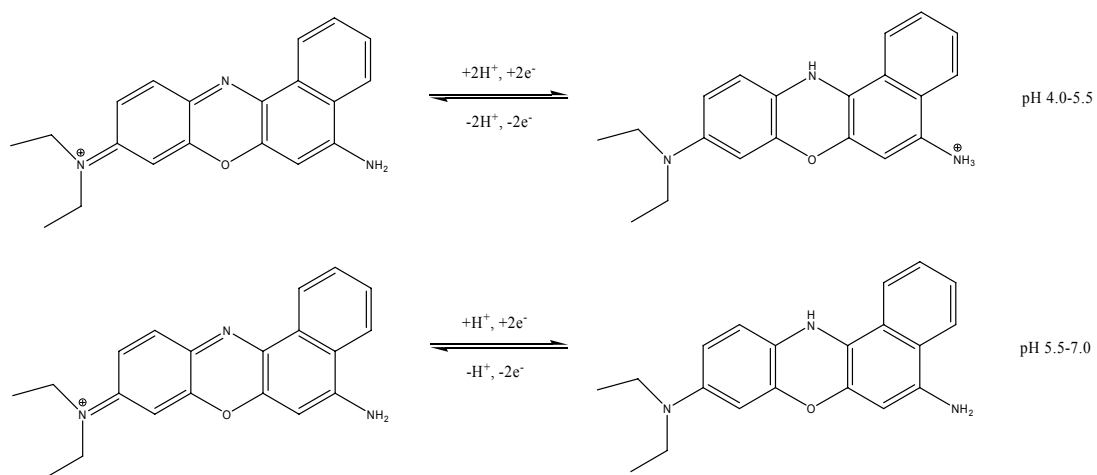
dissociate from the DNA duplex in the film. Assays using non-tethered intercalators require that DNA duplexes are densely packed on the electrode surface confining the intercalators to the top of the monolayers.⁶ Unlike MB, DM is usually covalently tethered to the duplex.³ The advantage of covalent tethering is obvious: the probe can be used on both loosely and densely packed films. Additionally, the ratio of DNA to the intercalator is strictly determined by the stoichiometry of the tethering reaction. Consequently, the amount of DNA on the surface can be easily derived from the charge accumulated during reduction of the intercalator. Therefore, covalent tethering is usually preferred in electrochemical assays involving DNA-mediated CT.

Although DM is well coupled to the π -stack of DNA, it is not an appropriate redox active marker for DNA immobilized on a gold surface by thiol-Au bond. The reduction potential of DM bound to DNA is \sim -650 mV (vs. SCE), at the edge of the potential window of a DNA film on gold. In our experiments, we found that cyclic voltammetric scans beyond -700 mV (vs. SCE) resulted in significant and non-reversible desorption of thiolated DNA from the gold surface, seriously hindering the sensitivity and reliability of the assay. In addition, the linkage between guanine and DM is not very stable.^{7,8} Our experiments have shown that the DNA-DM adducts tend to dissociate in diluted solution ($<1 \mu\text{M}$). Hence, an intercalator with a more stable crosslink and appropriate reduction potential is needed to improve the sensibility and reliability of an electrochemical assay based on DNA-mediated CT.

Nile blue (NB) is a cationic phenoxazine dye that has been widely used as an acid-base indicator and as a stain for fat, tissues, and nuclei of living or dead cells.^{9,10} The heterocyclic, planar structure (Scheme 5.1) and positive charge of NB suggest that it



Scheme 5.1. Structure of Nile blue.



Scheme 5.2. Redox reactions of Nile blue at different pH.

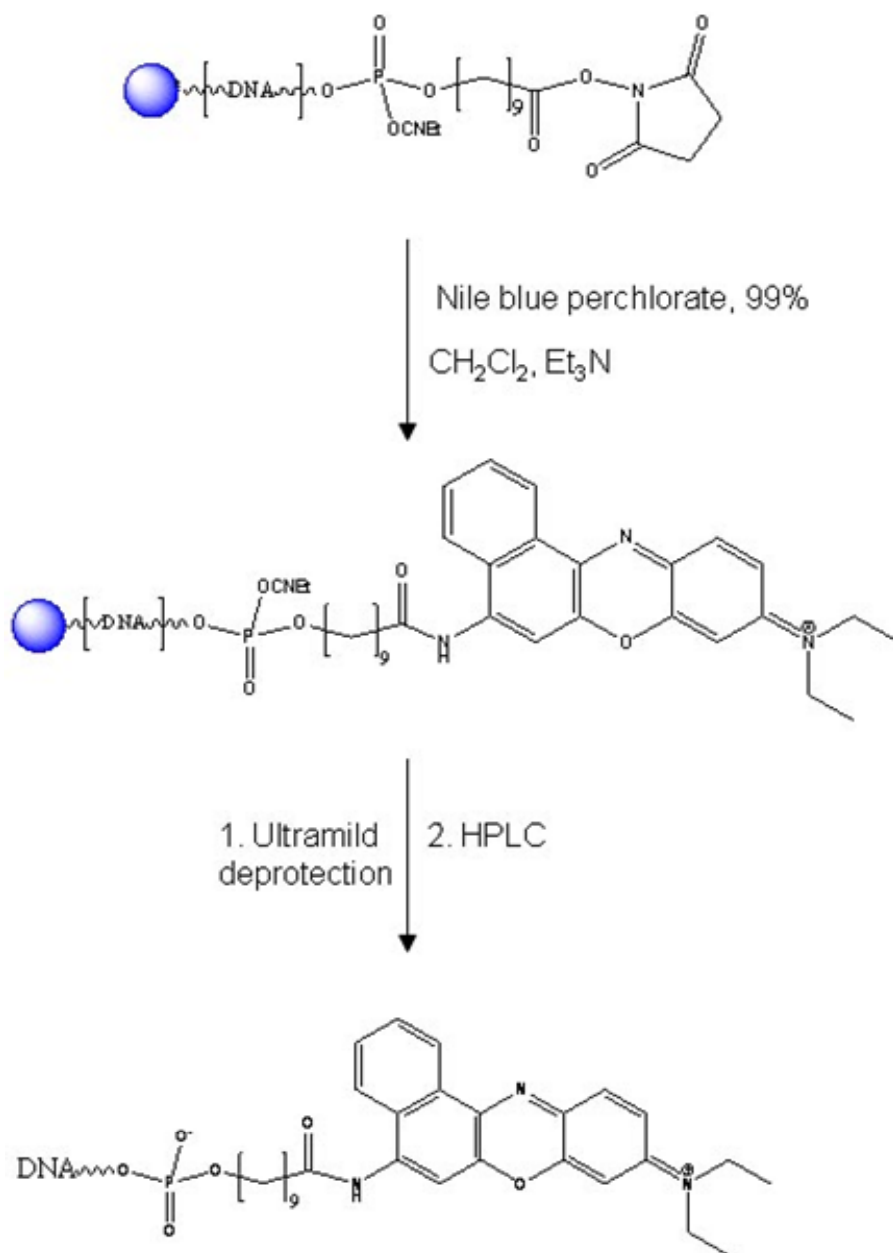
could interact strongly with the DNA base stack. It is believed that the planar hydrophobic phenoxazine moiety facilitates the intercalation of NB into the relatively nonpolar interior of the DNA double helix.¹¹ Indeed, spectral studies have shown that NB intercalates in the DNA helix and binds with high affinity.¹¹⁻¹⁵ A binding constant on the order of 10^6 M^{-1} was obtained by a fluorescence static quenching method.¹¹ Furthermore, NB is redox active with a formal potential of -360 mV (vs. SCE) in aqueous solution. At pH 7~8, it undergoes a quasi-reversible, $2 e^-$ reduction (Scheme 5.2).¹² NB has been generally used as an electron transfer mediator for the electrocatalytic reduction of biological molecules, such as hemoglobin,¹⁶ NADH,^{17, 18} and horseradish peroxidase.¹⁸ Because of its high affinity for duplex DNA, it has also been used as a redox active reporter of DNA hybridization.¹² The excellent intercalative and electrochemical characteristics of NB suggest that it may function as an efficient redox active probe for DNA-mediated CT.

In this Chapter, we develop a method to covalently tether NB to the 5'-end of an oligonucleotide and explore the DNA-NB conjugate electrochemically. Based on the electrochemical properties of the DNA-NB conjugate, we propose a label-free method for mismatch detection in which the modification of target DNA is not required. These studies may help to develop a new generation of DNA sensors for mutation detection based on DNA-mediated CT.

5.2 MATERIALS AND METHODS

5.2.1 Materials

DNA synthesis reagents were obtained from Glen Research. Nile blue A



Scheme 5.3. Scheme for the synthesis of DNA-NB conjugate.

perchlorate (laser grade, 99+%) was obtained from Acros Organics. Dry organic solvents (dichloromethane, DMF, methanol, acetonitrile, triethylamine) were obtained from Fluka in the highest available grade for the synthesis of the DNA-NB conjugate. Mercaptohexanol (MCH) and mercaptoundecanoic acid (MUA) were purchased from Aldrich at the highest purity available. For DNA synthesis and purification, a 50 mM, pH 7.4 sodium phosphate buffer (PBS) was used. A 5 mM sodium phosphate, 50 mM sodium chloride buffer was used for electrochemical analysis (Echem buffer, pH 7.4). Millipore Milli-Q water (18 M Ω cm) was used for all experiments.

5.2.2 *Synthesis of DNA-NB conjugate*

A scheme for the synthesis of the DNA-NB conjugate is illustrated in Scheme 5.3. Oligonucleotides (3.0 μ mol) modified with an N-hydroxysuccinimide ester at the 5' end were synthesized on an ABI 392 model DNA synthesizer using the ultramild synthesis method, in which phenoxyacetyl (Pac) protected dA and 4-isopropylphenoxyacetyl (iPr-Pac) protected dG were used instead of the normal CE phosphoramidites.¹⁹ The controlled pore glass (CPG) beads supporting the oligonucleotides were then rinsed by dry acetonitrile and dichloromethane in a glass coupling tube. A 10-fold excess of NB (30 μ mol, 12.5 mg) was dissolved in 2 ml dry DMF with 10% triethylamine and the mixture was added to the coupling tube containing the CPG beads. After being vortexed for 20 hours, the solution was removed and the beads were washed sequentially with DMF, methanol, acetonitrile and dichloromethane. The DNA-NB conjugates were then cleaved from the CPG resin and the protecting groups were removed by incubating with 50 mM K₂CO₃/methanol for 8 hours at room

temperature. The liquid phase was neutralized by 2 mL of 2 M acetic acid-triethylamine solution and was desalted by NAP-10 column (Amersham Biosciences). After being dried in a lyophilizer, the DNA-NB conjugate was purified twice by reverse phase HPLC on a C-18 300 Å column.

The purified product was dried in the lyophilizer and was characterized by UV-visible spectroscopy and mass spectrometry. The sequence and mass of the DNA-NB conjugates are shown in Table 5.1. The extinction coefficient of DNA ($\lambda_{\text{max}} = 260 \text{ nm}$, $\epsilon_{\text{DNA}}(\text{M}^{-1}\cdot\text{cm}^{-1})$) was calculated by OligoAnalyzer 3.0 provided by IDT. The contribution of NB moiety to the extinction coefficient of the conjugate is $15,500 \text{ M}^{-1}\cdot\text{cm}^{-1}$ at 260 nm, determined by measuring the UV-visible absorption of a mixture of equimolar oligonucleotide and acetyl-NB in Echem buffer.

5.2.3 Preparation of DNA-modified surfaces

Thiol-modified single-stranded oligonucleotides were prepared as previously described in Chapter 2. All oligonucleotides were purified by reverse phase HPLC and characterized by UV-visible spectroscopy and mass spectrometry. The sequences of oligonucleotides used in the experiments are listed in Table 5.2.

For experiments with blunt DNA, the thiol-modified single strands were hybridized with their NB modified complements by heating equimolar amounts of each strand in Echem buffer to 90°C followed by slow cooling to ambient temperature. The thiol-modified duplexes were deposited on a gold electrode surface for 12-24 hours and backfilled with 1 mM mercaptoundecanoic acid (MUA) for 1 hour. The electrode was then thoroughly rinsed in Echem buffer before use in electrochemical experiments. When

Table 5.1. DNA-NB conjugates*

	Sequence	Mass (by ESI-MS)	Calculated Mass
NB-1	NB-5' -CGCGATGACTGTACT-3'	5118.0	5117.4
NB-2	NB-5' -ACGATGTCATGCGATGACTGCACT-3'	7902.6	7902.2
NB-3	NB-5' -ACGATGACTCCTAGTGTCTC-3'	6617.6	6617.4

*Nile blue (NB) is covalently tethered to the 5'-end of DNA through a decyl amide linkage.

Table 5.2. DNA sequences[†]

B-TA	HS-5' -AGTACAGTCATCGCG-3' 3' -TCATGTCAGTAGCGC-5' -NB
B-CA	HS-5' -AGTACAG CC ATCGCG-3' 3' -TCATGTC AG TAGCGC-5' -NB
P1	HS-5' -AGTGCAGTCATC-3'
T1-TA	5' -GCATGACATCGT-3' 3' -TCACGTCAGTAGCGTACTGTAGCA-5' -NB
T1-CA	5' -GCA CG ACATCGT-3' 3' -TCACGTCAGTAGCGT ACT GTAGCA-5' -NB
P2	HS-5' -AGTACAGTCATC-3'
M-TA	5' -AGCAGTATAGATGACGAGACACTAG-3' 3' -TCATGTCAGTAGTCGTCATATCTACTG-5'
M-CA	5' -AGCAGTA CA GATGACGAGACACTAG-3' 3' -TCATGTCAGTAGTCGTCAT AT CTACTG-5'
T2	5' -GAGTCATCGT-3' 3' -CTCTGTGATCCTCAGTAGCA-5' -NB

[†]The positions of mismatches are highlighted in bold and italics.

tightly packed monolayers were required, 0.1 M MgCl_2 was added to the duplex solution before deposition on the gold surfaces and the electrodes were not backfilled after the deposition.

For experiments on DNA containing a base overhang, the thiol-modified oligonucleotides (10 μM) were deposited on the gold electrode surface for 6 hours and backfilled with 1 mM MCH for 1 hour. The electrode was subsequently rinsed in Echem buffer. The modified electrode was then incubated with 1 μM DNA containing an overhang at room temperature for hybridization. The electrode was again thoroughly rinsed in Echem buffer before use in electrochemical experiments.

5.2.4 Electrochemical measurements

Cyclic voltammetry and square wave voltammetry were carried out under an Ar atmosphere on 0.02 cm^2 gold electrodes using a CH Instruments 760B electrochemical analyzer. A normal three-electrode configuration was used, consisting of a modified gold-disk working electrode, a platinum wire auxiliary electrode, and a saturated calomel reference electrode (SCE, Fisher Scientific). A modified Luggin capillary separated the working compartment of the electrochemical cell from the reference compartment. Potentials are reported versus SCE. Polycrystalline gold electrodes were polished sequentially with 1.0, 0.3, and 0.05 micron alumina slurry, followed by etching in 1.0 M H_2SO_4 and thorough rinsing with Milli-Q water prior to DNA deposition. For electrocatalytic experiments and AC impedance measurements, 2 mM $[\text{Fe}(\text{CN})_6]^{3-}$ in Echem buffer was used. All electrochemical measurements were carried out at room temperature.

5.3 RESULTS AND DISCUSSION

5.3.1 Electrochemistry of blunt DNA-NB conjugates

A schematic representation of the DNA-NB modified electrode and the DNA sequences used in these studies is illustrated in Figure 5.1. NB is covalently tethered to the 5' end of DNA in order to restrict the intercalation site of NB to the top of the DNA film. The UV-visible absorption profile of DNA-NB features a characteristic peak at 600 nm which corresponds to absorption of acyl-NB (Figure 5.2). The reported extinction coefficient of acetyl-NB is $30,000 \text{ M}^{-1}\cdot\text{cm}^{-1}$ at 600 nm.²⁰ Using this number, the ratio of DNA to NB is determined to be 1:1. A change in HPLC retention time and the mass spectrometry also confirmed the tethering of NB to DNA. Melting temperature experiments indicate that the duplexes with tethered NB melt at 58 °C (3.3 μM DNA-NB, 5 mM sodium phosphate, 50 mM NaCl, pH 7.4), which is ~ 5 °C higher than that of the unmodified DNA duplex. This stabilization of the duplex can be attributed to intercalation of the NB moiety into the base stack.

DNA-modified electrodes are prepared with the DNA-NB adducts hybridized to the thiol-derivatized complements. A solution of 100 μM duplexes (**B-TA**) in Echem buffer containing 100 mM Mg^{2+} is added to the gold electrodes to yield a densely packed monolayer. We estimate the surface coverage of the duplexes to be $\sim 20 \text{ pmol}/\text{cm}^2$, as quantified by $[\text{Ru}(\text{NH}_3)_6]^{3+}$ assay. The cyclic voltammetric response of the **B-TA** modified electrode exhibits a pronounced electrochemical signal at $\sim -250 \text{ mV}$ versus SCE (Figure 5.3). The amount of NB reduced is determined to be $18.7(\pm 2) \text{ pmol}/\text{cm}^2$ by integration of the cathodic peak assuming a two-electron reduction. This is consistent with the quantification of DNA coverage by $[\text{Ru}(\text{NH}_3)_6]^{3+}$ measurements, and indicates a

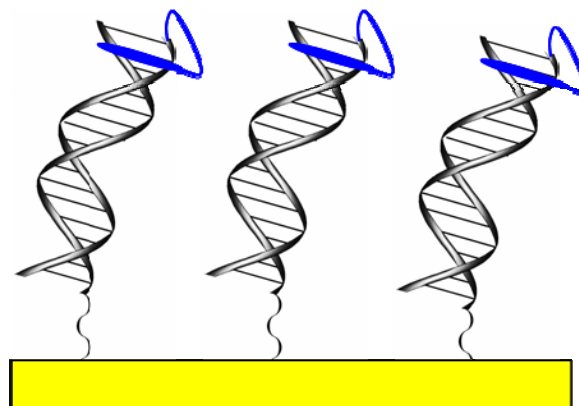


Figure 5.1. Schematic illustration of a gold electrode (yellow) modified with DNA duplexes with covalently tethered Nile blue (blue). Also shown is the sequence of the DNA duplex, with the position of an intervening CA mismatch highlighted in red.

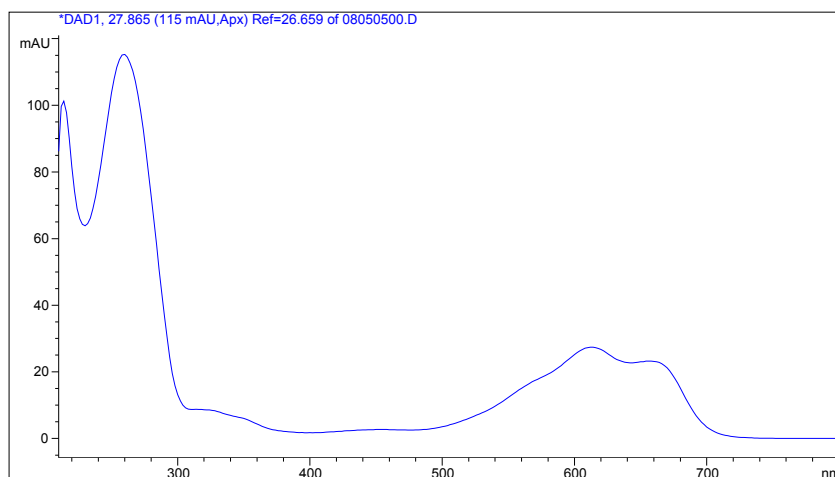


Figure 5.2. UV-visible absorption profile of DNA-NB conjugate. It features a characteristic peak at 600 nm which corresponds to absorption of acyl-NB.

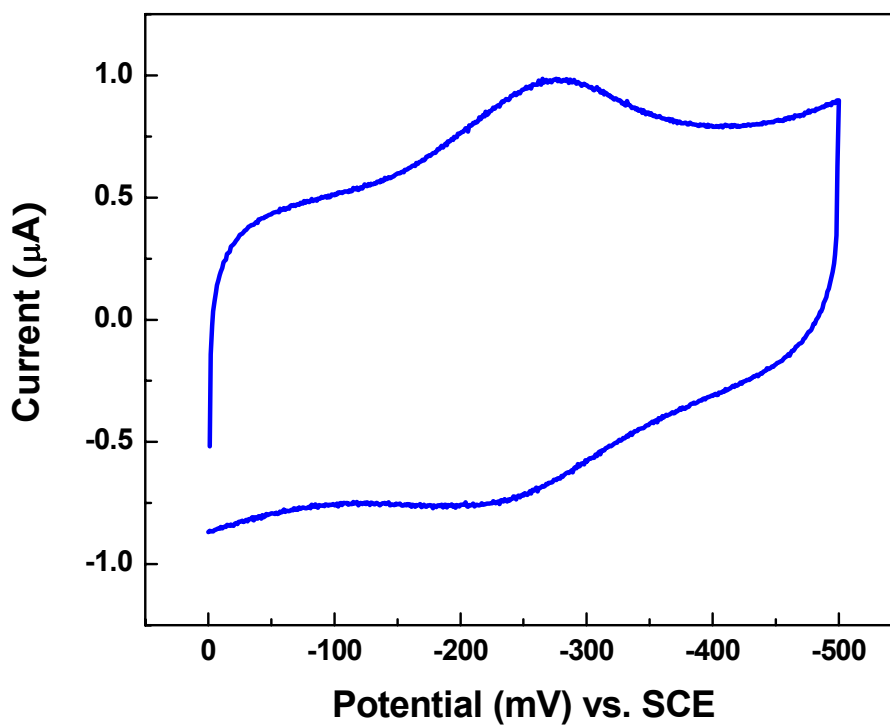
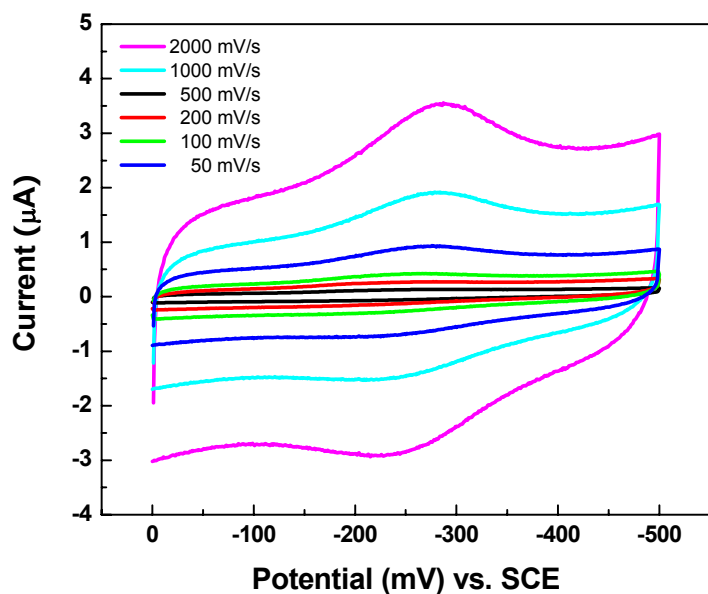


Figure 5.3. Cyclic voltammetry of a gold electrode modified with a densely packed **B-TA** film in Echem buffer (scan rate = 500 mV/s). A pronounced electrochemical signal is observed at ~ -250 mV (vs. SCE). The amount of NB reduced is determined to be $18.7 (\pm 2)$ pmol/cm² by integration of the cathodic peak, assuming a two-electron reduction.

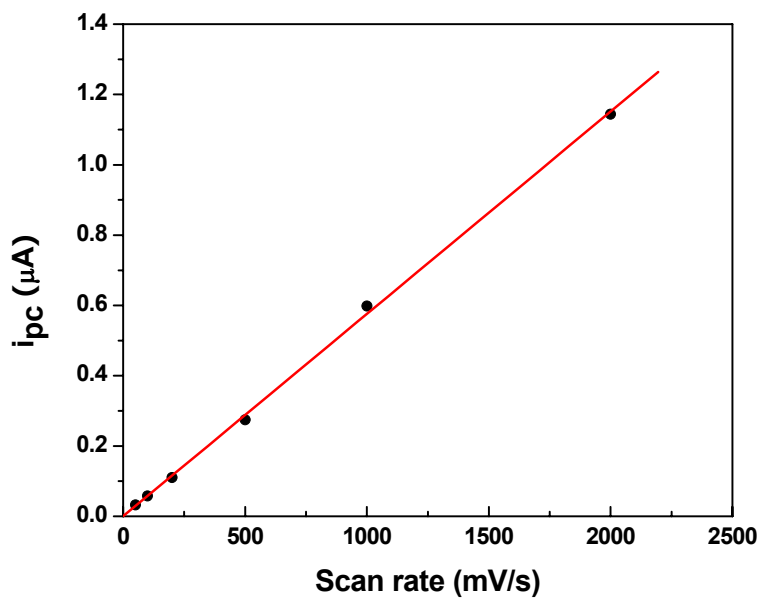
1:1 ratio of NB to DNA on the surface. Furthermore, by varying the scan rate, we obtain a linear dependence of peak current on scan rate which confirms that the NB is surface bound (Figure 5.4).

It is noteworthy that the peak-to-peak separation in the cyclic voltammograms of DNA-NB films is very similar to that of DNA-DM conjugates. The electron transfer rate constant (k_s) is estimated from the characteristic splittings between cathodic and anodic peaks as a function of scan rate, following Laviron's approach.^{21, 22} Indeed, we estimate that the rate constant of electron transfer via the DNA-NB film is $\sim 30 \text{ s}^{-1}$, which is on the same order of magnitude as that of the DNA-DM conjugates (Figure 5.5).^{3, 23} This similarity in electron transfer rate indicates that NB is coupled to the base pair stack of the DNA duplex in a manner similar to DM.

Furthermore, the signal observed for the DNA-NB film is at a potential different from NB on bare gold, without DNA. It has been reported that the formal potential of a NB self-assembled monolayer (SAM) on a gold electrode is -0.388 V (vs. SCE) in 100 mM pH 7.0 PBS.¹⁸ Here we obtain a formal potential of -0.250 V (vs. SCE) in Echem buffer (5 mM, pH 7.4 PBS with 50mM NaCl). This significant potential shift likely results from the change of the environment around the NB moiety, which implies a strong interaction between NB and the DNA duplexes. Indeed, we have observed similar positive potential shifts in our studies with anthraquinone derivatives, and found that the differences in reduction potentials of the redox probe reflect differences in the binding mode of the probe to DNA. All of these data suggest that the NB moiety in the DNA-NB film is reduced via a DNA-mediated pathway, rather than directly at the electrode surface.



(a)



(b)

Figure 5.4. (a) Cyclic voltammograms of B-TA modified electrode at various scan rates. (b) Plot of cathodic peak current vs. scan rate. Peak current is proportional to scan rate. This linearity demonstrated that the redox active species, NB, was bound to surface.

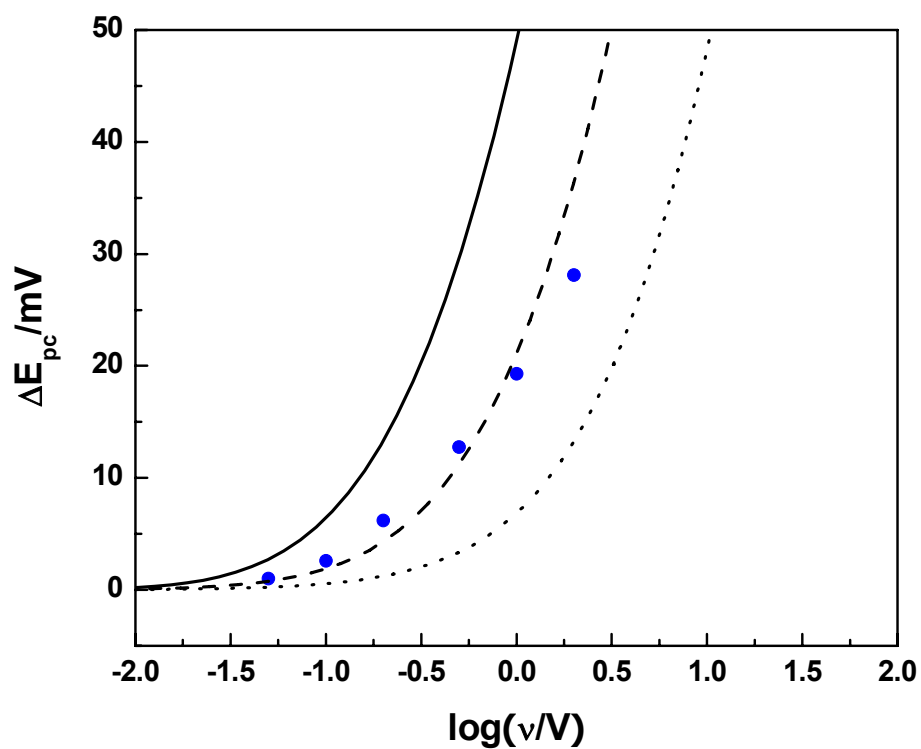


Figure 5.5. Plot of peak splitting ΔE_{pc} (where $\Delta E_{pc} = E_{pc} - E^\circ$) versus $\log(v)$ (where $v =$ scan rate) for electrode modified with **B-TA** (blue dots). Working curves corresponding to standard rate constants of 10 s^{-1} (—), 30 s^{-1} (- - -), and 100 s^{-1} ($\cdot\cdot\cdot$) are shown for comparison.^{21,22}

DNA-mediated electrochemistry is perhaps best demonstrated in comparative experiments with intervening base pair mismatches. We find here too that reduction of the DNA-NB films containing an intervening CA mismatch yields a significant attenuation in the electrochemical signal compared to that of the fully matched DNA-NB film (Figure 5.6). This confirms that the electrochemistry is DNA mediated.

5.3.2 *Electrocatalysis of Nile blue*

Although mismatches in DNA can be distinguished by direct voltammetry of redox active intercalators (i.e., DM, MB), there are inherent limitations to the sensitivity of such assays. In order to improve the discrimination between fully base-paired and mismatched DNA duplexes, the Barton group has previously coupled the direct electron transfer event to an electrocatalytic process involving a species (i.e., $[\text{Fe}(\text{CN})_6]^{3-}$) freely diffusing in solution.⁶ This effectively amplifies the signal corresponding to the reduction of intercalator bound to DNA. Using this method of electrocatalysis, all single base mismatches, including thermodynamically stable GT and GA mismatches, have been detected within DNA and DNA/RNA hybrid duplexes.²⁴ In those experiments, however, a noncovalent intercalator (MB) was used as the redox probe and the DNA duplexes had to be densely packed in the film to assure the intercalator is bound only to the top of the DNA film. Here we explore the possibility of using NB as the covalent intercalator in an electrocatalytic analysis of DNA-mediated electron transfer.

The gold electrode is first modified with a film of densely packed DNA-NB conjugates, and $[\text{Fe}(\text{CN})_6]^{3-}$ is used as the solution-borne substrate. Strikingly, a pronounced electrochemical signal is observed at the fully base-paired DNA-NB

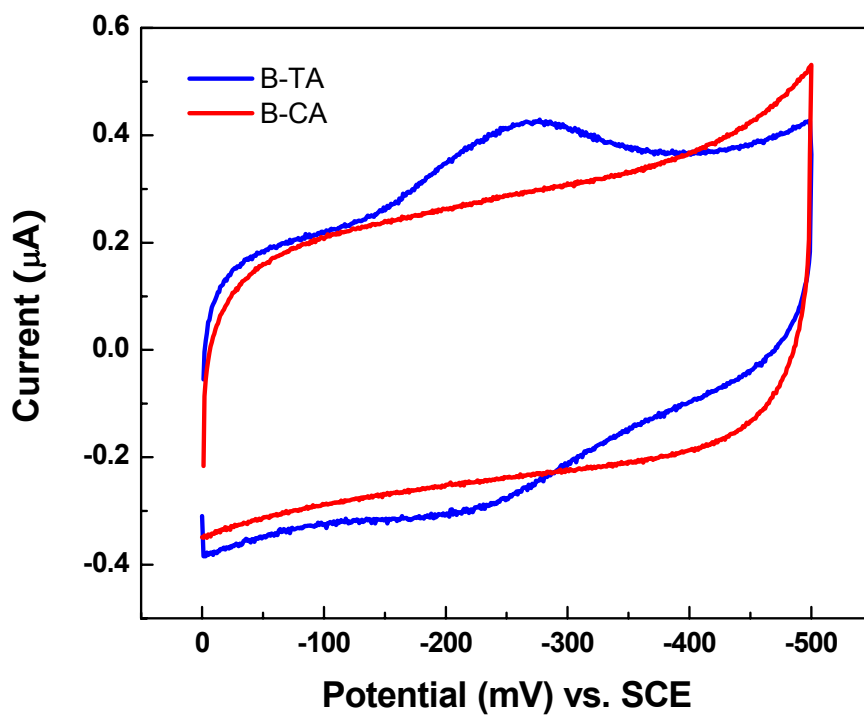


Figure 5.6. Cyclic voltammetry of electrodes modified with fully base paired DNA-NB duplex (**B-TA**, blue) and CA mismatched DNA-NB duplex (**B-CA**, red) in Echem buffer (scan rate = 200 mV/s). The intervening CA mismatch results in a significant attenuation of the electrochemical signal.

modified electrode in Echem buffer with 2.0 mM $[\text{Fe}(\text{CN})_6]^{3-}$ (Figure 5.7.). Notably, this signal comes at the reduction potential of intercalated NB and is completely irreversible. The qualitative shape of the signal resembles MB/ $\text{K}_3\text{Fe}(\text{CN})_6$ electrocatalysis experiments. These data are consistent with the idea that the covalent intercalator of NB can be used in the electrocatalytic assay as effectively as noncovalent intercalators.

We further use electrocatalysis to detect mismatches in loosely packed DNA films. As illustrated in Figure 5.8, the DNA-NB conjugate (1 μM DNA in Echem buffer in the absence of Mg^{2+}) is deposited on a gold electrode for 6 hours at room temperature to yield a loosely packed film. The surface of the electrode is backfilled with mercaptoundecanoic acid (MUA) for 1 hour. This backfilling effectively blocks access of $[\text{Fe}(\text{CN})_6]^{3-}$ to the gold surface so that it can not be reduced directly at the electrode surface (Figure 5.9). Figure 5.10(a) illustrates cyclic voltammograms of electrodes modified with fully base paired DNA-NB conjugates (**B-TA**) and electrodes modified with DNA-NB conjugates containing an intervening CA mismatch (**B-CA**) in Echem buffer without $[\text{Fe}(\text{CN})_6]^{3-}$. The corresponding cyclic voltammograms after adding 2 mM $[\text{Fe}(\text{CN})_6]^{3-}$ are shown in Figure 5.10(b). Notably, adding $[\text{Fe}(\text{CN})_6]^{3-}$ drastically amplifies the difference in the electrochemical signals between fully base paired duplexes (**B-TA**) and mismatched duplexes (**B-CA**). This difference could barely be observed in cyclic voltammograms without $[\text{Fe}(\text{CN})_6]^{3-}$. More specifically, the difference between the peak currents of **B-TA** and **B-CA** is 80-fold larger in the presence of $[\text{Fe}(\text{CN})_6]^{3-}$. Hence, electrocatalysis both increases the sensitivity of mismatch detection and provides larger absolute signals.

It is noteworthy that densely a packed DNA film is not required, as an

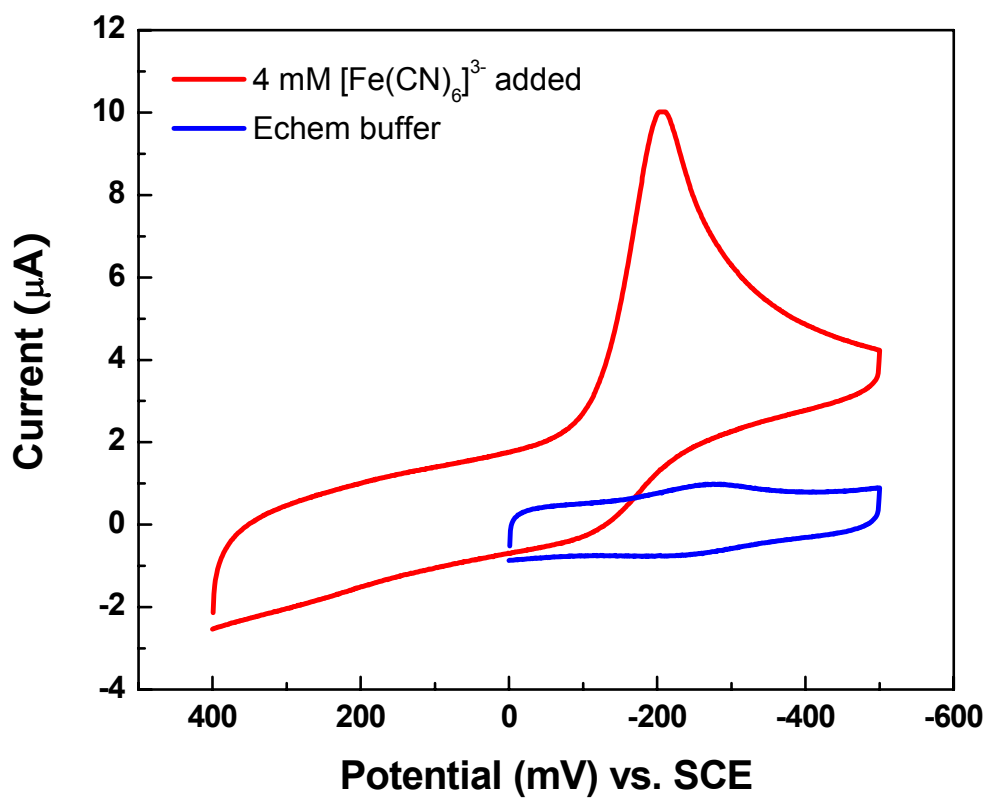


Figure 5.7. Cyclic voltammetry (scan rate = 500 mV/s) of an electrode modified with a densely packed DNA-NB duplex (**B-TA**) in Echem buffer (blue) and in 2 mM $[\text{Fe}(\text{CN})_6]^{3-}$ (red).

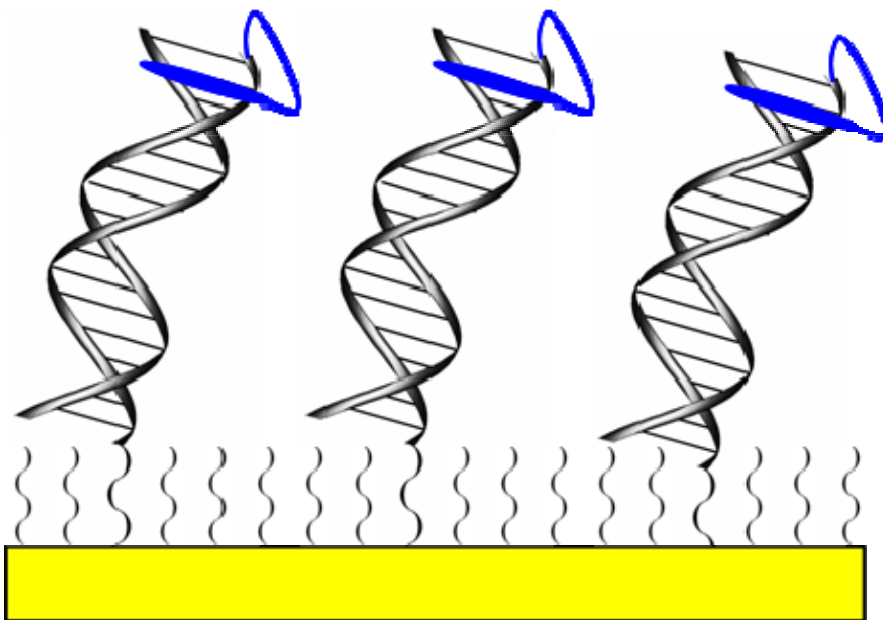


Figure 5.8. Schematic illustration of a gold electrode modified with loosely packed DNA-NB duplexes, backfilled with mercaptoundecanoic acid (MUA).

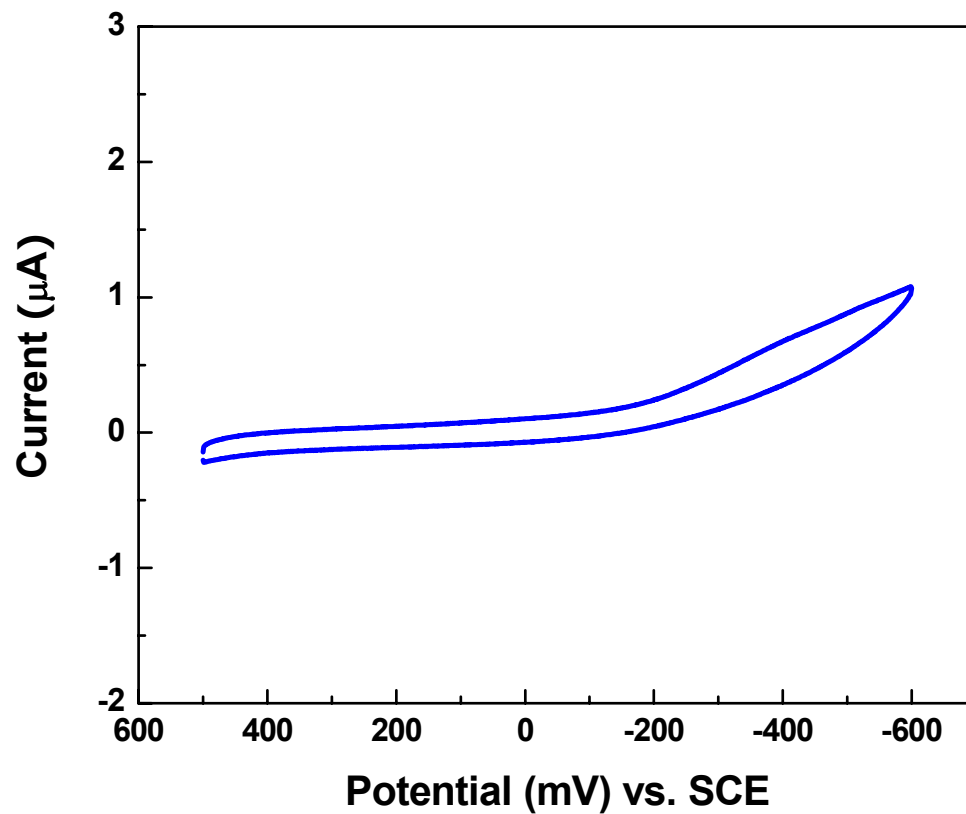
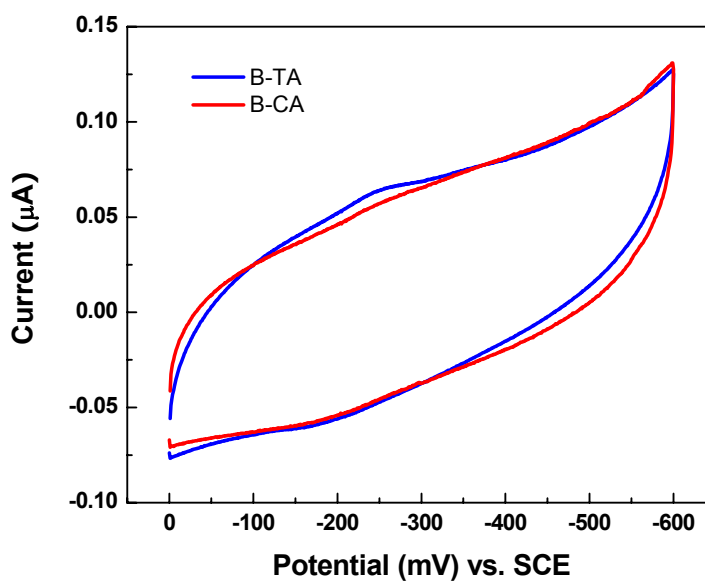
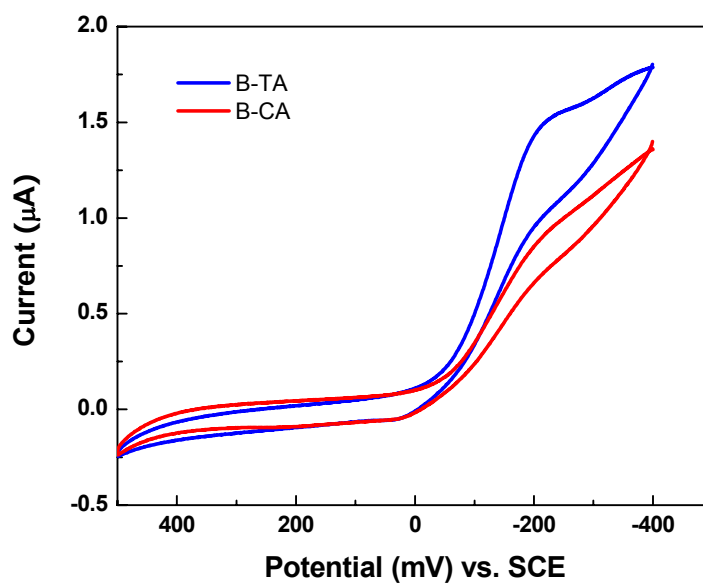


Figure 5.9. Cyclic voltammetry of a gold electrode modified with MUA monolayer in Echem buffer containing 2 mM $[\text{Fe}(\text{CN})_6]^{3-}$ (scan rate = 0.2 mV).



(a)



(b)

Figure 5.10. Cyclic voltammetry of electrodes modified with loosely packed **B-TA** (blue) and **B-CA** (red) which were backfilled with MUA, in Echem buffer (scan rate = 50 mV/s) in the absence (a) and the presence (b) of 2 mM $[\text{Fe}(\text{CN})_6]^{3-}$.

advantageous result of the covalent tethering of NB. By integrating the charge accumulated in the observed cathodic peak, we can estimate the DNA coverage to be $<1 \text{ pmol/cm}^2$. Therefore, by using covalently tethered NB and electrocatalysis, we can greatly increase the viability of electrochemical mismatch detection by charge transport via DNA.

5.3.3 Detection of the trapping of DNA duplexes containing base overhangs on electrodes

A possible application of the DNA-NB conjugate is to monitor the trapping of DNA duplexes with base overhangs onto electrodes modified with single stranded probes. We have previously described a similar strategy in which duplexes containing a base overhang were used as the anchored probes and daunomycin was used as the covalently tethered intercalator (see Chapter 3). However, because of the aforementioned problems with the reduction potential and the crosslink stability issues, covalently tethered DM is inherently limited in sensitivity and viability. Therefore, here we use NB as a substitute for daunomycin and couple the trapping event with an electrocatalytic assay in order to improve the method.

As shown in Figure 5.11, gold electrodes are modified with loosely packed single stranded probes (**P1**) and backfilled with MCH (1mM, for 1 hour) to remove nonspecifically absorbed probes. A solution of 1 μM DNA-NB duplex (**T1-TA**) containing a base overhang is added to the electrode (5 mM sodium phosphate, 1 M NaCl, pH 7.4). The electrode is interrogated by square wave voltammetry in Echem buffer and by AC impedance measurements in Echem buffer containing 4 mM $[\text{Fe}(\text{CN})_6]^{3-}$ at 0.155 V (vs. SCE) from 0.1 Hz to 100 kHz.

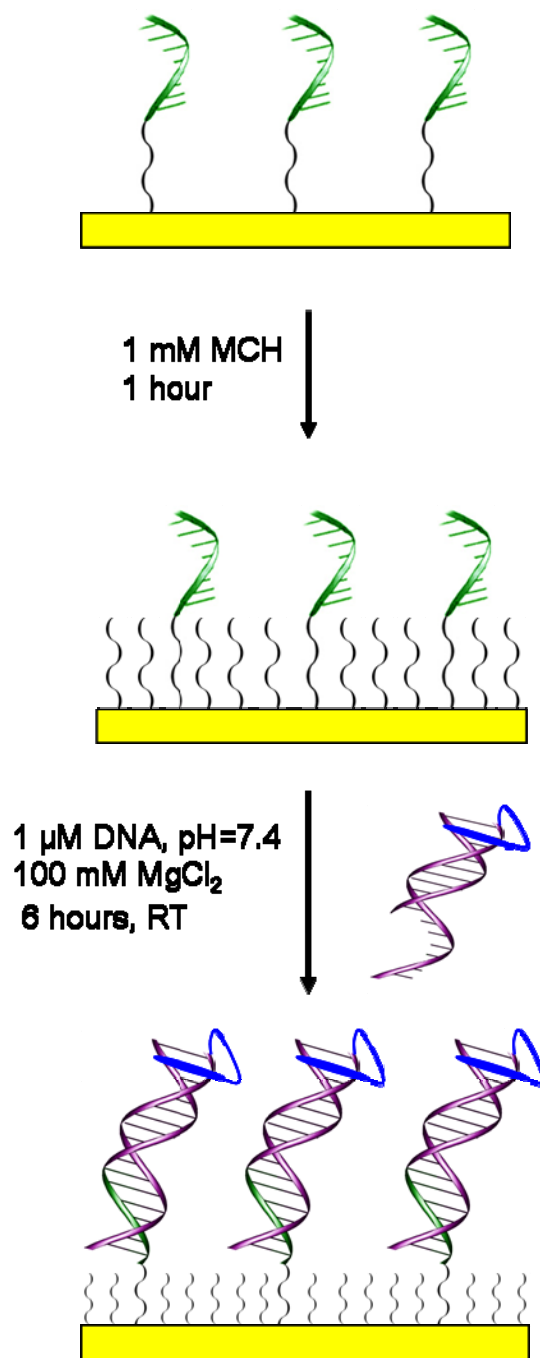


Figure 5.11. Schematic illustration of the trapping of DNA duplexes containing an overhang (violet) on a gold electrode modified with single stranded probe (green). The covalently tethered NB is in blue.

AC impedance measurements have been used as a label-free method for the detection of *in situ* hybridization of DNA on an electrode surface.²⁵⁻²⁹ The method is simple, sensitive and requires no labeling of the analyte with a redox active moiety. Using AC impedance measurements, we monitor *in situ* hybridization of **T1-TA** to the **P1** probe and explore its reversibility. Figure 5.12 illustrates the Nyquist plots for **P1** modified electrodes incubated with **T1-TA** solution, heat denatured, and reincubated with a noncomplementary strand and **T1-TA** again. Notably, the trapping of **T1-TA** is fast as the impedance of the electrode reaches its maximum in 18 minutes. Furthermore, it is highly reversible and the probe modified electrodes can be used repeatedly. The trapped duplexes are completely removed by heating the electrode at 70 °C in Milli-Q water; reincubation with the **T1-TA** solution resulted in restoration of the AC impedance. On the other hand, incubation with a noncomplementary strand causes no change in impedance.

Experiments by square wave voltammetry confirm the findings obtained by AC impedance measurements. The results of these experiments are shown in Figure 5.13. In these experiments, a **P1** modified electrode is first incubated with **T1-TA** solution for 1 hour and is then heated in Milli-Q water at 70 °C for 15 minutes. After the removal of **T1-TA**, the electrode is incubated with **T1-CA** which contains an intervening CA mismatch. As shown in Figure 5.13, a signal consistent with the reduction of NB is detected at -250 mV (vs. SCE) after the incubation with **T1-TA**; this signal almost vanishes after heat denaturing. Reincubation with **T1-CA** hardly causes any change in the signal, although AC impedance measurements indicate that a significant amount of **T1-CA** is trapped at the surface; subsequent reincubation with **T1-TA** results in the restoration of the electrochemical signal. These observations confirm that trapping the

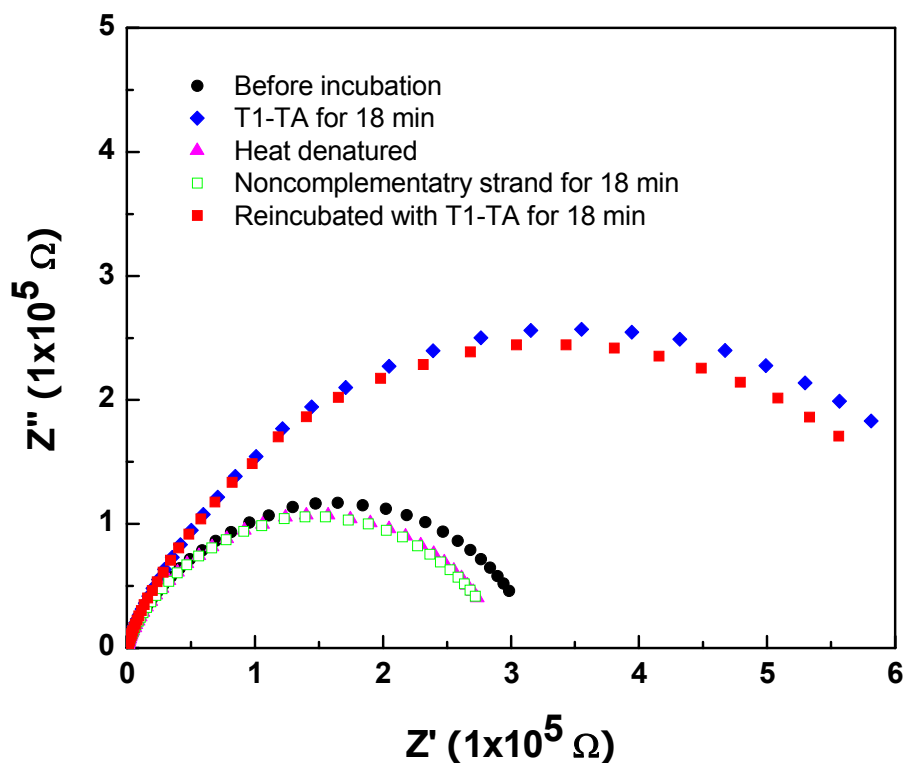


Figure 5.12. Nyquist plots of the probe modified electrode response at different stages in the study of trapping DNA duplexes. Before incubation with **T1-TA** (●), after incubating with **T1-TA** (1 μM) for 18 minutes (◆), after heat denatured in Milli-Q water at 70 °C for 15 minutes (▲), after incubating with a noncomplementary strand for 18 minutes (□), and after reincubating with **T1-TA** (1 μM) for 18 minutes (■).

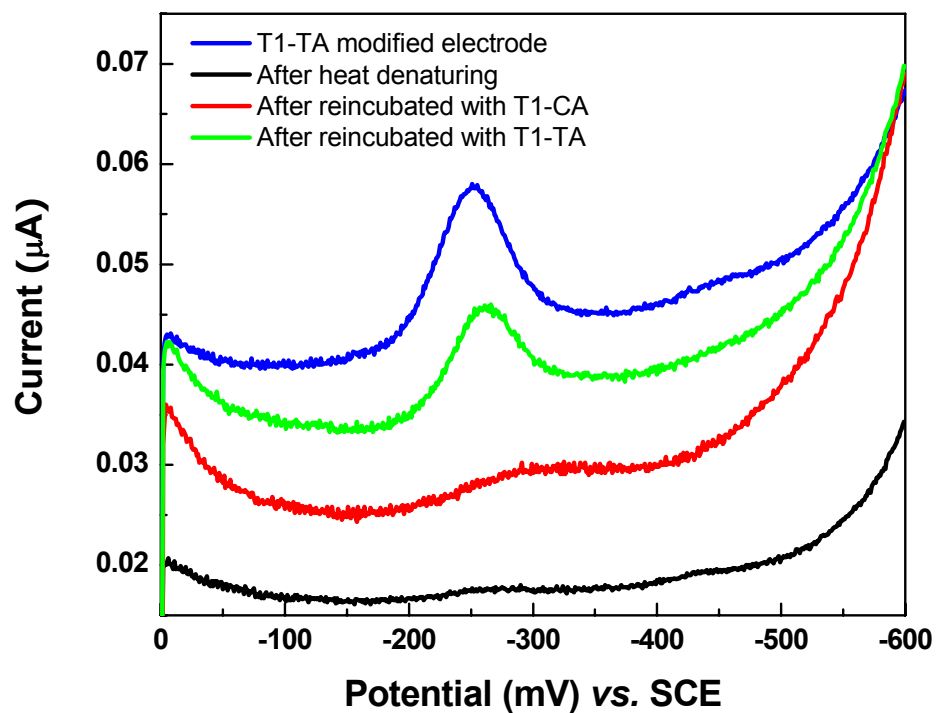


Figure 5.13. Square wave voltammetry of the electrode responses at different steps in the reversible hybridization experiment. In this experiment, the probe modified electrode was first incubated with **T1-TA** (blue), heat denatured in Milli-Q water (black), reincubated with **T1-CA** (red), heat denatured once more, and reincubated with **T1-TA** again (green).

DNA duplex containing a base overhang at the surface is highly reversible. Moreover, a CA mismatch in the duplex can be effectively detected by the change in the redox signal of NB.

The electrochemical sensitivity to the mismatch within the trapped duplex can be significantly enhanced by coupling the trapping event to an electrocatalytic assay. Two **P1** modified electrodes are incubated with **T1-TA** and **T1-CA** respectively, and are interrogated by cyclic voltammetry in Echem buffer containing 4 mM $[\text{Fe}(\text{CN})_6]^{3-}$. As previously observed, both the reduction signal of the **T1-TA** modified electrode and the differentiation between **T1-TA** and **T1-CA** are dramatically amplified (~100-fold) (Figure 5.14).

Again, with covalently tethered NB, we have demonstrated that DNA duplexes containing base overhangs can be reversibly trapped at DNA modified electrodes. A CA mismatch in the duplex can be effectively detected by the change in the redox signal of the covalent intercalator. Furthermore, the sensitivity of mismatch detection is significantly enhanced by electrocatalysis. The methodology presented here provides a suitable means to fabricate reusable electrodes for mutation detection based on DNA-mediated charge transport.

5.3.4 Label-free mismatch detection with DNA-NB conjugates

By a simple modification to the trapping strategy described above, we have developed a label-free method for base pair mismatch detection that eliminates the need for chemical modification of the samples being tested. As illustrated in Figure 5.15, a gold electrode is modified with a thiol-terminated single stranded probe. The electrode is

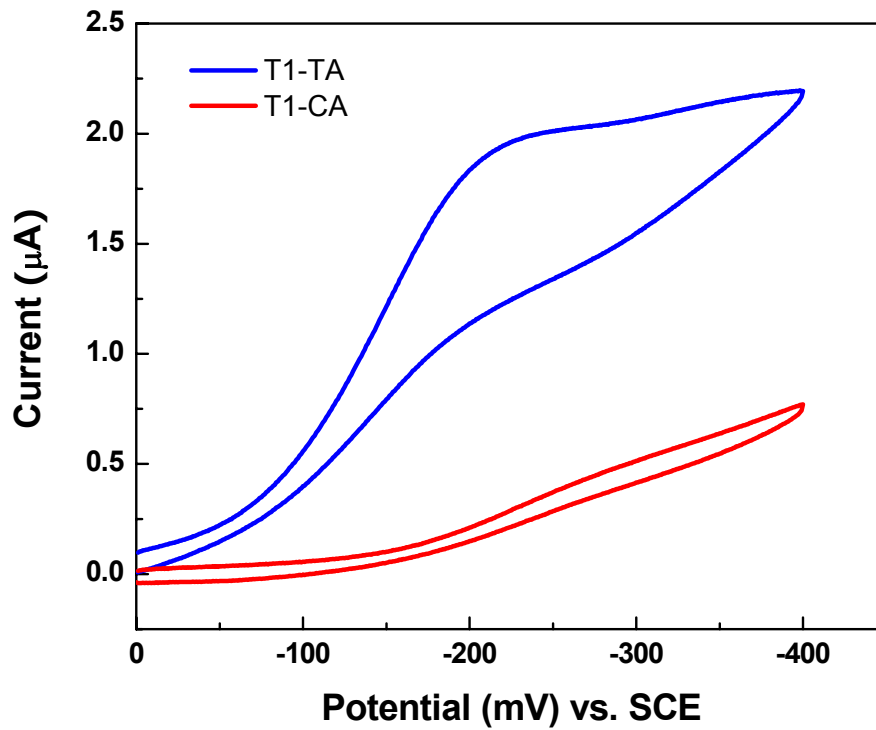


Figure 5.14. Cyclic voltammogram of probe modified electrodes incubated with **T1-TA** (blue) and **T1-CA** (red), respectively. Cyclic voltammetry was carried out in Echem buffer containing 4 mM $[\text{Fe}(\text{CN})_6]^{3-}$ (scan rate = 50 mV/s).

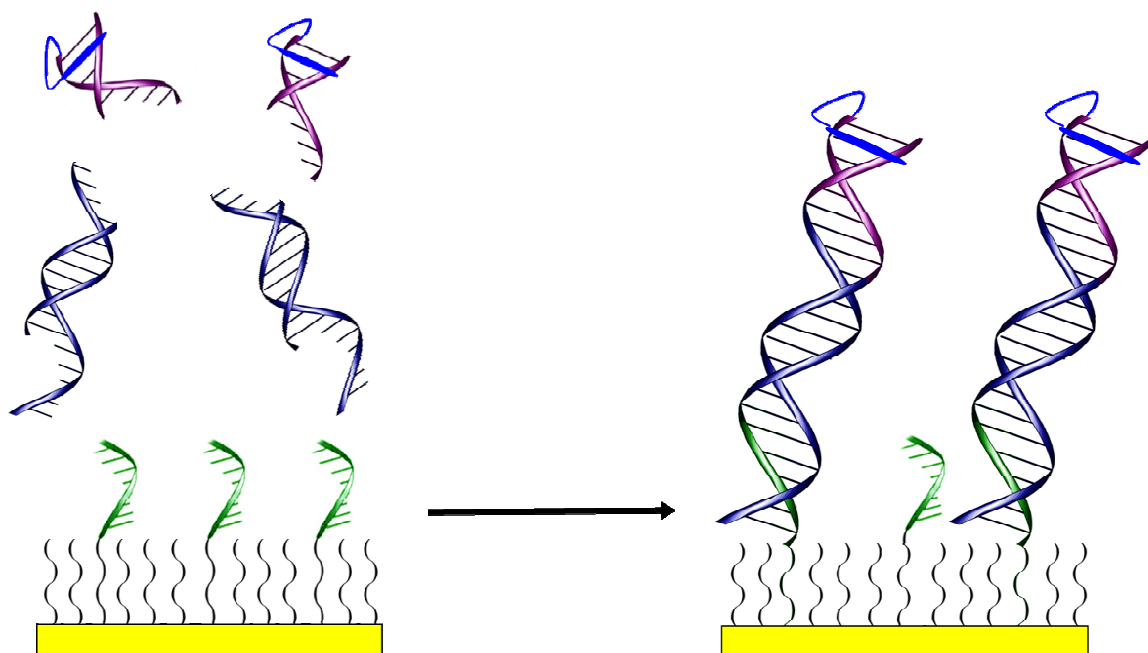


Figure 5.15. Schematic representation of label-free mutation detection based on DNA-mediated charge transport. The gold electrode is modified with thiol-terminated single stranded probe (green), incubated with a mixture of target duplexes containing two overhangs (navy blue) and signaling duplexes (violet) with covalently tethered Nile blue (blue). An intervening mismatch in the target duplex can be detected by the diminished electrochemical response caused by the presence of the mismatch.

then incubated with a mixture of target duplexes bearing two overhangs and signaling duplexes with covalently the tethered redox active intercalator. An intervening mismatch in the target duplex can be detected by a diminished electrochemical response due to the perturbation of the electron transfer pathway within the DNA film. The probe modified electrode can be easily regenerated by heat denaturing, which removes the target duplex and the signaling duplex. Compared to our previous mismatch detection methods using methylene blue and daunomycin,^{3, 6, 24} this detection strategy avoids time-consuming chemical crosslinking and eliminates the need for a tightly packed DNA film. Furthermore, the probe modified electrodes in this method are reusable. These advantages significantly simplify the assay process and increase the viability of mismatch detection based on DNA-mediated charge transport.

Using the DNA-NB conjugate as the signaling duplex, we carry out an experiment to detect a CA mismatch in a DNA sample (**M-CA**) without any chemical modification. In this experiment, three electrodes are modified with 1 μM single stranded probes (**P2**) in Echem buffer and are backfilled with 1 mM MCH for 1 hour. We estimate the surface coverage of the electrodes to be ~ 15 pmol/cm², quantified by $[\text{Ru}(\text{NH}_3)_6]^{3+}$. The first electrode (electrode 1) is incubated with a solution of 1 μM fully base paired sample (**M-TA**), 1 μM signaling duplex (**T2**), and 1 M NaCl. The second electrode (electrode 2) is incubated with a solution of 1 μM CA-mismatched sample (**M-CA**), 1 μM **T2**, and 1 M NaCl. As a control, the third electrode (electrode 3) is incubated with a solution containing only 1 μM **T2** and 1 M NaCl. Each incubation is carried out for 1 hour at room temperature.

The trapping of the sample duplexes and signaling duplexes is monitored by AC

impedance measurements in Echem buffer containing 4 mM $[\text{Fe}(\text{CN})_6]^{3-}$. As shown in Figure 5.16, both electrode 1 and electrode 2 show a significant increase in impedance while the impedance of electrode 3 only changes slightly. This indicates that the trapping event is sequence specific and the signaling duplex (**T2**) does not nonspecifically adsorb to the electrode surface in the absence of the sample duplexes. On the other hand, the sample duplexes are readily immobilized on the electrode. It is noteworthy that the Nyquist plots are almost semicircular and no linear region is observed. The absence of a linear region indicates that the $[\text{Fe}(\text{CN})_6]^{3-}$ ions are well blocked from the electrode surface and can not be reduced directly.

DNA-mediated charge transfer events at the modified electrodes are further investigated by square wave voltammetry. The results of these experiments are shown in Figure 5.17. Only electrode 1, which contains the fully base-paired sample, shows a signal at -250 mV (vs. SCE), consistent with the reduction of NB. No reduction signal is observed on either electrode 2, which contains a CA mismatched sample, or electrode 3, on which the sample duplex is absent. This indicates that a CA mismatch in the sample duplex can be readily detected by attenuation of the reduction signal, and an excess of **T2** does not cause false signals.

Further experiments demonstrate that mismatch detection can also be achieved with the samples trapped reversibly *in situ* at the electrode surface. In these experiments, electrode 1 and electrode 2 are heated in Milli-Q water to remove the trapped **M-TA** and **M-CA**, respectively. New duplexes are then formed by incubation of the electrodes with the swapped samples (**M-TA** \rightarrow **M-CA**, **M-CA** \rightarrow **M-TA**) and **T2**. As shown in Figure 5.17(b), the electrochemistry of **T2** at the modified electrodes exhibits the characteristic

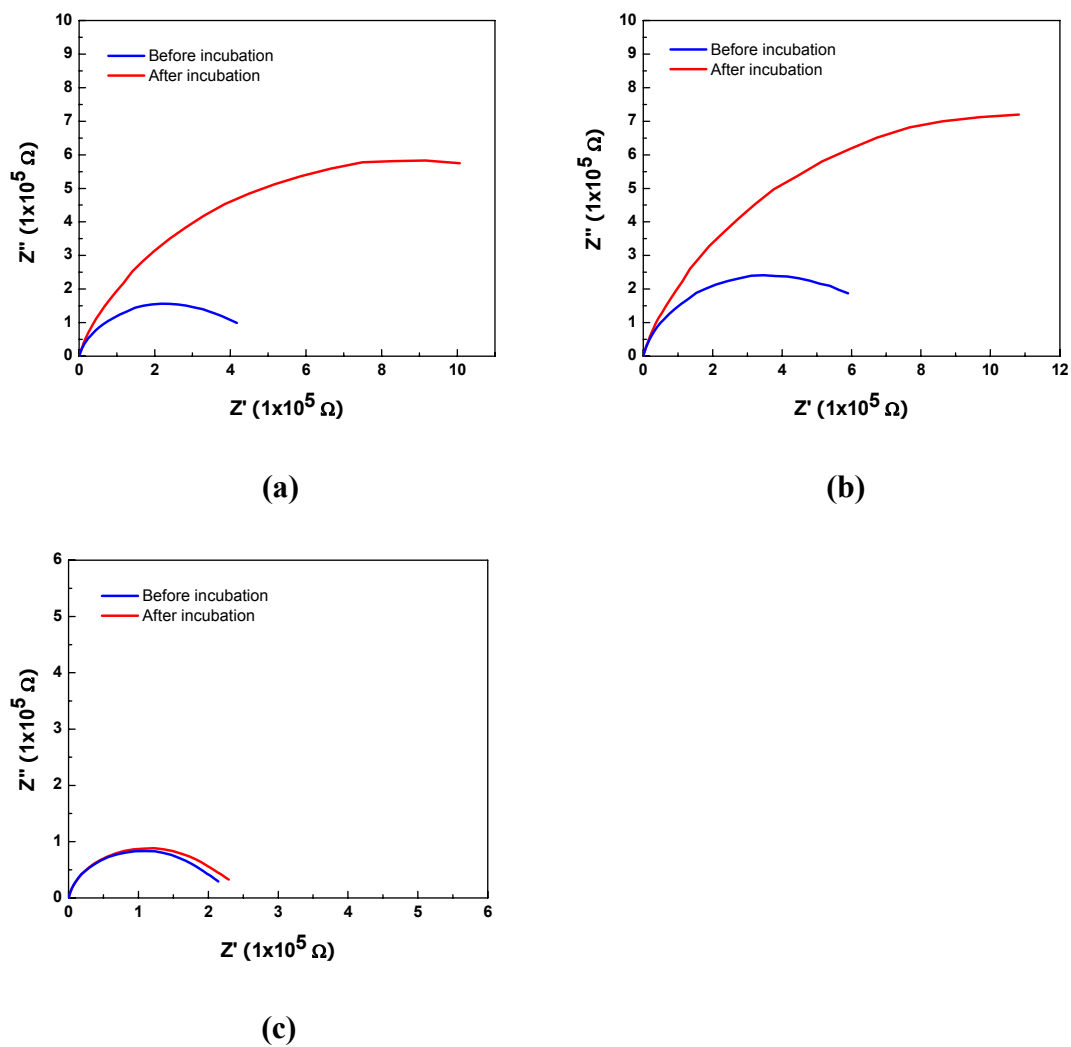
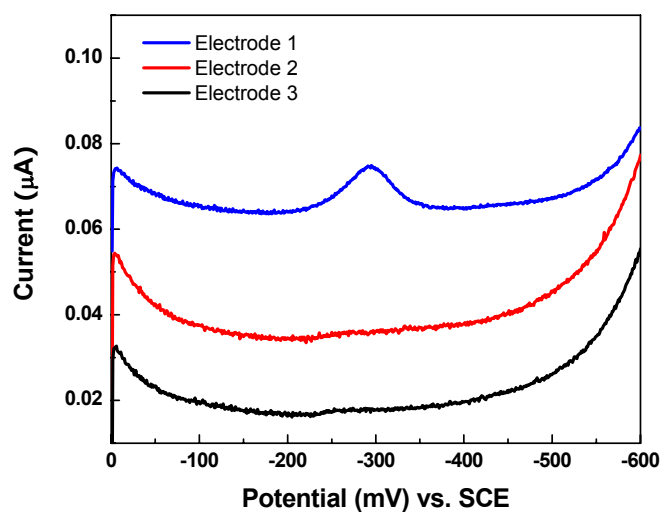


Figure 5.16. Nyquist plots for P2 modified electrodes before (blue) and after (red) incubation with different solutions.

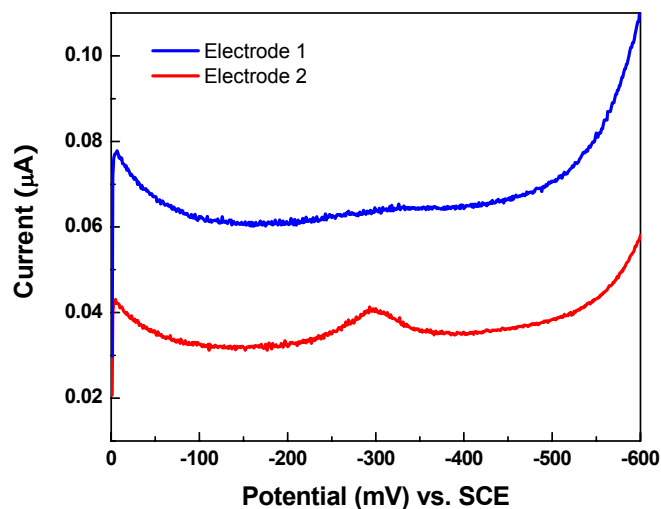
(a) A solution of 1 μM M-TA and 1 μM T2;

(b) A solution of 1 μM M-CA and 1 μM T2;

(c) A solution of 1 μM T2 only.



(a)



(b)

Figure 5.17.

(a) Square wave voltammetry of **P2**-modified electrodes incubated with different solutions: electrode 1, incubated with **M-TA** and **T2** (blue); electrode 2, incubated with **M-CA** and **T2** (red); electrode 3, incubated with **T2** only (black).

(b) Square wave voltammetry of electrode 1 and electrode 2 after they were heat denatured and incubated with the swapped solutions (**M-TA** \rightarrow **M-CA**, **M-CA** \rightarrow **M-TA**).

behavior corresponding to the type of sample trapped on the electrode.

Although duplexes containing mismatches can be distinguished by the reduction signal of **T2** in square wave voltammetry, the absolute electrochemical signals are limited by the surface coverage of the trapped samples and **T2**. In order to increase the inherent sensitivity of this assay, we have coupled electrocatalysis to the trapping event. In this experiment, electrode 1 and electrode 2 modified with M-TA and M-CA respectively are interrogated by cyclic voltammetry in Echem buffer containing 4mM $[\text{Fe}(\text{CN})_6]^{3-}$. As shown in Figure 5.18, electrocatalysis effectively amplifies the electrochemical signal of NB and improves the discrimination between the signals obtained for **M-TA** versus **M-CA** modified electrodes.

Because electrocatalysis involving intercalators bound to DNA-modified electrodes requires a catalyst that can dynamically shuttle electrons to solution-borne acceptors,⁶ the linkage between NB and DNA duplex should be flexible enough so that the NB moiety can reversibly bind to and dissociate from the DNA duplex to which it is tethered. The flexibility of the linker also sterically affects the coupling between NB and the base pair stack. Indeed, we find that, with less flexible linkers, the covalently tethered NB can not be reduced on DNA modified electrodes. For the same reason, daunomycin, which has a stronger affinity for DNA,³⁰ may have slower exchange dynamics that would not allow the passage of electrons out to the acceptor. Hence, daunomycin is not expected to be suitable for electrocatalytic assays.

Here we have presented a label-free method for mismatch detection using DNA-NB conjugates. Compared to other mismatch detection methods that are also based on DNA-mediated charge transport, this method avoids the time-consuming chemical

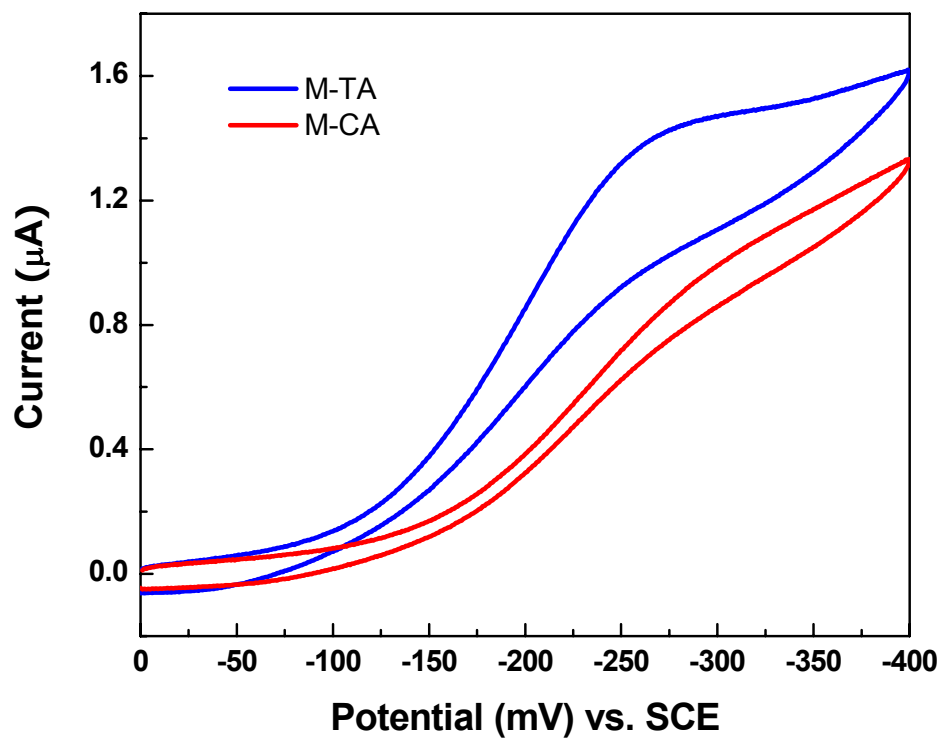


Figure 5.18. Cyclic voltammogram of P2-modified electrodes incubated with M-TA+T2 (blue) and M-CA+T2 (red), respectively. Cyclic voltammetry was carried out in Echem buffer containing 4 mM $[\text{Fe}(\text{CN})_6]^{3-}$ (scan rate = 50 mV/s).

modification of the samples and eliminates the requirements for densely packed DNA films. Furthermore, because the probe modified electrodes are addressable and can be easily regenerated by heat denaturing, this method shows a great potential for high throughput DNA assays. As a result, it may provide a practical detection system for inexpensive detection of single nucleotide polymorphisms (SNPs).

5.4 SUMMARY

We have covalently tethered Nile blue (NB) to DNA strands and used it as a redox active intercalator to examine DNA-mediated charge transfer in various contexts. We have observed that the reduction of the covalently tethered NB is very sensitive to charge transfer events in DNA films. An intervening CA mismatch significantly diminished the reduction signal of NB. The DNA-NB conjugates have also been used to monitor the trapping of DNA duplexes containing a base overhang at gold electrodes modified with single stranded probes. Moreover, a CA mismatch in the trapped duplex is effectively detected based on electron transfer through the DNA film. Based on these discoveries, we have developed a label-free method for mismatch detection using DNA-NB conjugates as signaling probes. Compared to previous mismatch detection methods based on DNA-mediated charge transfer, this method avoids the time-consuming chemical modifications of DNA samples and eliminates the requirements for densely packed DNA films. Using this method, we have successfully detected a CA mismatch in the duplex sample. Furthermore, by coupling the reduction of NB to an electrocatalytic process, we have significantly improved the sensitivity and reliability of this assay. Our studies provide a novel approach to the development of DNA sensors for mutation detection.

5.5 REFERENCES

1. Delaney, S.; Pascaly, M.; Bhattacharya, P. K.; Han, K.; Barton, J. K., Oxidative Damage by Ruthenium Complexes Containing the Dipyridophenazine Ligand or Its Derivatives: A Focus on Intercalation. *Inorganic Chemistry* **2002**, 41, (7), 1966-1974.
2. Boon, E. M.; Jackson, N. M.; Wightman, M. D.; Kelley, S. O.; Hill, M. G.; Barton, J. K., Intercalative stacking: A critical feature of DNA charge-transport electrochemistry. *Journal of Physical Chemistry B* **2003**, 107, (42), 11805-11812.
3. Kelley, S. O.; Jackson, N. M.; Hill, M. G.; Barton, J. K., Long-range electron transfer through DNA films. *Angewandte Chemie-International Edition* **1999**, 38, (7), 941-945.
4. Yu, H. Z.; Luo, C. Y.; Sankar, C. G.; Sen, D., Voltammetric Procedure for Examining DNA-Modified Surfaces: Quantitation, Cationic Binding Activity, and Electron-Transfer Kinetics. *Analytical Chemistry* **2003**, 75, (15), 3902-3907.
5. Liu, T., Ph.D thesis, Chapter 4.
6. Kelley, S. O.; Boon, E. M.; Barton, J. K.; Jackson, N. M.; Hill, M. G., Single-base mismatch detection based on charge transduction through DNA. *Nucleic Acids Research* **1999**, 27, (24), 4830-4837.
7. Taatjes, D. J.; Gaudiano, G.; Resing, K.; Koch, T. H., Redox pathway leading to the alkylation of DNA by the anthracycline, antitumor drugs adriamycin and daunomycin. *Journal of Medicinal Chemistry* **1997**, 40, (8), 1276-1286.
8. Houeelevin, C.; Gardesalbert, M.; Rouscilles, A.; Ferradini, C.; Hickel, B., Intramolecular Semiquinone Disproportionation in DNA - Pulse-Radiolysis Study of the One-Electron Reduction of Daunorubicin Intercalated in DNA. *Biochemistry* **1991**, 30, (33), 8216-8222.
9. Gurr, E., *Synthetic dyes in biology, medicine and chemistry*. Academic Press: London, England, 1971.
10. Lillie, R. D., *Conn's Biological Stains*. Williams & Wilkins: Baltimore, MD., U.S.A., 1977.
11. Chen, Q. G., Interaction of a novel red-region fluorescent probe, Nile blue, with DNA

and its application to nucleic acids assay. *The Analyst* **1999**, 124, (6), 901-906.

12. Ju, H.; Ye, Y.; Zhu, Y., Interaction between Nile blue and immobilized single- or double-stranded DNA and its application in electrochemical recognition. *Electrochimica Acta* **2005**, 50, (6), 1361-1367.

13. Zhao, G. C.; Zhu, J. J.; Chen, H. Y.; Wang, X. M.; Lu, Z. H., Spectroscopic and spectroelectrochemical studies of interaction of Nile blue with DNA. *Chinese Journal of Chemistry* **2002**, 20, (1), 57-62.

14. Huang, C. Z.; Li, Y. F.; Pu, Q. H.; Lai, L. J., Interactions of Nile blue sulphate with nucleic acids as studied by resonance light-scattering measurements and determination of nucleic acids at nanogram levels. *Analytical Letters* **1999**, 32, (12), 2395-2415.

15. Lakowicz, J. R.; Piszczek, G.; Kang, J. S., On the Possibility of Long-Wavelength Long-Lifetime High-Quantum-Yield Luminophores. *Analytical Biochemistry* **2001**, 288, (1), 62-75.

16. Kuramitz, H., Electrocatalytic reduction of hemoglobin at a self-assembled monolayer electrode containing redox dye, Nile blue as an electron-transfer mediator. *Analytical sciences* **1999**, 15, (6), 589-592.

17. Cai, C. X., Electrocatalytic oxidation of NADH at glassy carbon electrodes modified with an electropolymerized film of Nile blue A. *Chinese journal of chemistry* **2000**, 18, (2), 182-187.

18. Liu, H. H.; Lu, J. L.; Zhang, M.; Pang, D. W., Electrochemical properties of Nile blue covalently immobilized on self-assembled thiol-monolayer modified gold electrodes. *Analytical Sciences* **2002**, 18, (12), 1339-1344.

19. Glen Research, <http://www.glenres.com/Catalog/ultramild.html>.

20. Sugawara, K.; Yamauchi, Y.; Hoshi, S.; Akatsuka, K.; Yamamoto, F.; Tanaka, S.; Nakamura, H., Accumulation voltammetry of avidin and biotin using a biotin labeled with Nile blue A. *Bioelectrochemistry and Bioenergetics* **1996**, 41, (2), 167-172.

21. Laviron, E., General Expression of the Linear Potential Sweep Voltammogram in the Case of Diffusionless Electrochemical Systems. *Journal of Electroanalytical Chemistry* **1979**, 101, (1), 19-28.

22. Tender, L.; Carter, M. T.; Murray, R. W., Cyclic Voltammetric Analysis of Ferrocene

Alkanethiol Monolayer Electrode-Kinetics Based on Marcus Theory. *Analytical Chemistry* **1994**, 66, (19), 3173-3181.

23. Liu, T.; Barton, J. K., DNA Electrochemistry through the Base Pairs Not the Sugar-Phosphate Backbone. *Journal of the American Chemical Society* **2005**, 127, (29), 10160-10161.

24. Boon, E. M.; Ceres, D. M.; Drummond, T. G.; Hill, M. G.; Barton, J. K., Mutation detection by electrocatalysis at DNA-modified electrodes. *Nature Biotechnology* **2000**, 18, (10), 1096-1100.

25. Ruan, C.; Yang, L.; Li, Y., Immunobiosensor Chips for Detection of *Escherichia coli* O157:H7 Using Electrochemical Impedance Spectroscopy. *Analytical Chemistry* **2002**, 74, (18), 4814-4820.

26. Yan, F.; Sadik, O. A., Enzyme-Modulated Cleavage of dsDNA for Supramolecular Design of Biosensors. *Analytical Chemistry* **2001**, 73, (21), 5272-5280.

27. Patolsky, F.; Katz, E.; Bardea, A.; Willner, I., Enzyme-Linked Amplified Electrochemical Sensing of Oligonucleotide-DNA Interactions by Means of the Precipitation of an Insoluble Product and Using Impedance Spectroscopy. *Langmuir* **1999**, 15, (11), 3703-3706.

28. Patolsky, F.; Lichtenstein, A.; Willner, I., Electronic Transduction of DNA Sensing Processes on Surfaces: Amplification of DNA Detection and Analysis of Single-Base Mismatches by Tagged Liposomes. *Journal of the American Chemical Society* **2001**, 123, (22), 5194-5205.

29. Pan, S.; Rothberg, L., Chemical Control of Electrode Functionalization for Detection of DNA Hybridization by Electrochemical Impedance Spectroscopy. *Langmuir* **2005**, 21, (3), 1022-1027.

30. Chaires, J. B., Binding of daunomycin to calf thymus nucleosomes. *Biochemistry* **1983**, 22, (2), 284-292.